ABSTRACT

TUOHY, JOANNE L. Characterization of the Effects of Bacteria-Induced Inflammation and Hyperthermia Therapy on Monocytes and Macrophages in Osteosarcoma. (Under the direction of Dr. Duncan Lascelles and Dr. Jonathan Fogle).

Osteosarcoma (OS) survival has not improved substantially for humans and dogs in the past 30 years. OS is the 3rd most commonly diagnosed tumor in adolescents 12-18 years of age, and is the most common primary bone tumor in the dog. Despite attempts with various permutations of adjunctive therapies, the median survival for OS dogs remains at 10-12 months. Similarly, the 5-year survival rate in humans with non-metastatic OS remains around 70%, with no better than 20-30% long-term survival in OS patients with metastatic disease. Despite progress made in surgical resection of the primary tumor, metastases continue to impede efforts to improve OS survival. The problem of metastatic disease in OS thus needs a new and innovative approach. An approach with exciting potential is immunotherapy. The investigations outlined in this dissertation build the foundation for development of novel immunotherapy against OS by understanding the role of monocytes and macrophages in the immune environment of OS, and the influence of bacteria-induced and hyperthermia therapy-induced inflammation on monocyte/macrophage phenotype in the tumor microenvironment. Our overall hypothesis is that bacteria-induced and hyperthermia therapy-induced inflammation reverses the immunosuppressive effects of OS on monocytes and macrophages, and induces an inflammatory anti-tumor phenotype in macrophages under the influence of OS. Specific objectives were to evaluate the effect of OS on monocytes and macrophages, to determine if the addition of bacteria or administration of hyperthermia therapy induces an inflammatory phenotype distinct from the effects of OS.

We carried out studies in the dog, human and mouse to increase the specificity of our findings with cross-species comparisons. The biological similarity between canine and human OS makes the dog a promising model for translational research. In contrast to inbred laboratory rodents, the dog has the advantage of being an outbred species, like humans, with an intact immune system that develops spontaneously occurring OS. Utilizing the canine model of OS gives us the distinct advantage of producing highly applicable and translatable results for progressing human OS research.

In our studies that recruited clinical canine patients with OS, we demonstrated that OS influences host immune response in dogs by downregulating monocyte chemokine receptor expression and inhibiting monocyte chemotaxis. This dampening effect on monocyte chemokine receptors appears to be attenuated by the presence of a bacterial infection, as dogs with OS and a concurrent surgical site infection have significantly higher monocyte chemokine receptor expression than dogs with untreated OS. We also demonstrated increased PGE_2 secretion from monocytes of untreated OS dogs, which correlates with inhibition of monocyte chemotaxis, causing immunopathology in OS. We did not demonstrate parallel observations in human and murine monocytes, but our cross-species studies have identified monocyte surface receptors that are dysregulated in OS across species, specifically CCR2, CCR7, CXCR2, and CX3CR1. We demonstrated with our human and canine macrophage *in vitro* studies that although OS can induce a protumorigenic inflammatory response in macrophages, the additional influence of bacteria can upregulate the macrophage inflammatory response to a higher intensity, potentially turning it into an M1-like macrophage anti-tumor response.

These results improved our understanding of the monocyte / macrophage response to OS, and the immunostimulatory effects of bacteria-induced inflammation. The studies outlined help direct our future work aimed at manipulating macrophage differentiation in OS to induce an anti-tumor immune response. Using the dog as a model for comparative OS research takes advantage of the biologic similarity between canine and human OS to produce maximally translatable results to improve survival for dogs and humans.

Characterization of the Effects of Bacteria-Induced Inflammation and Hyperthermia Therapy on Monocytes and Macrophages in Osteosarcoma.

by
Joanne L. Tuohy

A dissertation submitted to the Graduate Faculty of
North Carolina State University
in partial fulfillment of the
requirements for the degree of
Doctor of Philosophy

Comparative Biomedical Sciences

Raleigh, North Carolina

2018

APPROVED BY:

_____	_____
Dr. Duncan Lascelles Committee Chair	Dr. Jonathan Fogle Committee Co-Chair
_____	_____
Dr. Mark Dewhirst	Dr. William Eward (External member)
_____	_____
Dr. Paul Hess	Dr. Steve Dow (External member)

DEDICATION

To Michael Tuohy, my loving husband and dearest friend, and to Dougal, Railay, and Tasker, who make me laugh and inspire me.

BIOGRAPHY

Joanne Tuohy received a Bachelor of Arts in Greek and Latin from Mount Holyoke College, and her Doctor of Veterinary Medicine from the Colorado State University. She completed her rotating small animal internship and residency program in small animal surgery at North Carolina State University, and achieved board certification from the American College of Veterinary Surgeons. She then matriculated into the Comparative Biomedical Sciences graduate program at North Carolina State University.

ACKNOWLEDGMENTS

These dissertation studies have allowed me to combine my research and clinical passions, and build a foundation for future work to improve survival outcomes for canine and human osteosarcoma patients. I cannot thank everyone enough who have guided and encouraged me through this process. I could not have accomplished any of this work without the support and dedication of my advisors, Drs. Duncan Lascelles and Jonathan Fogle. I would also like to thank the members of my committee, Drs. Eward, Dewhirst, Dow, and Hess, for sharing their expertise and helping me elevate the quality of my research. I would like to thank Dr. Sam Jones, the director of the CBS program, for his support, and acknowledge the NIH T32 Comparative Medicine and Translational Research Training Program for making this work possible. Without the collaboration and assistance from the following laboratories and their personnel, this work could not have been accomplished – Borst Laboratory (Mitsu Suyemoto), Messenger Laboratory (Alex Taylor), and the Hess Laboratory (Jenny Holmes). I would also like to thank all the individuals who have so graciously lent their expertise and taken the time along the way to help answer my many questions as I worked through the experiments. I have been very fortunate to meet many loving and dedicated pet owners, some of whom have become firm friends, most notably Betty and Ed Woodard, who have shown endless support for me and my work. Last but not least, I would like to thank my husband, all my mentors, and my friends who have given me invaluable encouragement along this journey.

TABLE OF CONTENTS

LIST OF TABLES

Chapter 2

Chapter 3

Chapter 5

LIST OF FIGURES

Chapter 2

Chapter 3

CHAPTER 1

Literature Review

Overview of canine and human osteosarcoma

Osteosarcoma (OS), a malignant primary tumor of bone, is a devastating disease for both human and canine patients. It is the most common primary bone tumor in children and adolescents, as well as in the dog, and arises from mesenchymal cells that produce osteoid.[1,2] Treatment of OS involves removal of the primary tumor, and chemotherapy to address metastatic disease. The initial treatment option for the primary tumor in appendicular OS was amputation of the affected limb. Subsequently, major advances made in surgical tumor removal have enabled successful limb salvage surgeries to be performed in humans and dogs. A recent meta-analysis of surgical treatment for human OS concluded that limb salvage surgery was associated with increased 5-year survival rates without increased risk of local disease recurrence.[3] Similarly, limb salvage surgery in dogs yields comparable survival rates to limb amputation when combined with adjuvant therapy.[4] More recently, stereotactic radiotherapy (SRT) has been reported in dogs as a non-surgical limb sparing method of primary tumor control, with similar survival rates as surgical primary tumor resection.[5,6] Adjuvant and neoadjuvant chemotherapeutic regimens are used in OS to target metastatic disease, where chemotherapy is administered before (neoadjuvant), and after (adjuvant) primary tumor removal. However, the main cause of death in human and canine OS is still metastatic disease, even though at time of diagnosis, only 11-20% of human patients and under 15% of canine patients present with pulmonary metastases.[1,7] The introduction of adjuvant and neoadjuvant chemotherapy initially increased disease-free intervals and survival

rates for both humans and dogs, but improvements in outcomes have plateaued for the past 30 years. The 5-year disease-free interval for human patients with non-metastatic OS remains around 70%, with only 20-30% long-term survival in patients with metastatic disease, and the median survival in dogs with OS remains between 10-12 months despite various permutations of chemotherapeutic regimens.[1,8-10] Advancements in OS therapy clearly need to target metastatic disease in order to improve survival.

Canine OS as a translational research model for human OS

Dogs and humans with OS share multiple similarities that make the dog an exceptional translational research model. These similarities include matching biological behavior, similar response to treatments, almost identical histological characteristics, and shared global gene expression signatures.[11-15] For example, a majority of OS lesions occur in the appendicular skeleton around the metaphyseal region of long bones in both dogs and humans, and the disease tends to be associated with large and/or tall individuals more frequently.[2,11] Radiographically, OS appears identical in humans and dogs, displaying a lesion with a combination of lytic and proliferative bone.[11,16]

OS is aggressively metastatic in both dogs and humans, with the lung being the most frequent site of metastasis. Despite the relatively low percentage (<20%) of human and canine OS patients that present with gross metastasis at time of diagnosis, approximately 85-90% of patients will eventually develop metastatic disease.[7,16] Both canine and human OS patients respond similarly to treatment strategies – removal of the primary tumor and the use of chemotherapeutics to address metastatic disease. Human OS patients have more diverse

treatment options, with chemotherapeutic options such as methotrexate and ifosfamide in addition to doxorubicin and carboplatin / cisplatin combinations. The introduction of neoadjuvant chemotherapy and histologic assessment of response to therapy in human OS patients have improved prognostication of outcomes and awareness of the need for adjusted treatment regimens for poor responders.[17] The use of neoadjuvant chemotherapy is currently not a widely adopted practice for canine OS patients, with a scarcity of data to support its use. One retrospective study did not find a survival advantage with use of neoadjuvant chemotherapy in dogs with OS.[18] Additional data are needed in order to adequately assess the efficacy of neoadjuvant regimens in dogs. The dose intensity (DI) of chemotherapeutic protocols, defined as the dose administered per body surface area / body weight, does not appear to have a significant impact on survival in canine patients, and increased DI in human protocols do not necessarily produce improved survival.[8,17,19]

Canine and human OS patients share similar prognostic factors such as the presence of metastatic disease at time of diagnosis. Human patients presenting with gross metastases have a decreased 5-year survival of 20-30%; canine patients with metastases also experience decreased survival, and the varied range of treatments reported for stage III (presence of metastatic disease) canine OS patients yielded a median survival of 76 days.[10,20] Tumor location is also an important prognosticator for human and canine OS – proximal humeral OS carries a poorer prognosis compared to other appendicular sites.[21,22] Interestingly, the development of a postoperative infection at surgical limb salvage sites is associated with an improved survival in dogs and humans with OS, though this survival advantage is not consistently reported across human studies.[23-27] Serum alkaline phosphatase (ALP) levels are

similarly prognostic for human and canine OS – OS dogs with serum ALP levels above the reference range have significantly shorter survival and disease-free interval compared to dogs with levels within the reference range, and a similar observation has been made in human OS patients.[17,21]

Histologically, canine and human OS are difficult to distinguish from each other. OS in both species is a tumor that arises from primitive precursors of mesenchymal cells that can produce osteoid, is most commonly a high grade tumor, and is classified into various histologic subtypes including chondroblastic, fibroblastic, telangiectatic, and osteoblastic. Histologic subtypes carry no prognostic significance for both canine and human OS patients, however, the histologic grade of the tumor does influence prognosis, with high grade tumors associated with a worse prognosis than low grade OS such as parosteal OS.[28,29]

On a molecular level, canine and human OS share genetic dysregulations such as p53 tumor suppressor gene mutations – up to 65% of primary canine OS overexpress the p53 protein, and about 20-60% of human OS cases exhibit p53 mutations.[30-33] Normal functioning of the p53 gene and nuclear phosphoprotein protects from carcinogenesis by preventing cells with genomic aberrations from replicating by inducing cell cycle arrest or apoptosis, thus its deregulation is common in many cancers. Other genes similarly dysregulated in canine and human OS include PTEN (phosphatase and tensin homolog), RB1 (retinoblastoma), and β–catenin. The PTEN gene encodes for the PTEN protein, another tumor suppressor; decreased PTEN expression and copy number losses have been reported in human and canine OS.[34,35] The RB1 gene encodes for the pRB protein, which is also a tumor suppressor, regulating processes critical to cell growth and differentiation, especially the cell cycle transition from

G1 to S phase, as well as cell survival and apoptosis. Dysregulation of the RB1 gene has been noted in 30-75% of human OS cases, with 29% of canine OS cases displaying DNA copy number loss in the RB1 gene, and 45% of canine OS reported to exhibit disrupted Rb pathways.[33,36] Metastatic lesions from human OS patients have low RB1 expression, supporting the hypothesis that the resultant loss of cell cycle regulation can lead to promotion of metastases.[37] The expression of β–catenin, an important regulator of the Wnt signaling pathway that helps regulate stem cell pluripotency, occurs with similar frequency (~70-80%) in canine and human OS, but does not appear to be associated with survival or disease-free outcomes.[38,39] Nonetheless, the Wnt / β–catenin signaling pathway is dysregulated in many cancers, including OS, where its role in physiologic skeletal development can be subsumed to promote tumorigenesis and metastasis.[40-42] Both humans and dogs display germline genetic aberrations that can increase risk of OS development. In humans, survivors of familial retinoblastoma, a disease associated with germline mutations of the RB1 gene, have increased occurrences of other malignancies later in life, including a 12% incidence of OS.[33] The Li-Fraumeni syndrome is a genetic disorder characterized by a mutation in the p53 gene, and up to 3% of pediatric OS cases are associated with a germline mutation of p53.[43] In dogs, the controlled breeding of specific breeds has decreased the species' genetic diversity, and breeds such as Scottish deerhounds, Rottweilers, and Greyhounds are associated with increased incidence of OS. A genetic variant linked to the CFA34 locus (synthetic to human chromosome 3q26) is associated with a 15-fold increased risk of OS in Scottish deerhounds, and a recent report suggests the role of additional genetic factors in the risk inheritance of OS in this breed.[44,45] A genome-wide association analysis study in 3 breeds (Rottweilers, Irish

wolfhounds and Greyhounds) identified 33 inherited risk loci, with the strongest associated found in the Greyhound locus, which incidentally was the locus with the most rearrangements in canine OS.[46] Identification of cross-species germline risk factors in humans and dogs informs our understanding of the etiopathogenesis of OS and helps identify potential prognostication target candidates. A strong similarity in global gene expression signatures exists between human and canine OS, with the disease in both species indistinguishable by gene expression analyses.[12,47] Recent identification of orthologous high frequency DNA copy number aberrations in canine and human OS confirmed the importance of genes such as RUNX2 in OS pathogenesis.[34] Overexpression of IL-8 and SCL1A3 genes was reported in canine OS, and expression of these genes in human OS was associated with a poorer prognosis in human OS.[12] Such cross-species comparative genomic studies assist in increasing the specificity of our focus in OS, a disease marked by complex genomic instability, enabling the de-emphasis of unshared alterations and the focused identification of the most relevant targets for prognosis and treatment.

The strength of naturally occurring OS in the dog as a model for translational oncological research lies not only in the multitude of similarities of the disease in both species, but also in extrinsic factors. The dog has the advantage of being an outbred species with an intact immune system that develops spontaneously occurring OS over an extended period of time, just as humans do, unlike inbred laboratory rodents that are not syngeneic host-tumor models. Dogs and humans are more akin anatomically and physiologically than are mice to humans, and share the same physical environments and stressors, unlike mice maintained in a highly controlled research facility environment.[15] Canine OS patients mirror

the heterogeneity of human patients, with interindividual variations in disease manifestations and tumor characteristics. The behavior of canine OS parallels the biological complexity of the naturally occurring human disease, with both species sharing similar clinical disease manifestations and outcomes, especially in the development of recurrent resistant disease. The >10-fold increased incidence of canine OS (estimated incidence of 13.9/100,000) compared to human OS (1.02/100,000), the shorter lifespan of dogs, the rapid progression to OS metastasis in dogs enable outcomes to be assessed in relatively short periods of time.[11,48,49] In contrast, OS is considered an ultra-orphan disease in humans (worldwide average 3-4 cases / million individuals ≤24 years), and together with the relatively longer lifespan and OS survival in humans compared to dogs, create a substantial hurdle to obtaining study results in a rapid fashion to allow for accelerated advances to therapeutic regimens.[49] Dogs with OS represent powerful tools for drug development and clinical trials, as they are a biologically relevant disease model that can serve to better bridge preclinical murine study findings with human clinical trials. The larger size of dogs compared to mice improves the assessment of parameters such as pharmacologic dosing and kinetic studies, the availability of canine patients and the willingness of their owners to engage in repeated sample collections and procedures such as biopsies make dogs an invaluable model for clinical testing. Dogs also serve as valuable models for evaluating novel therapeutics. For example, canine studies initially reported the efficacy of the novel immunomodulating therapeutic, liposomal muramyl tripeptide phosphatidylethanolamine (L-MTP-PE) in improving OS outcomes.[50,51] Subsequently, human clinical trials have been initiated to assess

the use of L-MTP-PE in OS patients, and the drug has been approved for post-operative use in Europe for OS patients with minimal residual disease.[52]

The dog thus represents a unique and highly relevant translational large animal model for human OS, with the two species sharing strong similarities in many aspects of the disease including biologic behavior, clinical manifestations, global gene expressions and genetic aberrations. Cross-species comparative approaches can increase the specificity and relevance of identified shared prognostic and therapeutic targets, inform and optimize human clinical trial designs so as to decrease drug attrition / failure rates, and improve outcomes for human and canine patients suffering from this devastating disease.

Monocytes and macrophages in osteosarcoma

Overview of monocytes and macrophages

Monocytes are mononuclear leukocytes primarily found in the peripheral circulation, making up approximately 10% of total circulating leukocytes in humans, and approximately 2-4% of murine leukocytes.[53] Monocytes are an important player in the innate immune system, which provides first-line defense against invading pathogens by mounting an inflammatory response. A physiologically appropriate inflammatory response begins with the initial phase of inflammation to destroy pathogens, followed by a clean-up phase to remove dead cells, damaged extracellular matrix, and the final recovery and repair phase when injured tissue is restored to a healthy condition. Monocytes, together with resident macrophages and dendritic cells (DCs) form the mononuclear phagocyte system (MPS), which orchestrates the different phases of the inflammatory response. Monocytes begin their

development in the bone marrow as the common myeloid progenitor, and go through the stages of differentiation (granulocyte-macrophage progenitor, common macrophage and dendritic cell (DC) precursor) to become the committed monocyte progenitor. The primary factors important for regulation of monocyte development are macrophage stimulating factor (M-CSF), also known as colony stimulating factor 1 (CSF1), and granulocyte-macrophage colony stimulating factor (GM-CSF), also known as colony stimulating factor 2 (CSF2). M-CSF mainly regulates monocytes under homeostatic conditions, whereas GM-CSF functions under inflammatory responses.[53] More recently, IL-34 has been reported as an additional factor capable of binding the M-CSF receptor (CSF-1R) and inducing monocyte differentiation.[54] One of the main functions of monocytes as key players in the inflammatory response to pathogens is circulation in the peripheral blood to be recruited to replace tissue macrophage populations.[55] However, recent studies reporting the presence of tissue macrophages derived from embryonic origins with the ability for self-renewal, suggest that there may be a more complex role for monocytes besides simply being circulating macrophage precursors.[56,57] For example, Kupffer cells populate the liver during embryonic development and are self-renewing, independent of circulating monocytes.[57] Lineage-tracing studies have demonstrated that peripheral monocytes are not precursors of tissue macrophages in all tissues, instead, there are some tissues such as the intestinal lamia propria and colon, which have higher dependence on monocytes to repopulate resident macrophages, compared to other tissues such as the lung and kidney, which house mixed populations of macrophages that have both embryonic and adult hematopoietic origins.[57-59]

Monocytes are a heterogeneous population of cells whose subpopulations have been described for various species, including humans and mice. In 2010, the Nomenclature Committee of the International Union of Immunological Societies approved the terminology describing the 3 main human monocyte subsets.[60] The main population of monocytes (~90% of monocytes) are termed classical monocytes, and are characterized by high CD14 with no CD16 expression ($CD14^{++}CD16^{-}$ or $CD14^{+}CD16^{-}$), and the minor population of monocytes (~10% of monocytes) are subdivided into the intermediate and non-classical subsets. Intermediate monocytes are characterized by high CD14 with low CD16 expression ($CD14^{++}CD16^{+}$ or $CD14^{+}CD16^{+}$), and non-classical monocytes are characterized by lower CD14 expression relative to the high CD16 expression ($CD14^{+}CD16^{++}$ or $CD14^{dim}CD16^{+}$).[60] Gene expression profiling studies of the 3 monocyte subsets reveal different findings indicating the proximity of relationship between the subsets, but there appears to be more data supporting a closer relationship between the intermediate and non-classical subsets.[61] The 3 monocyte subsets are postulated to have different functions, but there is not universal agreement on specific parameters such as cytokine secretion profiles and antigen processing and presenting abilities. For example, both the intermediate and non-classical subsets have been shown to be highest producers of tumor necrosis factor alpha (TNF-α) in response to LPS stimulation, but differences in these results may be due to use of different isolation and staining techniques.[61] Despite the lack of universal agreement on the specific characteristics of the human monocyte subsets, these subsets are recognized to mirror murine monocyte subpopulations to a large extent. Murine monocytes are divided into inflammatory and alternative subpopulations, with the inflammatory monocytes exhibiting high Ly6C

expression and alternative monocytes exhibiting low or negative Ly6C expression. Murine Ly6C^{hi} inflammatory and human CD16^{-} monocytes both exhibit high expression of CCR2, a chemokine receptor that responds to the ligand CCL2, and is important for monocyte migration and recruitment to inflammatory foci.[62] Ly6C^{hi} inflammatory monocytes are akin in gene expression patterns to human classical CD16^{-} monocytes, whereas Ly6C^{lo} alternative monocytes are more similar to the non-classical CD16^{+} monocytes.[53,63] Ly6C^{lo} alternative murine monocytes, like their human non-classical counterparts, have high expression of another chemokine receptor, CX3CR1, thus directing their response to the ligand CX3CL1, found on endothelial cells and tissues. These alternative and non-classical monocytes have been shown to exhibit patrolling behavior, as they crawl along quiescent endothelium.[64] However, unlike their human counterparts, murine Ly6C^{hi} and Ly6C^{lo} monocytes have close to equal distribution, with inflammatory monocytes making up ~60% and alternative monocytes making up ~40% of peripheral monocytes. Just as for human monocytes, signaling via CSF-1R is important for murine monocytes, allowing for the differentiation from Ly6C^{hi} to Ly6C^{lo} monocytes under homeostatic conditions.[65]

In the acute inflammatory response to pathogens, monocytes are responsible for phagocytosing microbial invaders, and produce inflammatory cytokines and antimicrobial substances to enhance the destruction of pathogens.[66] Monocytes can also influence the adaptive immune reaction by shaping T cell responses.[66] Recent data support the hypothesis that monocytes have more complex effector cell functions and are not just phagocytes that replenish tissue macrophages – a distinct Ly6C^{hi} monocyte phenotype has been reported to be able to migrate to non-lymphoid organs and become “tissue monocytes” without necessarily

differentiating into tissue macrophages. These monocytes have the potential to upregulate MHCII expression, migrate to lymph nodes for antigen presentation to T cells while retaining a monocyte-gene profile.[67] Another effector function of monocytes, specifically the $Ly6C^{lo}$ and $CD14^{+}CD16^{++}$ subsets, is that of patrolling the endothelium and coordinating the repair of damaged endothelium. These terminally differentiated monocytes that crawl along the endothelial lumina can react to pathogens and endothelial damage with a variety of responses such as phagocytosis, recruitment of intravascular neutrophils, secretion of inflammatory cytokines, and cellular debris clean-up.[68,69] Despite these more recent elucidations on the variety of monocyte functions, an important long recognized role of monocytes, especially the $Ly6C^{hi}$ and the $CD14^{++}CD16^{-}$ classical monocytes, remains their ability to differentiate into M1-like macrophages during an inflammatory response.

Macrophages are an extremely heterogeneous cell population found in almost all adult mammalian tissues, making up 10-15% of total cells under physiologic conditions. Resident macrophages in various tissues are given different names, for example, Kupffer cells of the liver, alveolar macrophages of the lung, microglial cells of the central nervous system, and osteoclasts of the bone. Despite their different names, resident macrophages share basic primary responsibilities, namely shaping physiologic tissue development, surveilling for and responding to tissue damage, effecting tissue remodeling and repair, and participating in the immune response to pathogens by coordinating an inflammatory reaction. Macrophages were originally thought to solely come from peripheral monocytes migrating to tissues and differentiating into macrophages, however this theory is being revised with more recent data.[55] The characterization of fetal tissue macrophages that arise from macrophage

embryonic precursors has challenged the long-held view that circulating monocytes are primarily responsible for populating tissue macrophage pools.[70] Some organs only have fetal tissue macrophages, for example, the brain has yolk-sac derived microglia, whereas other organs such as the heart contain a mixed population of macrophages of embryonic origins and macrophages derived from circulating blood monocytes.[70] Additionally, these macrophages of embryonic origins have the capacity to proliferate and maintain their numbers independent of replenishment from circulating monocytes.[56] Essentially, macrophages are a much more complex cell population than originally thought, and they also possess tremendous ability to respond rapidly and effectively to changing physiological conditions.

The macrophage's ability to respond to different environments lie in their capacity to polarize to functionally appropriate phenotypes with a high degree of plasticity, with M1 (pro-inflammatory)/M2 (anti-inflammatory) macrophages being the most commonly recognized phenotypes, representing both ends of the polarization spectrum. However, M1 and M2 macrophages should not be viewed as discrete subsets, instead, they represent macrophages over the spectrum of continuum of macrophage activation and polarization. M1 macrophages are induced by bacterial products such as lipopolysaccharide (LPS), cytokines such as IFN-γ, and they metabolize arginine to nitric oxide (NO) and citrulline, enabling their killing function, as NO is a potent microbicidal molecule.[53] M1 macrophages display increased expression of markers such as MHCII, CD80/86, and efficiently produce inflammatory cytokines (e.g. TNF-α, IL-1β, IL-12) and cytotoxic mediators (e.g. reactive oxygen species, NO).[53] M2 macrophages are induced by cytokines like IL-10, IL-4, and

TGF-β, and they metabolize arginine to ornithine and polyamines, molecules that assist in tissue healing and remodeling.[53] M2 macrophages display increased expression of markers such as mannose and scavenger receptors, and secrete anti-inflammatory molecules such as TGF-β.[53] Attempts have been made to subclassify M2 macrophages into M2a, M2b and M2c macrophages to further reflect the variety of functional macrophage responses, with M2a macrophages responding primarily to IL-4 and IL-13, M2b macrophages responding to binding of Fc and Toll-like receptors, and M2c macrophages responding to IL-10 and TGF-β.[71] It is important to note that both monocyte differentiation and macrophage polarization are dynamic processes, and the classifications given to these cells provide a conceptual organizational framework to describe a continuum of differentiation and polarization states. Macrophages can switch between polarization states depending on contextual environmental cues, *in vitro* studies have demonstrated the ability of macrophages to switch from M1 to M2, and vice versa, depending on the changes in environmental stimuli.[72,73] Besides their functions of mounting a host defense against pathogens and initiating tissue healing and recovery responses, macrophages are also extremely important in coordinating the adaptive T cell response, as they are capable of directing T cells towards Th1 or Th2 responses and inducing T cell proliferation.[74,75] Tissue macrophages can present antigen to T cells initially primed in the lymph nodes that subsequently travel to tissue sites of inflammation, enabling the T cell's full activation.[76] The tremendous plasticity of the macrophage enables it to carry out its wide range of functions effectively, but it is also an attribute that can be subverted by pathologies to contribute to disease progression.

Tumor-associated macrophages

Macrophages have been recognized to play an important role in cancer, representing a large proportion (as high as 50%) of the leukocyte infiltrate in the tumor microenvironment.[77] Macrophages within the tumor environment are referred to as tumor-associated macrophages (TAMs). Similar to the heterogeneity of resident macrophage ontogeny in tissues in physiologic environments, the tumor microenvironment is populated both by macrophages that are derived from embryonic precursors of the affected tissue, and macrophages differentiated from circulating monocytes migrating to the tumor.[78,79] Whether macrophage ontogeny influences the TAM's contribution to the tumor microenvironment is currently unclear, however, the recruitment of circulating monocytes appears to be an integral process for maintaining the TAM population.[79,80] Peripheral cells in circulation that are commonly recruited to the tumor microenvironment include Ly6C^{hi} inflammatory monocytes and monocytic myeloid-derived suppressor cells (M-MDSCs).[80,81] Interestingly, in contrast, Ly6C^{lo} alternative monocytes have been shown to reduce tumor growth in murine models of pulmonary metastatic disease by activating an NK cell response and scavenging tumor debris, which contain tumor-derived extracellular vesicles implicated in the promotion of tumor progression and immune suppression.[82] The main chemoattractants recruiting Ly6C^{hi} monocytes and M-MDSCs to the tumor include CCL2 and CSF-1.[83] In addition to attracting TAM precursors from circulation, molecules such as CSF-1 also have substantial effects on macrophage growth and differentiation, inducing growth and pushing macrophages towards an M2-like phenotype often associated with tumor promotion.[84] In skeletal neoplasms, CSF-1 becomes an important player in promoting tumor progression as it directs the differentiation

of osteoclasts, which are in turn influenced by tumor cells to cause osteolysis.[84] A study utilizing a murine model of mammary carcinoma demonstrated that TAMs require the transcriptional regulator of Notch signaling, RBPJ, for differentiation from infiltrating Ly6C^{hi} inflammatory monocytes.[80] Also, depletion of TAMs derived from circulating monocytes inhibited tumor growth and rescued cytotoxic T cell responses, whereas depletion of TAMs from embryonic precursors did not have a similar effect.[80]

Macrophages play a prominent role in the process of cancer immunoediting, which consists of 4 phases – the elimination, equilibrium, immunosuppression and escape phases. In the elimination phase, macrophages work with other immune cells to eliminate nascent tumor cells. In that capacity, they assume an M1-like phenotype with the ability to kill tumor cells with secretion of cytotoxic mediators and inhibit angiogenesis.[85,86] The crosstalk between M1-like macrophages and T cells can induce Th1-type responses and potentiate M1-type macrophage activity – for example, M1-like macrophages secrete CXCL9 and CXCL10, which are chemoattractants for Th1 T cells, and Th1 cells secrete IFNγ, amplifying M1 macrophage polarization.[85] All this culminates in an innate and adaptive anti-tumor response that can destroy tumor cells. Successful tumor cell elimination results in an endpoint of cancer immunoediting. In some situations, the cancer cells are not completely eliminated, and enter instead into a phase of equilibrium, where the immune cells are able to maintain the cancer cells in functional dormancy, thus inhibiting their growth. During this phase, immune cells such as the macrophage can be influenced by signals and mediators from the tumor cells to start polarizing towards an M2-like phenotype. Eventually, this can lead to a breakdown of the immune defense against the tumor cells, resulting in suppression of the immune response

and escape of the tumor cells to create clinically apparent disease.[87] A complex mix of various mediators in the tumor microenvironment leads to recruitment of peripheral monocytes and initiation of M2-like polarization. Factors such as IL-4, IL-13, and CSF-1 within the microenvironment skew macrophages towards an M2-like phenotype, which can be exploited by the tumor to promote growth and metastasis.[81,84] TAMs are a heterogeneous population with phenotypes that vary between tumor types and also between different locations within the same tumor, with the common thread connecting diverse TAM phenotypes being their predisposition towards an M2 phenotype.[81]

M2-like TAMs effect tumorigenesis via multiple mechanisms, which include promotion of cellular proliferation, tissue remodeling, matrix invasion and metastasis, angiogenesis, epithelial-to-mesenchymal transition (EMT), genetic instability, and suppression of the immune response while providing a protective environment for cancer stem cells. For example, TAMs can produce epidermal growth factor (EGF), which induces cellular proliferation.[81] Additionally, as an illustration of the complexity of interactions within the tumor microenvironment, carcinoma cells secreting CSF-1 can stimulate macrophages to produce EGF, which promotes directed migration of tumor cells together with macrophages along collagen fibers that guide the cells towards blood vessels.[88,89] This paracrine loop involving EGF and CSF-1 directing the migration of carcinoma cells depends on the presence of macrophages.[88] As the carcinoma cells and macrophages cluster around the vasculature, under the influence of EGF and CSF-1 respectively, tumor cells form invadopodia and macrophages form podosomes that increase their invasiveness and ability to degrade the extracellular matrix and intravasate.[90] Production of proteolytic enzymes by

TAMs such as matrix metalloproteinases (MMPs) also break down the extracellular matrix to facilitate local tumor cell invasion and intravasation into the vasculature.[81] For instance, M2-like TAMs were reported to increase MMP-9 expression and activity, thus degrading the extracellular matrix to facilitate colon cancer cell invasion.[91]

Promotion of angiogenesis is another hallmark of TAMs' protumoral abilities. The tumor angiogenic switch is required for tumors to acquire a vasculature capable of supporting its growth and to progress malignancy, and this switch is dependent on macrophages.[92] TAMs, under the influence of CSF-1, produce growth factors such as vascular endothelial growth factor (VEGF), and MMP-9, which promotes angiogenesis via release of VEGF.[92,93] More recently, the expression of WNT7b by TAMs in a human breast carcinoma model is reported to promote angiogenesis and metastasis, partly through induction of VEGF, and inactivation of WNT7b decreased pulmonary metastasis.[94] Expression of TIE2, an endothelial cell tyrosine kinase receptor, in TAMs has also been shown to be an important player in promoting angiogenesis, as $TIE2^{+}$ TAMs align along vasculature in response to expression of angiopoietin-2 (ANG2), the TIE2 ligand, by endothelial cells, thus promoting tumor angiogenesis.[95] Inhibiting either TIE2 or ANG2 can break this link between TAMs and the vasculature, leading to decreased angiogenesis, reducing subsequent tumor growth and metastasis.[95] Treatment with CSF-1 in a mammary carcinoma model led to increased numbers of TIE2-expressing monocytes and macrophages, in turn increasing angiogenesis.[96]

TAMs can induce EMT, a process in which epithelial cells lose their epithelial phenotype and take on increasingly mesenchymal features such as increased migratory abilities, resistance to apoptosis, invasiveness and production of extracellular matrix.[97] EMT

occurs under physiologic conditions to assist in embryonic cell dispersion and recovery from tissue injury. However, it can also be subsumed by epithelial neoplasias to promote invasiveness and metastasis. TAMs have been shown to induce EMT through various mechanisms, including secretion of inflammatory cytokines such as TNF-α and cysteinyl leukotriene D_4 (LTD_4).[91] Anti-inflammatory cytokines secreted by TAMs such as TGF-β are also capable of inducing EMT, as demonstrated in a F9-teratocarcinoma murine model where co-culture with macrophage-conditioned medium resulted in EMT activation via macrophage-derived TGF-β.[98] Co-culture with M2-like TAMs also induced EMT in pancreatic cancer cells partly via increase in TLR4 and IL-10 signaling.[99] In addition, the inflammatory reactive oxygen and nitrogen intermediates secreted by TAMs can cause genetic instability in cancer cells, allowing for mutations that build resistance to cancer therapies.[81] Human TAMs have been shown to overexpress the cancer protooncogene c-MYC, which is required for activation of M2-like macrophages, and inhibition of c-MYC in TAMs resulted in blockade of tumorigenic gene expression, such as VEGF, TGF-β, and MMP9.[100] Similarly, inhibition of MYC in murine tumors decreased expression of immune checkpoint proteins CD47 and programmed cell death ligand-1 (PD-L1), thus activating the antitumor immune response, as CD47 expression inhibits macrophage phagocytosis and PD-L1 inhibits T cell activation.[101]

An important mechanism of tumorigenesis effected by TAMs is suppression of an effective anti-tumor immune response. Macrophages normally express ligands of the inhibitory receptors programmed cell death protein 1 (PD-1), and cytotoxic T-lymphocyte antigen 4 (CTLA-4), which are PD-L1, PD-L2, and B7-1 (CD80), B7-2 (CD86) respectively.

Expression of these ligands are usually found on activated immune cells such as macrophages to control the intensity of the immune response and to aid in the physiologic resolution of inflammation. Binding of these ligands with their respective receptors result in dampening of T and B cell receptor signaling, T cell activation and cytotoxic function.[84] A study evaluating PD-L1 expression in canine myeloid cells found low to negative PD-L1 expression in quiescent peripheral monocytes and monocyte-derived macrophages from healthy dogs.[102] However, PD-L1 expression in these cells was significantly increased in response to IFN-γ exposure, supporting the observation that PD-L1 expression is physiologically important for resolving inflammation.[102] In the tumor microenvironment, TAMs can upregulate inhibitory ligand expression to suppress T cell responses. A study highlighting the importance of the PD-1 / PD-L1 axis in creating an immunosuppressive tumor environment demonstrated PD-1 mediated T cell exhaustion and depletion, with increases in TAMs paralleling decreases in $CD8^+$ T cell numbers.[103] PD-L1 expression has also been found to be increased in murine macrophages within the tumor in a squamous cell carcinoma model, with corresponding increased percentage of T cell expression of PD-1, and inhibition of PD-1 reduced the incidence of papilloma formation.[104] In human oral squamous cell carcinoma, M2-like TAMs exhibited higher expression of PD-L1 and the immunosuppressive IL-10 compared to non M2-like TAMs, and co-culture with these M2-like TAMs resulted in decreased numbers of activated T cells.[105] Secretion of immunosuppressive cytokines is another mechanism by which TAMs dampen the anti-tumor immune response. As mentioned above, TAMs secrete IL-10, and they also secrete TGF-β as well as induce latent TGF-β into their activated forms.[106] TGF-β exerts a multitude of

immunosuppressive effects, including the co-induction, together with IL-10, of T regulatory cells (Tregs) within the tumor, whose function is to dampen the immune / inflammatory response via inhibition of cytotoxic T cells and $CD4^+$ T cells.[107,108] Additionally, TAMs can recruit Tregs to the tumor microenvironment via secretion of a variety of cytokines including CCL20, CCL22, and CCL5.[84] TAMs suppress T cell function also by secretion of arginase I into the tumor microenvironment, which metabolizes L-arginine to L-ornithine and urea.[109] A study reports the Ron receptor tyrosine kinase activating arginase I expression in TAMs, and that Ron expression was found specifically in the TIE2 TAM subset.[109] L-arginine metabolism essentially depletes L-arginine from the environment, which is required by T cells for the re-expression of the CD3ζ chain after internalization due to antigen stimulation.[110] TAM expression of B7-H4, a member of the B7 superfamily, can suppress T cell function. A study reported the stimulation of B7-H4 expression in TAMs by Treg-induced IL-10 secretion by TAMs, thereby promoting the immunosuppressive activity of TAMs.[111] Clinically, increased levels of B7-H4 expressing macrophages correlated with higher clinical stages and hence poorer prognosis in human lung cancer.[112]

Another tumor-promoting mechanism of TAMs is the provision of a nurturing niche for cancer stem cells. A murine study described TAMs protecting cancer stem cells from the cytotoxic effects of chemotherapy and promoting their chemotherapeutic drug resistance via secretion of milk-fat globule-epidermal growth factor VIII (MFG-E8).[113] Inhibition of TAMs can reduce the number of cancer stem cells in pancreatic tumors and increase the effectiveness of chemotherapeutics.[114] TAMs also help establish pre-metastatic niches, preparing distant sites for metastatic seeding and assisting metastatic cells in their

intravasation, extravasation, survival and growth.[115] An important component of the pre-metastatic niche is the bone marrow-derived immature myeloid cell expressing VEGF receptor 1 (VEGFR1), which seeds in pre-metastatic sites and increases the permissiveness of these sites before the arrival of metastatic tumor cells.[116] MMP9, which can be secreted by TAMs, is an example of a molecule important in establishing the pre-metastatic niche - it is induced in macrophages by distant tumor cells, resulting in increased myeloid cell recruitment via VEGFR1 signaling, facilitation of tumor cell invasion, and subsequent promotion of lung metastasis.[117] Ablation of $CD11b^{+}VEGFR1^{+}$ myeloid cells can inhibit formation of these pre-metastatic niches.[116,118] Tumor-derived exosomes are another factor capable of stimulating myeloid cells at pre-metastatic niches to increase their angiogenic capabilities via the receptor tyrosine kinase MET, thus priming the sites for metastatic seeding.[119] Once tumor cells seed at the pre-metastatic sites, they can release CCL2 to attract circulating $Ly6C^{hi}$ monocytes, which in turn enhance the ability of metastatic tumor cells to extravasate partially via expression of VEGF.[120] These $Ly6C^{hi}$ monocytes eventually differentiate into macrophages at the metastatic site, which continue to enhance extravasation and promote tumor cell survival.[120]

Given the widely reported pro-tumorigenic characteristics of TAMs, it is not surprising that the presence and level of TAM infiltration into a tumor carry prognostic significance for many tumors. A meta-analysis of the prognostic significance of TAMs in human solid tumors demonstrated TAM infiltration as a negative prognosticator.[121] However, in some cases such as colorectal, gastric, and non-small-cell lung cancers, TAM infiltration can be associated with a favorable prognosis.[77,121,122] As we gain increased understanding of

TAMs, it becomes apparent that TAM distribution within a tumor is not homogeneous, and TAM phenotypic signatures range across the M1-M2 spectrum. For instance, M1-like TAMs can be found in normoxic areas of the tumor compared to M2-like TAMs, which populate hypoxic regions instead.[77] Such heterogeneity can potentially account for the differences in prognostic significance of TAMs in various reports. It has been reported since the 1970s that macrophages, if appropriately activated by e.g. bacterial products, can take on tumoricidal properties, thus suggesting that manipulating TAM phenotype has antitumor potential.[78,123,124] TAMs can also affect responses to chemotherapy. Chemotherapeutic agents such as doxorubicin can effect immunogenic cell death in tumor cells by activating the innate and adaptive immune responses, and TAM infiltration in turn can be predictive of responses to chemotherapy.[125] For example, in follicular lymphoma, increased TAM numbers was a good prognosticator for patients treated with a chemotherapeutic regimen that included doxorubicin, whereas in patients that did not receive doxorubicin, high TAMs were a poor prognosticator, therefore suggesting TAMs as important regulators of the antitumor effects of doxorubicin.[126] Pancreatic adenocarcinoma patients with high TAM infiltration were reported to respond positively to gemcitabine chemotherapy, and the authors demonstrated *in vitro* activation of gemcitabine-treated macrophages to an antitumor phenotype.[127] Strategies for TAM re-education to stimulate an antitumor phenotype thus represent an exciting therapeutic avenue. In OS, TAM infiltration interestingly has not uniformly represented an unfavorable prognosis, and TAMs could represent a therapeutic target against the disease, especially metastatic OS.

Tumor-associated macrophages in osteosarcoma

TAMs have been associated with variable prognoses in OS. Some OS studies show M2-like TAMs to be tumorigenic – a murine OS study reported M1-like TAMs polarizing to M2-like TAMs within the first 3 weeks after OS implantation, and depletion of M2-like TAMs resulted in significantly decreased tumor growth.[128] A study evaluating tumor and peripheral blood samples from human OS patients demonstrated a smaller proportion of T cells but higher expression of T cell exhaustion markers (TIM3, PD1) in tumor samples compared to peripheral blood.[129] These $TIM3^{+}PD1+$ T cells exhibited lower proliferation capacity and decreased cellular expression of inflammatory cytokines such as IFN-γ and TNF-α compared to peripheral T cells.[129] The percentage of the $TIM3^{+}PD1+$ T cells within the tumor positively correlated with M2-like TAM frequency, and specific depletion of this M2-like population of TAMs resulted in increased T cell proliferation and heightened cellular expression of IFN-γ and TNF-α.[129] Another study utilizing human OS patient tumor samples demonstrated that infiltration of tumor specimens with macrophages and dendritic cells (DCs) was associated with decreased event-free survival compared to tumors that had less than 1% tumor volume infiltrated with macrophages or DCs.[130] In this study, tumors positive for PD-L1 were more likely to contain immune cell infiltrates including macrophages, DCs, T cells, and NK cells, and tumor PD-L1 expression was associated with a shorter event-free survival.[130] The study did not attempt to classify the tumor infiltrating macrophages into subsets to ascertain whether specific subsets had differential associations with survival or PD-L1 expression. Additionally, it is interesting that even though the infiltrating T cells were more likely to express PD-1 in PD-L1 positive tumors, this T cell

presence was not significantly associated with a poorer event-free survival. There are also studies that suggest macrophage infiltration to be a favorable finding - in one report evaluating biopsy samples from human high-grade OS patients who did or did not develop metastases within 5 years of diagnosis, increased infiltration of M1/M2 TAMs was associated with decreased metastasis and improved survival.[131] The study also found that about 45% of the genes (e.g. CD14, TLR4, CD86, HLA-DR) overexpressed in samples from patients without metastases compared the patients that metastasized were expressed by infiltrating hematopoietic cells and were associated with macrophage functions.[131] These macrophage-associated genes were also upregulated in post-chemotherapy samples, and there was a trend for increased macrophage infiltration in pre-chemotherapy samples to predict a good histological response to neoadjuvant chemotherapy.[131] There was a mixture of M1-like and M2-like macrophages within the tumor tissue, with phenotypic prevalence not predictive of survival outcome, thus precluding conclusions about the anti-tumor mechanism.[131] Another study utilizing human OS tumor samples from patients that presented with and without metastasis at diagnosis showed a similar number of total tumor infiltrating macrophages between groups, but a higher number of M1-like macrophages in the non-metastatic group.[132] M2-like macrophages within the tumors were positively correlated with tumor vascular density, suggesting an angiogenesis-promoting effect of M2-like macrophages.[132] Similar to the findings by Buddingh et al., increased macrophage infiltration into tumors was associated with improved survival.[131,132] Such varied data on the implications of TAMs in OS make it clear that the interactions between macrophages and OS are complex and extremely plastic, and the mechanistic effects of macrophages in OS are clearly not well

understood. A recent study elucidated the role of IL-34 in promoting macrophage recruitment and OS growth – IL-34, recently identified as having similar effects as M-CSF in regulating differentiation of monocytes and macrophages, was overexpressed in a murine model of OS.[133] This overexpression resulted in increased endothelial cell proliferation and vascular cord formation, thus promoting angiogenesis.[133] Additionally IL-34 enhanced the recruitment of macrophages into the tumor microenvironment, as shown by the 3-fold increase in TAM infiltration and the increased number of M2-like macrophages in tumors overexpressing IL-34 compared to control tumors.[133] All these studies highlight the complexity of the interaction between macrophages and the tumor microenvironment in OS, and the need for increased understanding of the effects of different macrophage subtypes on the tumor. The phenotypic plasticity of the macrophage accounts for the heterogeneous phenotypes identified in OS tissues, manipulation of these plastic polarization phenotypes carries important therapeutic merit, as the malleability of macrophages to their environmental cues makes them promising therapeutic targets.

Potential role of monocytes and macrophages in immunotherapy against OS

An interesting phenomenon observed in OS is the improved survival associated with surgical site bacterial infections, which hearkens back to the findings of William B. Coley, who, based on anecdotal reports of patients who experienced malignant tumor regression concurrent with a bacterial infection, decided to test the potential beneficial effects of infections on tumor progression. Coley developed concoctions of bacterial organisms, most commonly heat-killed *Streptococcus* combined with *Serratia marcescens*, and administered

what became known as Coley's Toxins to hundreds of patients, some of whom reportedly experienced tumor regression.[134] However, due in part to the inconsistency of the treatment (e.g. in concoction preparations, route of administration, dose, treatment duration), and in part to the emergence of chemotherapy and radiation therapy, Coley's Toxins fell by the wayside until the recent advent of cancer immunotherapy as a promising adjunctive therapeutic.[134] In later years, a retrospective study of Coley's cases that were deemed inoperable sarcoma cases reported a remission rate of 64% and a 5-year survival rate of 44%, lending support to the validity of Coley's conviction that infection can have a positive effect on tumors.[135] It now recognized that Coley and his work have advanced our knowledge of immunology and immunotherapy, most notably in the discovery of TNF-α through the observation that a tumor-necrosing polysaccharide (endotoxin) indirectly kills tumor cells by inducing the release of a host factor (TNF-α) toxic to tumors.[136]

One of the earlier reports documenting improved survival in OS patients with surgical site infections was a veterinary retrospective series that aimed to assess the efficacy of preoperative radiation therapy in OS dogs undergoing limb salvage procedures.[137] This study found that dogs that developed a deep infection of the limb salvage site experienced significantly longer survival times compared to uninfected dogs (11 versus 5 months respectively), and infected dogs had better local tumor control rates.[137] In 2005, a veterinary retrospective series evaluating the effects of postoperative infections on OS outcomes noted dogs with OS that underwent surgical limb salvage procedures and developed a deep surgical site infection postoperatively survived a median of 252 days longer, and developed metastasis at a median of 300 days later compared to dogs without infection.[23] Considering

that the median survival time for dogs with OS ranges between 10-12 months, these numbers represent a near-doubling of overall survival and event-free survival times. Hazard ratios indicated that the OS dogs with a limb salvage associated infection were half as likely to die (HR 0.446) and half as likely to develop metastases (0.426), and the study demonstrated that the survival benefits were due to an inhibitory effect on metastasis rather than local disease recurrence.[23] A more recent retrospective veterinary study also identified the development of a surgical site infection was significantly associated with increased overall survival; another study evaluating OS dogs that underwent SRT and concurrent surgical stabilization of the treatment site reported a trend towards a significantly decreased hazard ratio for death with the development of infection.[25,138] This association of infection with survival has also been noted in human OS – a retrospective consecutive series of 547 human OS patients reported that the patients who developed a deep postoperative infection had significantly improved survival, with a 84.5% 10-year survival rate for the infected patients compared to the 62.3% 10-year survival rate for non-infected patients.[24] There was also a trend towards significantly decreased metastases in the infected patients, but infection appeared to have no impact on the incidence of local disease recurrence, similar to the finding in dogs.[23,24] In both the canine and human retrospectives, *Staphylococcus aureus* (*S. aureus*) was the most common organism isolated from infection sites, and in the human patients, significantly improved survival was noted in patients with a *S. aureus* infection.[23,24] Following the 2005 report by Jeys et al., a few other human studies have emerged exploring the relationship between infection and OS survival, and not all of them have uniformly reported an improvement in survival concurrent with infection. A report in 2009 of 347 patients did not find a survival advantage in patients

who developed a deep postoperative infection, with the 10-year survival rate for infected patients being 83.3%, compared to the 10-year survival for non-infected patients at 82%.[27] The study also reported that infected patients also frequently displayed good responses to chemotherapy, frequently had more proximal tibial tumors, and none of the infected patients experienced local disease recurrence.[27] The authors thus surmised that the influence of infection on survival may not only be due to local antitumor effects of the infection, but also due to clinical characteristics of the patients.[27] A study exploring whether postoperative infection affected outcomes in human soft tissue sarcoma did not find a protective effect of infection either.[139] The authors did not find a difference in survival, local recurrence or metastasis between patients that did or did not develop a postoperative infection after surgical resection of soft tissue sarcomas in combination with neoadjuvant and / or adjuvant radiation therapy.[139] The larger variation in treatment algorithms for soft tissue sarcoma compared to OS may have made it more challenging to fully evaluate the effects of infection. Recently, another study identified a positive benefit of infection on 5-year survival and event-free rates in human OS patients, with infected patients experiencing 100% survival and event-free rates compared to the 54% survival and 43% event-free rates in non-infected patients.[26] However, this study only included 6 infected patients out of a total of 125 study patients, thus these small sample sizes make it challenging to come to definitive conclusions about the effects of infection on OS outcomes.

The effects of infection on OS have been evaluated using murine models. A study utilizing a syngeneic subcutaneous model of murine OS and bacterial osteomyelitis demonstrated induction of anti-OS activity in tumor-bearing mice with concurrent bacterial

osteomyelitis.[140] Mice with OS and a bacterial osteomyelitis experienced significantly decreased tumor growth and significantly longer survival times compared to OS-bearing mice without an infection.[140] The effects of bacterial osteomyelitis on tumor growth was noted not only with *S. aureus*, it was also noted with other gram-positive as well as gram-negative bacteria.[140] Additionally, the protective effect of infection was recapitulated using different tumor types and mouse strains.[140] This anti-tumor response corresponded with an increase in total numbers of circulating monocytes caused by an increase specifically in the inflammatory monocyte compartment, as well as an increase in the splenic inflammatory monocyte population, suggestive of the hypothesis that bacterial infection causes an inflammatory response mobilizing inflammatory monocytes that can feed tumor macrophage populations.[140] In support of this hypothesis, the authors observed significantly increased numbers of TAMs in OS mice with osteomyelitis compared to uninfected OS mice.[140] These TAMs were not further identified as M1 versus M2 TAMs, thus this study raises the question whether the observed anti-tumor response was elicited by increased numbers of bacteria-induced M1 TAMs. Additionally, monocyte/macrophage depletion using liposomal clodronate resulted in significantly increased tumor growth in infected OS mice compared to infected OS mice that did not receive liposomal clodronate, supporting the hypothesis that monocytes and macrophages induced by bacterial osteomyelitis play a substantial role in tumor inhibition.[140] Depletion of natural killer (NK) cells in infected OS mice also resulted in significant increases in tumor growth compared to infected mice that did not undergo NK cell depletion, suggesting that NK cells, together with monocytes and macrophages, are important players in the anti-tumor response.[140]

Despite the conflicting studies regarding the effects of bacterial infection on OS outcomes, some of those results suggest the immunogenic nature of OS can be targeted by an upregulation of an immune / inflammatory response, leading to inhibition of tumor growth. Also, innate cells such as monocytes, macrophages and NK cells play important roles in this anti-tumor response. Immunotherapy, based on the principle of upregulating the immune response against a tumor, has been gaining attention as a promising adjuvant therapeutic modality in cancers such as melanoma.[141] However, despite these exciting developments of cancer immunotherapy, there is a lack of advancement in immunotherapies specifically for OS. Given the potential of macrophages to incite an anti-tumor response, understanding their responses within the OS tumor environment is important in any effort to harness the immune response against cancer. Due to their plasticity, macrophages can engage in pro- as well as anti-tumor activities – since the 1970s, investigators have noted that macrophages can be activated to mount an anti-tumor response, however it is also established that TAMs can promote tumorigenesis.[78,123,124] Thus it is crucial to find the balance between desirable and undesirable macrophage inflammatory responses to tip the scales in favor of an inflammatory anti-tumor response.

An immunotherapeutic agent that features prominently in OS studies is liposomal encapsulated muramyl tripeptide phosphatidyl ethanolamine (L-MTP-PE), a synthetic derivative of muramyl dipeptide (MDP), a bacterial cell wall component in both gram-positive and gram-negative bacterial cell walls. MDP is recognized both by the intracellular pattern-recognition molecule, NOD2, found primarily in monocytes, macrophages, dendritic cells and intestinal Paneth cells, and another NOD-like receptor, NLRP3.[142,143] Recognition of

MDP by NOD2 and NLRP3 results in an inflammatory response accompanied by inflammatory cytokine and antimicrobial peptide release, dendritic cell activation, activation of a T-helper cell response, and this response can potentially be tumoricidal as well.[143] Early canine studies demonstrated the efficacy of L-MTP-PE against OS – dogs with OS treated with amputation to remove the primary tumor that received L-MTP-PE experienced significantly longer survival times compared to dogs that received empty control liposomes.[50] Another canine clinical trial demonstrated a survival advantage when L-MTP-PE was administered following standard-of-care adjuvant treatment with cisplatin.[144] Monocytes and macrophages activated by L-MTP-PE have been evaluated as key players in the anti-OS response – a study utilizing normal canine pulmonary alveolar macrophages demonstrated significantly increased macrophage cytotoxicity against OS cells when dogs were treated with L-MTP-PE and doxorubicin.[51] A study of human macrophages showed *in vitro* anti-OS activity after macrophage stimulation with L-MTP-PE and IFN-γ.[145] The largest reported human clinical trial (INT 0133) to date that evaluated the efficacy of L-MTP-PE as one of the treatments in addition to standard chemotherapy did not initially show unequivocal advantage for event-free survival with the addition L-MTP-PE.[146] Subsequent analyses using overall survival as another endpoint demonstrated significantly increased 6-year survival with the addition of L-MTP-PE.[52] A recent analysis of the data from INT 0133 for lifetime effectiveness of adding L-MTP-PE to standard chemotherapy reported an increase in life-years gained for both non-metastatic and metastatic OS patients with the addition of L-MTP-PE.[147] The therapeutic potential of an anti-OS agent such as L-MTP-PE, which mimics the

effects of a bacterial infection, speaks to the importance of developing novel methods to stimulate macrophage anti-tumor activity against OS.

Dissertation Summary

The overall goal of this dissertation is to develop a foundation for understanding the monocyte and macrophage response to OS, bacteria-induced and hyperthermia therapy-induced inflammation to enhance our ability to develop novel immunotherapeutic strategies for monocyte/macrophage manipulation towards an anti-tumor phenotype. Comparing this response across species in the dog, human, and mouse wherever possible and identifying cross-species similarities and differences increases the robustness and therapeutic relevance of study findings. We hypothesize that bacteria-induced and hyperthermia therapy-induced inflammation reverses the immunosuppressive effects of OS on monocytes and macrophages, and induces an inflammatory anti-tumor phenotype in macrophages under the influence of OS. The biological similarity between canine and human OS makes such a cross-species comparative investigation a promising model for translational research, increasing the specificity and focus of follow-up studies. The additional strengths of using murine models include the ability to study the effects of bacterial-induced inflammation in an *in vivo* model. The goal of the first specific aim in this dissertation was to identify differences in monocyte phenotype and macrophage differentiation in OS compared to controls. The second specific aim then evaluated the influence of bacteria-induced inflammation on monocyte phenotype and macrophage differentiation in OS. The third specific aim evaluated the efficacy of a novel nanoparticle hyperthermia therapy in inducing an anti-OS response via

monocyte/macrophage activation. This dissertation seeks to add to the body of knowledge regarding phenotypic and functional profiles of monocytes and macrophages under the influence of OS, bacteria-induced inflammation, and hyperthermia therapy. These data will help build the foundation of knowledge required to investigate novel strategies for monocyte/macrophage immunomodulation in OS – utilizing microRNA (miRNA) manipulation and hyperthermia therapy to override OS-induced immunosuppression. Preliminary data will be presented on identification of commonly conserved microRNA signatures that influence monocyte/macrophage function in the presence of OS and bacteria.

REFERENCES

1. Friebele JC, Peck J, Pan X, et al. Osteosarcoma: A Meta-Analysis and Review of the Literature. *Am J Orthop (Belle Mead NJ)* 2015;44:547-553.

2. Fenger JM, London CA, Kisseberth WC. Canine osteosarcoma: a naturally occurring disease to inform pediatric oncology. *ILAR J* 2014;55:69-85.

3. He X, Gao Z, Xu H, et al. A meta-analysis of randomized control trials of surgical methods with osteosarcoma outcomes. *J Orthop Surg Res* 2017;12:5.

4. Mitchell KE, Boston SE, Kung M, et al. Outcomes of Limb-Sparing Surgery Using Two Generations of Metal Endoprosthesis in 45 Dogs With Distal Radial Osteosarcoma. A Veterinary Society of Surgical Oncology Retrospective Study. *Vet Surg* 2016;45:36-43.

5. Farese JP, Milner R, Thompson MS, et al. Stereotactic radiosurgery for treatment of osteosarcomas involving the distal portions of the limbs in dogs. *J Am Vet Med Assoc* 2004;225:1567-1572, 1548.

6. Kubicek L, Vanderhart D, Wirth K, et al. Association between Computed Tomographic Characteristics and Fractures Following Stereotactic Radiosurgery in Dogs with Appendicular Osteosarcoma. *Vet Radiol Ultrasound* 2016;57:321-330.

7. Ehrhart NR, S.; Fan, T. Tumors of the Skeletal System In: Vail DM, ed. *Withrow and MacEwen's Small Animal Clinical Oncology*. 5th ed: Saunders Elsevier, 2012;463-503.

8. Selmic LE, Burton JH, Thamm DH, et al. Comparison of carboplatin and doxorubicin-based chemotherapy protocols in 470 dogs after amputation for treatment of appendicular osteosarcoma. *J Vet Intern Med* 2014;28:554-563.

9. Alvarez FJ, Kisseberth W, Hosoya K, et al. Postoperative adjuvant combination therapy with doxorubicin and noncytotoxic suramin in dogs with appendicular osteosarcoma. *J Am Anim Hosp Assoc* 2014;50:12-18.

10. Meazza C, Scanagatta P. Metastatic osteosarcoma: a challenging multidisciplinary treatment. *Expert Rev Anticancer Ther* 2016.

11. Withrow SJ, Powers BE, Straw RC, et al. Comparative aspects of osteosarcoma. Dog versus man. *Clin Orthop Relat Res* 1991:159-168.

12. Paoloni M, Davis S, Lana S, et al. Canine tumor cross-species genomics uncovers targets linked to osteosarcoma progression. *BMC Genomics* 2009;10:625.

13. Mueller F, Fuchs B, Kaser-Hotz B. Comparative biology of human and canine osteosarcoma. *Anticancer Res* 2007;27:155-164.

14. Morello E, Martano M, Buracco P. Biology, diagnosis and treatment of canine appendicular osteosarcoma: similarities and differences with human osteosarcoma. *Vet J* 2011;189:268-277.

15. Rankin KS, Starkey M, Lunec J, et al. Of dogs and men: comparative biology as a tool for the discovery of novel biomarkers and drug development targets in osteosarcoma. *Pediatr Blood Cancer* 2012;58:327-333.

16. Gorlick R, Khanna C. Osteosarcoma. *J Bone Miner Res* 2010;25:683-691.

17. Bacci G, Longhi A, Versari M, et al. Prognostic factors for osteosarcoma of the extremity treated with neoadjuvant chemotherapy: 15-year experience in 789 patients treated at a single institution. *Cancer* 2006;106:1154-1161.

18. Phillips B, Powers BE, Dernell WS, et al. Use of single-agent carboplatin as adjuvant or neoadjuvant therapy in conjunction with amputation for appendicular osteosarcoma in dogs. *J Am Anim Hosp Assoc* 2009;45:33-38.

19. Lewis IJ, Nooij MA, Whelan J, et al. Improvement in histologic response but not survival in osteosarcoma patients treated with intensified chemotherapy: a randomized phase III trial of the European Osteosarcoma Intergroup. *J Natl Cancer Inst* 2007;99:112-128.

20. Boston SE, Ehrhart NP, Dernell WS, et al. Evaluation of survival time in dogs with stage III osteosarcoma that undergo treatment: 90 cases (1985-2004). *J Am Vet Med Assoc* 2006;228:1905-1908.

21. Boerman I, Selvarajah GT, Nielen M, et al. Prognostic factors in canine appendicular osteosarcoma - a meta-analysis. *BMC Vet Res* 2012;8:56.

22. Cho WH, Song WS, Jeon DG, et al. Differential presentations, clinical courses, and survivals of osteosarcomas of the proximal humerus over other extremity locations. *Ann Surg Oncol* 2010;17:702-708.

23. Lascelles BD, Dernell WS, Correa MT, et al. Improved survival associated with postoperative wound infection in dogs treated with limb-salvage surgery for osteosarcoma. *Ann Surg Oncol* 2005;12:1073-1083.

24. Jeys LM, Grimer RJ, Carter SR, et al. Post operative infection and increased survival in osteosarcoma patients: are they associated? *Ann Surg Oncol* 2007;14:2887-2895.

25. Culp WT, Olea-Popelka F, Sefton J, et al. Evaluation of outcome and prognostic factors for dogs living greater than one year after diagnosis of osteosarcoma: 90 cases (1997-2008). *J Am Vet Med Assoc* 2014;245:1141-1146.

26. Chen YU, Xu SF, Xu M, et al. Postoperative infection and survival in osteosarcoma patients: Reconsideration of immunotherapy for osteosarcoma. *Mol Clin Oncol* 2015;3:495-500.

27. Lee JA, Kim MS, Kim DH, et al. Postoperative infection and survival in osteosarcoma patients. *Ann Surg Oncol* 2009;16:147-151.

28. Klein MJ, Siegal GP. Osteosarcoma: anatomic and histologic variants. *Am J Clin Pathol* 2006;125:555-581.

29. Kirpensteijn J, Kik M, Rutteman GR, et al. Prognostic significance of a new histologic grading system for canine osteosarcoma. *Vet Pathol* 2002;39:240-246.

30. Loukopoulos P, Thornton JR, Robinson WF. Clinical and pathologic relevance of p53 index in canine osseous tumors. *Vet Pathol* 2003;40:237-248.

31. Wunder JS, Gokgoz N, Parkes R, et al. TP53 mutations and outcome in osteosarcoma: a prospective, multicenter study. *J Clin Oncol* 2005;23:1483-1490.

32. Gokgoz N, Wunder JS, Mousses S, et al. Comparison of p53 mutations in patients with localized osteosarcoma and metastatic osteosarcoma. *Cancer* 2001;92:2181-2189.

33. Ottaviani G, Jaffe N. The epidemiology of osteosarcoma. *Cancer Treat Res* 2009;152:3-13.

34. Angstadt AY, Motsinger-Reif A, Thomas R, et al. Characterization of canine osteosarcoma by array comparative genomic hybridization and RT-qPCR: signatures of genomic imbalance in canine osteosarcoma parallel the human counterpart. *Genes Chromosomes Cancer* 2011;50:859-874.

35. Freeman SS, Allen SW, Ganti R, et al. Copy number gains in EGFR and copy number losses in PTEN are common events in osteosarcoma tumors. *Cancer* 2008;113:1453-1461.

36. Thomas R, Wang HJ, Tsai PC, et al. Influence of genetic background on tumor karyotypes: evidence for breed-associated cytogenetic aberrations in canine appendicular osteosarcoma. *Chromosome Res* 2009;17:365-377.

37. Salinas-Souza C, De Oliveira R, Alves MT, et al. The metastatic behavior of osteosarcoma by gene expression and cytogenetic analyses. *Hum Pathol* 2013;44:2188-2198.

38. Stein TJ, Holmes KE, Muthuswamy A, et al. Characterization of beta-catenin expression in canine osteosarcoma. *Vet Comp Oncol* 2011;9:65-73.

39. Haydon RC, Deyrup A, Ishikawa A, et al. Cytoplasmic and/or nuclear accumulation of the beta-catenin protein is a frequent event in human osteosarcoma. *Int J Cancer* 2002;102:338-342.

40. Kansara M, Tsang M, Kodjabachian L, et al. Wnt inhibitory factor 1 is epigenetically silenced in human osteosarcoma, and targeted disruption accelerates osteosarcomagenesis in mice. *J Clin Invest* 2009;119:837-851.

41. Selvarajah GT, Kirpensteijn J, van Wolferen ME, et al. Gene expression profiling of canine osteosarcoma reveals genes associated with short and long survival times. *Mol Cancer* 2009;8:72.

42. Vega OA, Lucero CM, Araya HF, et al. Wnt/beta-catenin Signaling Activates Expression of the Bone-related Transcription Factor RUNX2 in Select Human Osteosarcoma Cell Types. *J Cell Biochem* 2017.

43. McIntyre JF, Smith-Sorensen B, Friend SH, et al. Germline mutations of the p53 tumor suppressor gene in children with osteosarcoma. *J Clin Oncol* 1994;12:925-930.

44. Phillips JC, Lembcke L, Chamberlin T. A novel locus for canine osteosarcoma (OSA1) maps to CFA34, the canine orthologue of human 3q26. *Genomics* 2010;96:220-227.

45. Dillberger JE, McAtee SA. Osteosarcoma inheritance in two families of Scottish deerhounds. *Canine Genet Epidemiol* 2017;4:3.

46. Karlsson EK, Sigurdsson S, Ivansson E, et al. Genome-wide analyses implicate 33 loci in heritable dog osteosarcoma, including regulatory variants near CDKN2A/B. *Genome Biol* 2013;14:R132.

47. Scott MC, Sarver AL, Gavin KJ, et al. Molecular subtypes of osteosarcoma identified by reducing tumor heterogeneity through an interspecies comparative approach. *Bone* 2011;49:356-367.

48. Rowell JL, McCarthy DO, Alvarez CE. Dog models of naturally occurring cancer. *Trends Mol Med* 2011;17:380-388.

49. Mirabello L, Troisi RJ, Savage SA. International osteosarcoma incidence patterns in children and adolescents, middle ages and elderly persons. *Int J Cancer* 2009;125:229-234.

50. MacEwen EG, Kurzman ID, Rosenthal RC, et al. Therapy for osteosarcoma in dogs with intravenous injection of liposome-encapsulated muramyl tripeptide. *J Natl Cancer Inst* 1989;81:935-938.

51. Kurzman ID, Shi F, Vail DM, et al. In vitro and in vivo enhancement of canine pulmonary alveolar macrophage cytotoxic activity against canine osteosarcoma cells. *Cancer Biother Radiopharm* 1999;14:121-128.

52. Meyers PA, Schwartz CL, Krailo MD, et al. Osteosarcoma: the addition of muramyl tripeptide to chemotherapy improves overall survival--a report from the Children's Oncology Group. *J Clin Oncol* 2008;26:633-638.

53. Italiani P, Boraschi D. From Monocytes to M1/M2 Macrophages: Phenotypical vs. Functional Differentiation. *Front Immunol* 2014;5:514.

54. Lin H, Lee E, Hestir K, et al. Discovery of a cytokine and its receptor by functional screening of the extracellular proteome. *Science* 2008;320:807-811.

55. van Furth R, Cohn ZA. The origin and kinetics of mononuclear phagocytes. *J Exp Med* 1968;128:415-435.

56. Sieweke MH, Allen JE. Beyond stem cells: self-renewal of differentiated macrophages. *Science* 2013;342:1242974.

57. Schulz C, Gomez Perdiguero E, Chorro L, et al. A lineage of myeloid cells independent of Myb and hematopoietic stem cells. *Science* 2012;336:86-90.

58. Bain CC, Scott CL, Uronen-Hansson H, et al. Resident and pro-inflammatory macrophages in the colon represent alternative context-dependent fates of the same Ly6Chi monocyte precursors. *Mucosal Immunol* 2013;6:498-510.

59. Varol C, Vallon-Eberhard A, Elinav E, et al. Intestinal lamina propria dendritic cell subsets have different origin and functions. *Immunity* 2009;31:502-512.

60. Ziegler-Heitbrock L, Ancuta P, Crowe S, et al. Nomenclature of monocytes and dendritic cells in blood. *Blood* 2010;116:e74-80.

61. Wong KL, Yeap WH, Tai JJ, et al. The three human monocyte subsets: implications for health and disease. *Immunol Res* 2012;53:41-57.

62. Tsou CL, Peters W, Si Y, et al. Critical roles for CCR2 and MCP-3 in monocyte mobilization from bone marrow and recruitment to inflammatory sites. *J Clin Invest* 2007;117:902-909.

63. Ingersoll MA, Spanbroek R, Lottaz C, et al. Comparison of gene expression profiles between human and mouse monocyte subsets. *Blood* 2010;115:e10-19.

64. Auffray C, Fogg D, Garfa M, et al. Monitoring of blood vessels and tissues by a population of monocytes with patrolling behavior. *Science* 2007;317:666-670.

65. Yona S, Kim KW, Wolf Y, et al. Fate mapping reveals origins and dynamics of monocytes and tissue macrophages under homeostasis. *Immunity* 2013;38:79-91.

66. Serbina NV, Jia T, Hohl TM, et al. Monocyte-mediated defense against microbial pathogens. *Annu Rev Immunol* 2008;26:421-452.

67. Jakubzick C, Gautier EL, Gibbings SL, et al. Minimal differentiation of classical monocytes as they survey steady-state tissues and transport antigen to lymph nodes. *Immunity* 2013;39:599-610.

68. Carlin LM, Stamatiades EG, Auffray C, et al. Nr4a1-dependent Ly6C(low) monocytes monitor endothelial cells and orchestrate their disposal. *Cell* 2013;153:362-375.

69. Cros J, Cagnard N, Woollard K, et al. Human CD14dim monocytes patrol and sense nucleic acids and viruses via TLR7 and TLR8 receptors. *Immunity* 2010;33:375-386.

70. Epelman S, Lavine KJ, Randolph GJ. Origin and functions of tissue macrophages. *Immunity* 2014;41:21-35.

71. Martinez FO, Sica A, Mantovani A, et al. Macrophage activation and polarization. *Front Biosci* 2008;13:453-461.

72. Mylonas KJ, Nair MG, Prieto-Lafuente L, et al. Alternatively activated macrophages elicited by helminth infection can be reprogrammed to enable microbial killing. *J Immunol* 2009;182:3084-3094.

73. Italiani P, Mazza EM, Lucchesi D, et al. Transcriptomic profiling of the development of the inflammatory response in human monocytes in vitro. *PLoS One* 2014;9:e87680.

74. Mills CD, Kincaid K, Alt JM, et al. M-1/M-2 macrophages and the Th1/Th2 paradigm. *J Immunol* 2000;164:6166-6173.

75. Unanue ER. Antigen-presenting function of the macrophage. *Annu Rev Immunol* 1984;2:395-428.

76. Ley K. The second touch hypothesis: T cell activation, homing and polarization. *F1000Res* 2014;3:37.

77. Goswami KK, Ghosh T, Ghosh S, et al. Tumor promoting role of anti-tumor macrophages in tumor microenvironment. *Cell Immunol* 2017.

78. Mantovani A, Bottazzi B, Colotta F, et al. The origin and function of tumor-associated macrophages. *Immunol Today* 1992;13:265-270.

79. Movahedi K, Van Ginderachter JA. The Ontogeny and Microenvironmental Regulation of Tumor-Associated Macrophages. *Antioxid Redox Signal* 2016;25:775-791.

80. Franklin RA, Liao W, Sarkar A, et al. The cellular and molecular origin of tumor-associated macrophages. *Science* 2014;344:921-925.

81. Mantovani A, Marchesi F, Malesci A, et al. Tumour-associated macrophages as treatment targets in oncology. *Nat Rev Clin Oncol* 2017.

82. Hanna RN, Cekic C, Sag D, et al. Patrolling monocytes control tumor metastasis to the lung. *Science* 2015;350:985-990.

83. Mantovani A, Allavena P, Sica A, et al. Cancer-related inflammation. *Nature* 2008;454:436-444.

84. Noy R, Pollard JW. Tumor-associated macrophages: from mechanisms to therapy. *Immunity* 2014;41:49-61.

85. Biswas SK, Mantovani A. Macrophage plasticity and interaction with lymphocyte subsets: cancer as a paradigm. *Nat Immunol* 2010;11:889-896.

86. Schmidt T, Carmeliet P. Blood-vessel formation: Bridges that guide and unite. *Nature* 2010;465:697-699.

87. Vesely MD, Kershaw MH, Schreiber RD, et al. Natural innate and adaptive immunity to cancer. *Annu Rev Immunol* 2011;29:235-271.

88. Wyckoff J, Wang W, Lin EY, et al. A paracrine loop between tumor cells and macrophages is required for tumor cell migration in mammary tumors. *Cancer Res* 2004;64:7022-7029.

89. Condeelis J, Pollard JW. Macrophages: obligate partners for tumor cell migration, invasion, and metastasis. *Cell* 2006;124:263-266.

90. Yamaguchi H, Pixley F, Condeelis J. Invadopodia and podosomes in tumor invasion. *Eur J Cell Biol* 2006;85:213-218.

91. Vinnakota K, Zhang Y, Selvanesan BC, et al. M2-like macrophages induce colon cancer cell invasion via matrix metalloproteinases. *J Cell Physiol* 2017.

92. Lin EY, Pollard JW. Tumor-associated macrophages press the angiogenic switch in breast cancer. *Cancer Res* 2007;67:5064-5066.

93. Bergers G, Benjamin LE. Tumorigenesis and the angiogenic switch. *Nat Rev Cancer* 2003;3:401-410.

94. Yeo EJ, Cassetta L, Qian BZ, et al. Myeloid WNT7b mediates the angiogenic switch and metastasis in breast cancer. *Cancer Res* 2014;74:2962-2973.

95. Mazzieri R, Pucci F, Moi D, et al. Targeting the ANG2/TIE2 axis inhibits tumor growth and metastasis by impairing angiogenesis and disabling rebounds of proangiogenic myeloid cells. *Cancer Cell* 2011;19:512-526.

96. Forget MA, Voorhees JL, Cole SL, et al. Macrophage colony-stimulating factor augments Tie2-expressing monocyte differentiation, angiogenic function, and recruitment in a mouse model of breast cancer. *PLoS One* 2014;9:e98623.

97. Kalluri R, Weinberg RA. The basics of epithelial-mesenchymal transition. *J Clin Invest* 2009;119:1420-1428.

98. Bonde AK, Tischler V, Kumar S, et al. Intratumoral macrophages contribute to epithelial-mesenchymal transition in solid tumors. *BMC Cancer* 2012;12:35.

99. Liu CY, Xu JY, Shi XY, et al. M2-polarized tumor-associated macrophages promoted epithelial-mesenchymal transition in pancreatic cancer cells, partially through TLR4/IL-10 signaling pathway. *Lab Invest* 2013;93:844-854.

100. Pello OM, De Pizzol M, Mirolo M, et al. Role of c-MYC in alternative activation of human macrophages and tumor-associated macrophage biology. *Blood* 2012;119:411-421.

101. Casey SC, Tong L, Li Y, et al. MYC regulates the antitumor immune response through CD47 and PD-L1. *Science* 2016;352:227-231.

102. Hartley G, Faulhaber E, Caldwell A, et al. Immune regulation of canine tumour and macrophage PD-L1 expression. *Vet Comp Oncol* 2017;15:534-549.

103. Duraiswamy J, Freeman GJ, Coukos G. Therapeutic PD-1 pathway blockade augments with other modalities of immunotherapy T-cell function to prevent immune decline in ovarian cancer. *Cancer Res* 2013;73:6900-6912.

104. Belai EB, de Oliveira CE, Gasparoto TH, et al. PD-1 blockage delays murine squamous cell carcinoma development. *Carcinogenesis* 2014;35:424-431.

105. Kubota K, Moriyama M, Furukawa S, et al. CD163+CD204+ tumor-associated macrophages contribute to T cell regulation via interleukin-10 and PD-L1 production in oral squamous cell carcinoma. *Sci Rep* 2017;7:1755.

106. Chong H, Vodovotz Y, Cox GW, et al. Immunocytochemical localization of latent transforming growth factor-beta1 activation by stimulated macrophages. *J Cell Physiol* 1999;178:275-283.

107. Ng TH, Britton GJ, Hill EV, et al. Regulation of adaptive immunity; the role of interleukin-10. *Front Immunol* 2013;4:129.

108. Oh SA, Li MO. TGF-beta: guardian of T cell function. *J Immunol* 2013;191:3973-3979.

109. Sharda DR, Yu S, Ray M, et al. Regulation of macrophage arginase expression and tumor growth by the Ron receptor tyrosine kinase. *J Immunol* 2011;187:2181-2192.

110. Rodriguez PC, Quiceno DG, Zabaleta J, et al. Arginase I production in the tumor microenvironment by mature myeloid cells inhibits T-cell receptor expression and antigen-specific T-cell responses. *Cancer Res* 2004;64:5839-5849.

111. Kryczek I, Wei S, Zou L, et al. Cutting edge: induction of B7-H4 on APCs through IL-10: novel suppressive mode for regulatory T cells. *J Immunol* 2006;177:40-44.

112. Chen C, Zhu YB, Shen Y, et al. Increase of circulating B7-H4-expressing CD68+ macrophage correlated with clinical stage of lung carcinomas. *J Immunother* 2012;35:354-358.

113. Jinushi M, Chiba S, Yoshiyama H, et al. Tumor-associated macrophages regulate tumorigenicity and anticancer drug responses of cancer stem/initiating cells. *Proc Natl Acad Sci U S A* 2011;108:12425-12430.

114. Mitchem JB, Brennan DJ, Knolhoff BL, et al. Targeting tumor-infiltrating macrophages decreases tumor-initiating cells, relieves immunosuppression, and improves chemotherapeutic responses. *Cancer Res* 2013;73:1128-1141.

115. Joyce JA, Pollard JW. Microenvironmental regulation of metastasis. *Nat Rev Cancer* 2009;9:239-252.

116. Kaplan RN, Riba RD, Zacharoulis S, et al. VEGFR1-positive haematopoietic bone marrow progenitors initiate the pre-metastatic niche. *Nature* 2005;438:820-827.

117. Hiratsuka S, Nakamura K, Iwai S, et al. MMP9 induction by vascular endothelial growth factor receptor-1 is involved in lung-specific metastasis. *Cancer Cell* 2002;2:289-300.

118. Psaila B, Lyden D. The metastatic niche: adapting the foreign soil. *Nat Rev Cancer* 2009;9:285-293.

119. Peinado H, Aleckovic M, Lavotshkin S, et al. Melanoma exosomes educate bone marrow progenitor cells toward a pro-metastatic phenotype through MET. *Nat Med* 2012;18:883-891.

120. Qian BZ, Li J, Zhang H, et al. CCL2 recruits inflammatory monocytes to facilitate breast-tumour metastasis. *Nature* 2011;475:222-225.

121. Zhang QW, Liu L, Gong CY, et al. Prognostic significance of tumor-associated macrophages in solid tumor: a meta-analysis of the literature. *PLoS One* 2012;7:e50946.

122. Welsh TJ, Green RH, Richardson D, et al. Macrophage and mast-cell invasion of tumor cell islets confers a marked survival advantage in non-small-cell lung cancer. *J Clin Oncol* 2005;23:8959-8967.

123. Evans R, Alexander P. Cooperation of immune lymphoid cells with macrophages in tumour immunity. *Nature* 1970;228:620-622.

124. Adams DO, Hamilton TA. The cell biology of macrophage activation. *Annu Rev Immunol* 1984;2:283-318.

125. Casares N, Pequignot MO, Tesniere A, et al. Caspase-dependent immunogenicity of doxorubicin-induced tumor cell death. *J Exp Med* 2005;202:1691-1701.

126. Kridel R, Xerri L, Gelas-Dore B, et al. The Prognostic Impact of CD163-Positive Macrophages in Follicular Lymphoma: A Study from the BC Cancer Agency and the Lymphoma Study Association. *Clin Cancer Res* 2015;21:3428-3435.

127. Di Caro G, Cortese N, Castino GF, et al. Dual prognostic significance of tumour-associated macrophages in human pancreatic adenocarcinoma treated or untreated with chemotherapy. *Gut* 2016;65:1710-1720.

128. Xiao Q, Zhang X, Wu Y, et al. Inhibition of macrophage polarization prohibits growth of human osteosarcoma. *Tumour Biol* 2014;35:7611-7616.

129. Han Q, Shi H, Liu F. CD163(+) M2-type tumor-associated macrophage support the suppression of tumor-infiltrating T cells in osteosarcoma. *Int Immunopharmacol* 2016;34:101-106.

130. Koirala P, Roth ME, Gill J, et al. Immune infiltration and PD-L1 expression in the tumor microenvironment are prognostic in osteosarcoma. *Sci Rep* 2016;6:30093.

131. Buddingh EP, Kuijjer ML, Duim RA, et al. Tumor-infiltrating macrophages are associated with metastasis suppression in high-grade osteosarcoma: a rationale for treatment with macrophage activating agents. *Clin Cancer Res* 2011;17:2110-2119.

132. Dumars C, Ngyuen JM, Gaultier A, et al. Dysregulation of macrophage polarization is associated with the metastatic process in osteosarcoma. *Oncotarget* 2016;7:78343-78354.

133. Segaliny AI, Mohamadi A, Dizier B, et al. Interleukin-34 promotes tumor progression and metastatic process in osteosarcoma through induction of angiogenesis and macrophage recruitment. *Int J Cancer* 2015;137:73-85.

134. McCarthy EF. The toxins of William B. Coley and the treatment of bone and soft-tissue sarcomas. *Iowa Orthop J* 2006;26:154-158.

135. Wiemann B, Starnes CO. Coley's toxins, tumor necrosis factor and cancer research: a historical perspective. *Pharmacol Ther* 1994;64:529-564.

136. Carswell EA, Old LJ, Kassel RL, et al. An endotoxin-induced serum factor that causes necrosis of tumors. *Proc Natl Acad Sci U S A* 1975;72:3666-3670.

137. Thrall DE, Withrow SJ, Powers BE, et al. Radiotherapy prior to cortical allograft limb sparing in dogs with osteosarcoma: a dose response assay. *Int J Radiat Oncol Biol Phys* 1990;18:1351-1357.

138. Boston SE, Vinayak A, Lu X, et al. Outcome and complications in dogs with appendicular primary bone tumors treated with stereotactic radiotherapy and concurrent surgical stabilization. *Vet Surg* 2017.

139. Behnke NK, Alamanda VK, Song Y, et al. Does postoperative infection after soft tissue sarcoma resection affect oncologic outcomes? *J Surg Oncol* 2014;109:415-420.

140. Sottnik JL, U'Ren LW, Thamm DH, et al. Chronic bacterial osteomyelitis suppression of tumor growth requires innate immune responses. *Cancer Immunol Immunother* 2010;59:367-378.

141. da Silveira Nogueira Lima JP, Georgieva M, Haaland B, et al. A systematic review and network meta-analysis of immunotherapy and targeted therapy for advanced melanoma. *Cancer Med* 2017.

142. Shaw MH, Reimer T, Kim YG, et al. NOD-like receptors (NLRs): bona fide intracellular microbial sensors. *Curr Opin Immunol* 2008;20:377-382.

143. Kager L, Potschger U, Bielack S. Review of mifamurtide in the treatment of patients with osteosarcoma. *Ther Clin Risk Manag* 2010;6:279-286.

144. Kurzman ID, MacEwen EG, Rosenthal RC, et al. Adjuvant therapy for osteosarcoma in dogs: results of randomized clinical trials using combined liposome-encapsulated muramyl tripeptide and cisplatin. *Clin Cancer Res* 1995;1:1595-1601.

145. Pahl JH, Kwappenberg KM, Varypataki EM, et al. Macrophages inhibit human osteosarcoma cell growth after activation with the bacterial cell wall derivative liposomal muramyl tripeptide in combination with interferon-gamma. *J Exp Clin Cancer Res* 2014;33:27.

146. Meyers PA, Schwartz CL, Krailo M, et al. Osteosarcoma: a randomized, prospective trial of the addition of ifosfamide and/or muramyl tripeptide to cisplatin, doxorubicin, and high-dose methotrexate. *J Clin Oncol* 2005;23:2004-2011.

147. Song HJ, Lee JA, Han E, et al. Lifetime effectiveness of mifamurtide addition to chemotherapy in nonmetastatic and metastatic osteosarcoma: a Markov process model analysis. *Tumour Biol* 2015;36:6773-6779.

CHAPTER 2

A cross-species evaluation of the effects of OS on monocytes and macrophages

2.1 Introduction

Of the many similarities between human and canine OS, perhaps the most dismal is the lack of significant improvement in survival over the past three decades. Despite attempts with various permutations of adjunctive chemotherapeutics, the median survival in dogs with OS remains between 10-12 months, and the 5-year disease-free interval for human patients with non-metastatic OS remains around 70%, with only 20-30% long-term survival in patients that present with metastases.[1-4] Therefore, it is imperative to identify unique avenues of investigation for the treatment of OS, and one of these avenues is immunotherapy. However, despite the rapid development of cancer immunotherapy for malignancies such as melanoma and non-small cell lung cancer, there is a lack of advancement in immunotherapies for OS, despite data indicating the immunogenicity OS.[5-9]

One of the hurdles to immunotherapy development in OS is the scarcity of information concerning the effects of OS on myeloid cells in sarcoma patients, despite observations suggesting that monocytes and macrophages are key players in shaping the immune environment in OS.[10-14] An evaluation of the immune profile in human pediatric sarcoma patients demonstrated an increase in $CD14^{+}HLA\text{-}DR^{lo/neg}$ immunosuppressive peripheral monocytes in sarcoma patients compared to healthy controls, and this abnormal monocyte profile was associated with poorer survival.[10] This subtype of $CD14^{+}HLA\text{-}DR^{lo/neg}$ monocytes has been shown to inhibit an effective immune response in cancers such as glioblastoma, lymphoma, and prostate cancer.[15-17] Interestingly, increased infiltration of

M1/M2 TAMs was associated with improved survival in high-grade human OS, though individual M1 or M2 phenotypes did not exhibit survival associations, thus the heterogeneous TAM population precluded conclusions about the anti-tumor mechanism.[14] An *in vitro* study demonstrated the ability of L-MTP-PE combined with IFN-γ to stimulate anti-tumor activity in macrophages against human OS cell lines.[11] Using a murine model of OS, a study showed that M1 macrophages within the tumor were polarized into M2-like TAMs within the first 3 weeks after tumor implantations, and depletion of TAMs using clodronate resulted in reduced tumor growth. A murine model of OS that documented improved survival with chronic bacterial osteomyelitis demonstrated increased numbers of TAMs in OS mice with osteomyelitis compared to uninfected OS mice, and an increase in total numbers of circulating monocytes caused by an increase specifically in the inflammatory monocyte compartment.[13] These data strongly support monocytes and macrophages as cells that modulate the immune response in OS, both in a pro-tumorigenic and anti-tumor fashion. Therefore, more data are needed to understand the effects of OS on immunomodulatory cells such as monocytes and macrophages to inform future investigations into reversing tumor-induced immune dysfunction. This chapter describes how OS influences the phenotype and chemotaxis of monocytes and differentiation of macrophages across species. Comparisons were made between the dog, human, and mouse, wherever possible, to increase the relevance of the findings. Our hypothesis was that evasion of the immune response by OS is due in part to expansion of the non-classical / alternatively activated monocyte subtype, down-regulation of monocyte chemokine receptor expression and migratory function, and suppression of host

immune responses as demonstrated by an immunosuppressive cytokine and mRNA signature in monocytes and macrophages.

Such cross-species comparison to expand our understanding of the immune environment in OS adds robustness to the results, and hones the focus for therapeutic target identification.

2.2. Materials and Methods

Monocyte Studies

2.2.1 Patient enrollment – canine and human

Canine monocyte samples: Client-owned dogs diagnosed with OS that had not received any tumor-directed therapy or immunomodulatory drugs were enrolled into the study at North Carolina State University (NCSU). Due to the enrollment of dogs at a tertiary referral center, some dogs with OS had been prescribed anti-inflammatory medications by their primary referring veterinarian. A similar population of age-matched medium and large-breed control dogs without known disease that were also not receiving any anti-inflammatory or immunomodulatory medications were recruited for the study as normal controls. Written owner consent was obtained for all dogs participating in the study, and peripheral blood samples were collected under an approved Institutional Animal Care and Use Committee (IACUC) protocol.

Human monocyte samples: Human patients newly diagnosed with OS were enrolled into the study at the Duke University Cancer Center by the Orthopedic Oncology service. Some of the enrolled patients had received neoadjuvant chemotherapy prior to starting the

study. A similar population of healthy human volunteers between the ages of 18 and 35 years were recruited as normal controls. Written consent was obtained for all humans participating in the study, and peripheral blood samples were collected under an approved Institutional Review Board (IRB) protocol.

2.2.2 Isolation of peripheral blood mononuclear cells (PBMCs) and of a purified monocyte population – canine and human

Approximately 20 ml of peripheral blood were collected into EDTA blood collection tubes via venipuncture from 14 control dogs and 18 dogs with OS, and 14 control human volunteers and 15 humans with OS. Canine and human peripheral blood mononuclear cells (PBMCs) were isolated by density gradient centrifugation using Histopaque®-1077. A portion of the canine PBMCs was preserved for cell surface staining, and a portion underwent cell sorting to isolate a purified monocyte population using a MoFlo® high-speed cell sorter. Monocyte cell isolation was performed based on forward (FSC) versus side scatter (SSC), and CD14+ expression, and the phenotype of the sorted monocytes were confirmed via light microscopy. Approximately 1 x 10^6 sorted monocytes from 7 healthy controls and 7 dogs with OS were centrifuged and resuspended in RNAprotect® cell reagent for PCR analysis. Sorted monocytes from 8 healthy controls and 7 dogs with OS were used for stimulation cultures, and sorted monocytes from 14 healthy controls and 5 dogs with OS were used for chemotaxis assays.

2.2.3 Murine models of OS

Syngeneic subcutaneous (SQ) OS model: A SQ syngeneic OS model was established in C3H-HeN mice with a subcutaneous injection of 2 x 10^8 DLM8 murine OS cells suspended in 30 µl HBSS into the right flank region.

Orthotopic OS model: An orthotopic OS model was established using Cre-LoxP recombination to generate tumors. In a modification of a previously described method, the Cre recombinase, enclosed in an adenovirus, was injected to induce OS formation via deletion of the floxed alleles (Rb and p53).[18]

2.2.4 Flow cytometry (FACS)

Canine and human monocytes: PBMCs from healthy controls and patients with OS were centrifuged, resuspended in 100 µl Phosphate-Buffered Saline (PBS) per tube, then stained with the following antibodies against cell surface receptors:

Canine monocytes: anti-CD14 (AbDSerotec), anti-CD16 (AbCam), anti- CD62L (BD BioSciences), anti-CD32 (AbCam), anti-CD11c (Thermo Scientific), anti-CCR2 (Bioss), anti-CCR7 (Bioss), anti- CD43 (Bioss), anti-CX3CR1 (Bioss), and anti-CXCR2 (Bioss). (Table 1)

Human monocytes: anti-CD14 (AbDSerotec), anti-CD16 (AbCam), anti- CD62L (BD BioSciences), anti-CD32 (AbCam), anti-CD11c (Thermo Scientific), anti-CCR2 (BioLegend), anti-CCR7 (BioLegend), anti- CD43 (Bioss), anti-CX3CR1 (eBioscience), and anti-CXCR2 (eBioscience), anti-CD163 (BD Pharmigen), anti-HLA-DR (BD Pharmigen), anti-CD64 (R&D), and anti-CD115 (eBioscience). (Table 2)

A tube containing unstained cells served as a negative control, and the appropriate isotype controls were applied. Single color compensation controls were established at the start of these experiments. The stained cells were incubated for 20 minutes on a shaker at low-speed, in the dark, at room temperature, after which the cells were washed twice with PBS. A FacsCaliber® or a LSRII® flow cytometer was used to perform FACS analysis. The canine data were analyzed using the accompanying Cell-Quest™ software, and the human data were analyzed using the Kaluza® software. Monocytes were gated based on FSC and SSC (Fig 1a), and gates for determining the percentage of monocytes that stained positive for antibody were set using isotype controls as guidelines.

Murine monocytes: Blood was collected from the mice at time of euthanasia using cardiac puncture, and the blood lysed with 1x RBC lysis buffer to remove the red blood cells. The cells were washed with 1x PBS and resuspended in 100 µl FACS buffer (1X HBSS with 2% FBS) per tube for staining with the following antibodies against cell surface receptors: anti-CD11b (BioLegend), anti-Ly6C (BioLegend), anti-Ly6G (eBioscience), anti-CCR2 (R&D), anti-CCR7 (eBioscience), anti-CXCR2 (BioLegend), anti-CXCR4 (BD BioSciences), anti-CX3CR1 (BioLegend), anti-CD62L (eBioscience). Normal donkey serum was added to the FACS buffer for blocking against non-specific staining. Monocytes were gated based on forward and side scatter, and on positive expression of CD11b, Ly6C, with negative expression of Ly6G. (Fig. 1b) Monocytes were further gated into subsets based on intensity of Ly6C expression, namely classical ($Ly6C^{hi}$) and non-classical ($Ly6C^{lo}$) monocytes. (Fig. 1c) The cells were stained with antibodies at 2-8°C for 30 minutes, after

which they were washed with FACS buffer and analyzed immediately. Samples were analyzed using a LSRII flow cytometer and data analysis was performed using Kaluza® software. Single color controls and compensation were performed using compensation beads, and positively staining cells were gated based on fluorescence-minus-one (FMO) cellular controls.

Table 1: List of antibodies used for canine flow cytometry

Antibodies	Clone	Fluorescence Labeling
CD14	TÜK4	APC, FITC
CD16	LNK16	PE
CD62L	SK11	PE
CD32	AT10	FITC
CD11c	BU15	FITC
CCR2	Polyclonal	FITC
CCR7	Polyclonal	FITC
CD43	Polyclonal	FITC
CX3CR1	Polyclonal	FITC
CXCR2	Polyclonal	FITC

Table 2: List of antibodies used for human flow cytometry

Antibodies	Clone	Fluorescence Labeling
CD14	TÜK4	APC, FITC
CD16	LNK16	PE
CD62L	SK11	PE
CD32	AT10	FITC
CD11c	BU15	FITC
CD43	Polyclonal	FITC
CD163	GHI/61	PE
CCR2	K036C2	BV510
CCR7	G043H7	BV421
CXCR2	5E8-C7-F10	PerCP-eFluor710
CX3CR1	2A9-1	APC
HLA-DR	G46-6	FITC
CD64	276426	APC
CD115	12-3A3-1B10	PE-Cy7

Table 3: List of antibodies used for murine flow cytometry

Antibodies	Clone	Fluorescence Labeling
CD11b	M1/70	BV421
Ly6C	HK1.4	BV570
Ly6G	1A8	FITC
CCR2	475301	AF-700
CXCR2	SA044G4	PE
CCR7	4B12	PE
CXCR4	2B11	AF700
CX3CR1	SA011F11	PE
CD62L	MEL-14	AF700

Figure 1: **Gating strategies for monocyte flow cytometry**

(a) Canine and human gating: Representative dot plot showing monocyte gating using forward and side scatter characteristics. CD14 staining was used to ensure that the majority of the gated monocytes exhibited positive CD14 cell surface expression. (b), (c) Murine gating: Representative dot plots showing monocyte (including neutrophils) gating using forward and side scatter characteristics (b, left), exclusion gating of neutrophils using Ly6G (neutrophils being Ly6G+) (b, right); gating of CD11b+ monocyte subsets into $Ly6C^{hi}$ and $Ly6C^{lo}$ subsets (c).

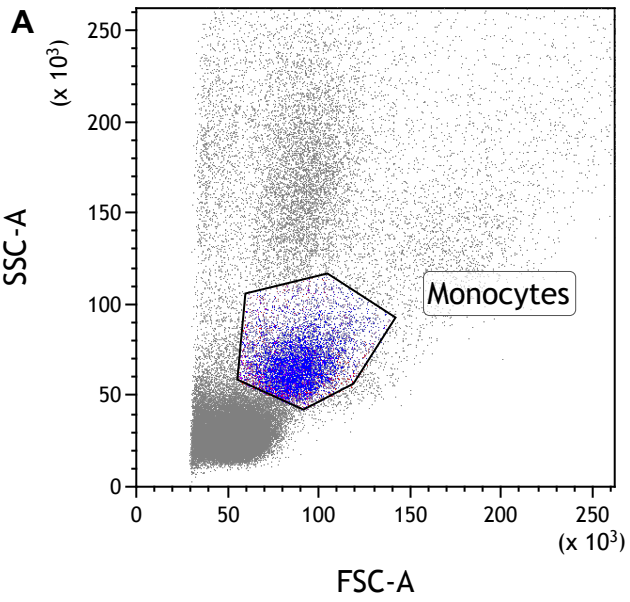
A
SSC-A
(x 10³)
250
200
150
100
50
0
0
50
100
150
200
250
(x 10³)
FSC-A
Monocytes

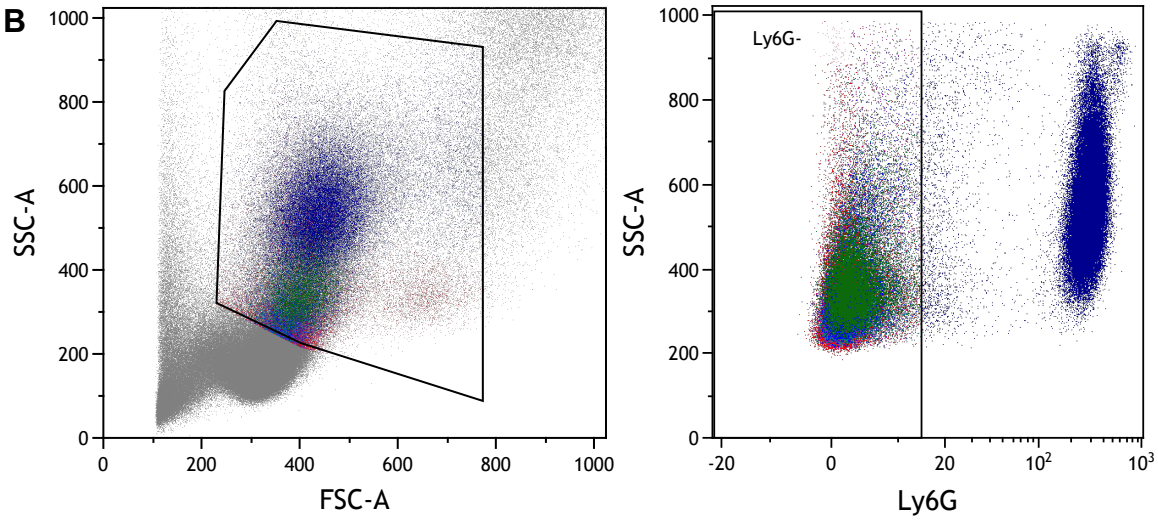
B
SSC-A
1000
800
600
400
200
0
0
200
400
600
800
1000
FSC-A
Ly6G-
-20
0
20
10²
10³
Ly6G

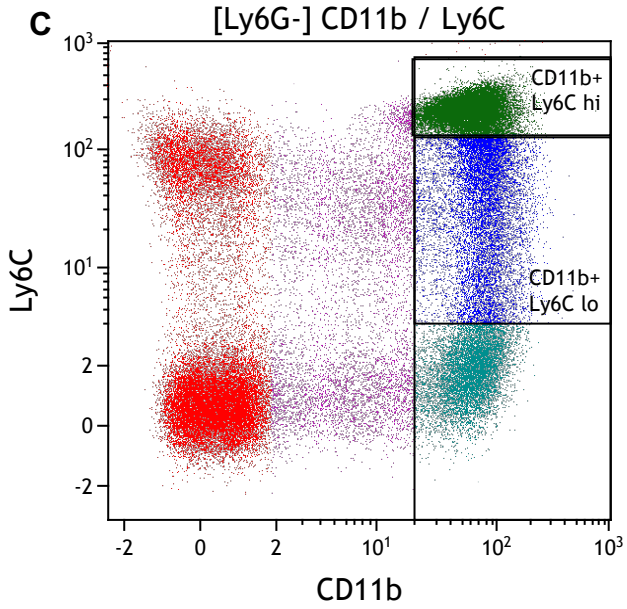
C
[Ly6G-] CD11b / Ly6C
CD11b+
Ly6C hi
CD11b+
Ly6C lo
Ly6C
CD11b
10^3
10^2
10^1
2
0
-2
-2
0
2
10^1
10^2
10^3

2.2.5 Total RNA extraction, reverse transcription, and quantitative RT-PCR

Canine monocytes: Sorted monocytes from healthy controls and dogs with OS were used for PCR analysis. The RNeasy minikit (Qiagen) was used to extract total RNA for quantitative RT-PCR (qPCR) from the sorted monocytes according to the manufacturer's protocol. We verified the quality and quantity of the purified RNA using a NanoDrop 2000c spectrophotometer (Thermo Scientific), and also used gel electrophoresis to confirm RNA quality. cDNA was subsequently synthesized in a Techne TC4000 (Bibby Scientific) thermal cycler using the Promega© RT kit (Promega) according to manufacturer's directions. Primers for qPCR to detect mRNA expression levels of Interleukin-10 (IL-10), Interleukin-12 (IL-12), Tumor Necrosis Factor-alpha (TNF-α), and Cyclooxygenase-2 (COX-2) were selected based on previous reports (Table 4),[19,20] and purchased from Integrated DNA Technologies. The PerfeCTa® SYBR® Green FastMix® for iQ™ PCR kit (Quanta BioSciences) was used for mRNA expression detection, and the reactions performed with the iCycler iQ™ real-time PCR detection system (BioRad). All samples were run in triplicate. The thermal cycling conditions were as follows: cycle 1 (95.0°C for 8 minutes) 1X, cycle 2 (95.0°C for 30 seconds, 56.0°C for 20 seconds, 72.0°C for 40 seconds) 40X, cycle 3 (melting curve starting at 60.0°C for 10 seconds, with stepwise increases of 0.5°C for 70X to achieve 95°C), cycle 4 (hold at 4.0°C). The housekeeping gene, Glyceraldehyde-3-Phosphate Dehydrogenase (GAPDH), was used for normalization of results. The CT value of GAPDH was consistent across experiments and between animals for all PCR results reported here (CT ~21). The PCR product was separated using agarose gel electrophoresis, the DNA was sequenced by GENEWIZ® DNA sequencing services, and the sequences were subjected to

alignment searches in the NCBI database to confirm matches with the gene of interest. The $2^{-\Delta\Delta CT}$ method was used to derive the normalized relative mRNA expression level of the target genes.

Table 4: **Quantitative RT-PCR primers to detect mRNA expression levels of pro-inflammatory and anti-inflammatory cytokines, and COX-2, in canine monocytes**

Target	(5' – 3')
IL-10 (F)	GCGACGCTGTCACCGATT
IL-10 (R)	CTGGAGCTTACTAAATGCGCTCTT
IL-12 (F)	TGGCTGCTATTCACAAGCTCAAGT
IL-12(R)	TGGTTTGATGATGTCTCTGATGAAG
TNF-α (F)	AGCCAGTAGCTCATGTTGTAGCAA
TNF-α (R)	GGCACTATCAGCTGGTTGTCTGT
COX-2 (F)	CTGTTCCCACCCATGTCAA
COX-2 (R)	GCAGTTTTCGCCGTAGAATC

2.2.6 Chemotaxis assay

Canine monocytes: Sorted monocytes from healthy controls and dogs with OS were used for chemotaxis assays. Monocyte migration was assessed using a NeuroProbe ChemoTx® 96-well disposable cell migration system with 8 μm polycarbonate framed filters. Sorted monocytes were resuspended in 10^6/ml of cell culture media, labeled with 1 μg calcein-AM/10^6 monocytes, and the cells incubated for 30 minutes in the dark at room temperature. Following incubation, the cells were resuspended at 10^6/ml in Dulbecco's Modified Eagle Medium (DMEM). Twenty-five μl of the cell suspension were deposited on each filter. The lower chamber, i.e. the 96-well plate, contained the following: 100% heat-inactivated fetal bovine serum (FBS), 100 ng/ml monocyte chemoattractant protein-1 (MCP-

1), 100nM N-Formyl-L-Methionyl-L-Leucyl-L-Phenylalanine (fMLP), 100 ng/ml CCL19 as positive chemoattractants, and PBS as a negative control. The positive chemoattractants were either placed individually in separate wells, or combined together in a single well. For total cell counts, 25 µl of cells were placed directly into the lower well to quantify maximal fluorescence. The plate was incubated for 4 hours at 37°C, after which the non-migrated cells on top of the filters were gently wiped off using a cell scraper. Cellular fluorescence in the bottom wells was quantified using a fMax fluorescence microplate reader (Molecular Devices) at 485 and 538 nm wavelength, and the corresponding SoftMax Pro® software. Filter fluorescence was also quantified to confirm that cells were not adherent to the underside of the filter. Degree of migration was calculated as a percentage of migrated cells out of the known cell numbers placed in bottom wells. Cell migration was expressed as a migration index, calculated by dividing directed cell chemotaxis (cells migrating in response to a chemokine, quantified by degree of fluorescence) by random cell chemotaxis (cells migrating in response to media alone, quantified by degree of fluorescence). Each sample was assayed in triplicate.

Murine monocytes: An *in vitro* transwell chemotaxis assay was used to assess monocyte migration. Single cell suspensions of the spleen were obtained at euthanasia by repeatedly flushing RPMI + 10% FBS through the spleen using a 20-gauge needle. The resultant cell suspension was filtered through a 0.4 µm filter to remove tissue debris, and the cells lysed with 1x RBC lysis buffer (eBioscience) to remove the red blood cells. Transwell inserts with a 3 µm membrane pore size (BD Biosciences) were loaded with 2 x 10^6 splenic cells suspended in 300 µl of RPMI + 10% FBS. The lower chamber, i.e., the 24-well cell

culture plate, was loaded with the following: 100 ng/ml monocyte chemoattractant protein-1 (MCP-1), 100 ng/ml stromal cell-derived factor-1 (SDF-1) as positive chemoattractants, and PBS + 1% bovine serum albumin (BSA) as a negative control. The cells were incubated at 37°C for 4 hours, after which the non-migrated cells remaining on the top of the membrane were removed with cotton swabs dampened with RPMI. The transmigrated cells on the underside of the membrane were fixed with ice-cold methanol before staining with 1% crystal violet aqueous solution. The membranes were air-dried overnight, then removed and mounted on glass microscope slides for counting. The membranes were counted in the following manner – for each membrane, monocytes in 5 random 40X fields were counted. For each mouse the ability of monocytes to move to the chemoattractants was measured in duplicate using aggregate counts from five microscope fields.

2.2.7 Prostaglandin ELISA

Sorted monocytes from healthy controls and dogs with OS were used for stimulation experiments – half of these monocytes served as unstimulated controls and incubated for 6 hours at 37°C and 5% CO_2. The other half were stimulated with 100ng/10^6 monocytes of lipopolysaccharide (LPS) and incubated similarly for 6 hours at 37°C and 5% CO_2. The resultant supernatants were collected, stored at -20°C until they were assessed for Prostaglandin E_2 (PGE_2) levels using a commercially available PGE_2 ELISA kit (Cayman Chemical) according to manufacturer's directions.

2.2.8 IL-10, IFN-γ, TNF-α magnetic bead panel assay

Sorted monocytes from healthy controls and dogs with OS were used for stimulation experiments as described for the prostaglandin ELISA (2.2.7). The resultant supernatants

were collected, stored at -20°C until they were assessed for IL-10, IFN-γ, and TNF-α levels using a commercially available canine cytokine magnetic bead panel kit, MILLIPLEX® MAP, (EMD Millipore) according to manufacturer's directions. IL-12 was not available as an analyte in the kit, thus IFN-γ levels were analyzed as a surrogate, since IL-12 is known to induce IFN-γ secretion.

Macrophage Studies

2.2.9 Volunteer enrollment – canine and human

A healthy volunteer population of dogs over 1 year of age was recruited for the study. Written owner consent was obtained for all dogs, and peripheral blood samples were collected under an approved IACUC protocol. A healthy volunteer population of humans between the ages of 18 and 25 years was recruited for the study. Written consent was obtained for all humans, and peripheral blood samples were collected under an approved IRB protocol.

2.2.10 Primary macrophage cultures – canine and human

Approximately 50 ml of peripheral blood were collected into EDTA blood collection tubes via venipuncture from canine and human volunteers. Canine and human PBMCs were isolated by density gradient centrifugation using Histopaque®-1077. The PBMCs were resuspended in culture media, placed in 12-well cell culture plates, and incubated at 37°C and 5% CO_2. After overnight incubation, the culture media was changed to remove non-adherent cells. The adherent cells were then incubated for another 96 hours to allow differentiation into macrophages. For experimental groups that required co-culture with OS cells, Abrams

OS cells and 143B OS cells were added at 36 hours to the canine and human macrophage cultures respectively. 200,000 OS cells suspended in 500 µl culture media were added to each 0.4 µm transwell insert and placed within each 12-well culture well for co-culture of OS cells with macrophages.

2.2.11 Flow cytometry (FACS)

Cultured primary macrophages were lifted from cell culture wells using Accutase® and resuspended in 100 µl FACS buffer (1X HBSS with 2% FBS) per tube for staining with the following antibodies against cell surface receptors:

Canine macrophages: anti-CD11b (AbCam), anti-MHCII (eBioscience), anti-CD80 (eBioscience), anti-CD11c (eBioscience) (Table 5). DAPI was used as a viability stain.

Human macrophages: anti-CD11b (BioLegend), anti-CD14 (AbD Serotec), anti-CD5 (BioLegend), anti-HLA-DR (BioLegend), anti-CD163 (BioLegend), anti-CD86 (BioLegend), anti-CD11c (BioLegend), anti-CD206 (BioLegend), anti-CCR2 (BioLegend) (Table 6). A fixable viability stain (eFluor 660, eBioscience) was used.

Normal donkey serum was added to the FACS buffer for blocking against non-specific staining. Macrophages were gated based on forward and side scatter, and on positive expression of CD11b after gating in the singlet cells (Figure 2). Any remaining lymphocytes were gated out using positive CD5 expression. The cells were stained with antibodies at 2-8°C for 30 minutes, after which they were washed with FACS buffer and the human macrophages were fixed with fixation buffer (eBiosciences) prior to analysis. Samples were analyzed using a LSRII flow cytometer and data analysis was performed using the Kaluza®

software. Single color controls and compensation were performed using compensation beads, and positively staining cells were gated based on fluorescence-minus-one (FMO) cellular controls.

Table 5: List of antibodies used for canine macrophage flow cytometry

Antibodies	Clone	Fluorescence Labeling
CD11b	M1/70	PE-Cy5
MHCII	YKIX334.2	FITC
CD80	16-10A1	PE
CD11c	BU15	APC-eFluor 780

Table 6: List of antibodies used for human macrophage flow cytometry

Antibodies	Clone	Fluorescence Labeling
CD11b	M1/70	Pacific Blue
CD14	TÜK4	FITC
CD5	L17F12	APC
HLA-DR	L243	APC-Fire 750
CD163	RM3/1	PerCp-Cy5.5
CD86	IT2.2	PE
CD11c	Bu15	APC-Cy7
CD206	15-2	PerCp-Cy5.5
CCR2	K036C2	BV510

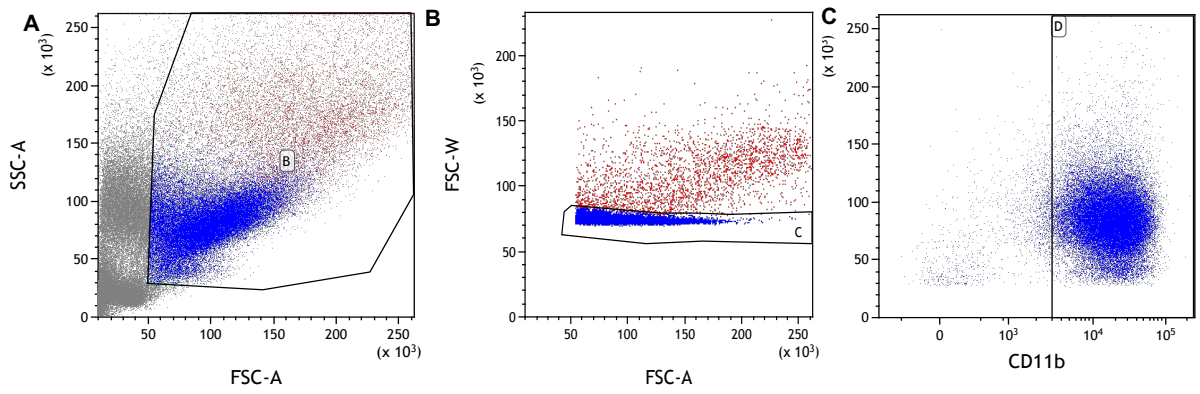

Figure 2: **Gating strategies for macrophage flow cytometry**

Representative dot plot showing macrophage gating using forward and side scatter characteristics (a); gating of singlet cells (b); gating of CD11b+ macrophages (c).

2.2.12 Magnetic bead panel assay

Supernatants from primary macrophage cultures were collected when the macrophages were harvested for assays, stored at -20°C for subsequent cytokine analysis. Canine macrophage supernatants were assessed for IL-10, IFN-γ, MCP-1, and TNF-α levels, and human macrophage supernatants were assessed for IL-10, IFN-γ, MCP-1, TNF-α, IL-12p40, and IL-12p70 levels using commercially available canine and human cytokine magnetic bead panel kits, MILLIPLEX® MAP, (EMD Millipore) according to manufacturer's directions.

2.2.13 TGF-β ELISA

Supernatants from primary macrophage cultures were collected when the macrophages were harvested for assays, stored at -20°C for subsequent cytokine analysis. Supernatants were assessed for TGF-β levels using a commercially available TGF-β ELISA kit (R&D) according to manufacturer's directions.

2.2.14 Total RNA extraction, reverse transcription, and quantitative RT-PCR

Macrophages were collected from culture wells by addition of Tri-Reagent (Zymo Research) directly into the wells to lyse the cells, and stored at -80°C for subsequent PCR analysis. The Direct Zol RNA Microprep™ kit (Zymo Research) was used to extract total RNA from macrophages according to the manufacturer's protocol. The concentration and quality of the extracted RNA was determined using a NanoDrop 2000c spectrophotometer (Thermo Scientific) as well as the Agilent Bioanalyzer (Agilent Technologies), and the RNA samples were stored at -80°C until processing. cDNA was synthesized from 100 ng RNA per sample using the QuantaBio qScript™ cDNA synthesis kit according to manufacturer's directions, and the RT reactions were carried out in a GeneAmp®PCR System 9700 thermal cycler (Applied Biosystems). mRNA gene expression was determined with SYBR Green qPCR using the QuantaBio PerfeCTa® SYBR Green FastMix® per manufacturer's directions, and reactions cycled in a Roche Lightcycler 480 (Roche Diagnostics Corporation). All samples were run in triplicate. PrimePCR™ PCR primers for detection of mRNA expression levels of Arginase (Unique assay ID: canine qCfaCED0035802; human qHsaCED0043785), IL-10 (Unique assay ID: canine qCfaCED0031300; human qHsaCED0003369), TNF-α (Unique assay ID: canine qCfaCED0030703; human qHsaCED003746), β-actin (Unique assay ID: canine qCfaCED0037901), and GAPDH (Unique assay ID: canine qCfaCED0036726; human qHsaCED0038674) were purchased from Bio-Rad. The qPCR cycling conditions were as follows: activation at 95°C for 2 minutes, followed by denaturation at 95°C for 5 seconds, annealing at 60°C for 30 seconds,

for a total of 45 cycles. Expression of the target genes was normalized to expression of the housekeeping genes GAPDH (human) and β-actin (canine). The $2^{-\Delta\Delta CT}$ method was used to calculate the normalized relative mRNA expression of the target genes.

2.2.15 Statistical analyses

Canine and human monocytes / macrophages: Statistical analyses were performed to compare monocyte cell surface receptor expression levels between groups using the non-parametric Mann-Whitney U-test due to the non-normal distribution of the data. Comparison of relative mRNA expression of each gene and of cytokine levels between groups were analyzed with the Mann-Whitney U-test. All statistical tests were carried out as 2-sided tests, and a p-value of <0.05 was considered significant. Comparison of peripheral blood monocyte counts between dogs with OS and healthy controls was performed using a 2-tailed T-Test. Pearson's correlation coefficient was used to determine the strength and direction of a possible linear relationship between monocyte surface receptors and peripheral blood monocyte counts. Two-way ANOVAs and least-squares means were used to test for differences in monocyte surface receptors due to status and monocyte counts (high versus low). Two-way ANOVAs and Tukey's multiple comparisons test were used to compare canine and human macrophage cell surface receptor expression and cytokine levels between groups. To analyze the chemotaxis data, one-way ANOVAs were run and means were compared using Welch's adjustment for heterogeneous variation. Kaplan-Meier survival analysis was used to compare survival between groups, with proportional hazards regression analysis to test the effect of chemokine receptor expression on survival. Survival was calculated as the number of days from diagnosis of disease to death attributed to disease, or

last follow-up if the patient was still alive. A dog was determined to have died of disease if metastasis or local tumor recurrence was the cause, and dogs with an unknown cause of death were presumed to be dead due to disease. Dogs were censored from the analysis if they were still alive at last follow-up. All analyses were performed using SAS software (Version 9.4, Cary, NC). All statistical analyses were performed in consultation with the NCSU Biostatistics consulting group.

Murine monocytes (SQ OS model): All statistical analyses were run in SAS (Version 9.4, Cary, NC) or Prism 7 (GraphPad Software, La Jolla, CA). For flow cytometric analyses, summary statistics were first calculated for all monocyte receptor values. Two-sample Wilcoxon rank-sum tests were used to test for differences between the nanoparticle groups when collected at euthanasia compared to before euthanasia. One-way ANOVAs were used to test for differences in the percent of Ly6c hi and lo monocytes between experimental groups as well as to test for differences between marker expressions within monocyte receptor subgroups for Ly6c hi, Ly6c lo, and CD11b hi. When statistical significance was indicated, post-hoc pairwise comparisons of means were performed. Pearson's correlation coefficient was calculated to examine the relationship between Ly6c hi and lo monocytes within each treatment group. ANCOVAs were used to test for the relationship between Ly6c hi and lo and its interaction with treatment groups. Differences between marker expressions within each experimental group and monocyte expression were tested using a series of Wilcoxon signed-rank tests comparing these pairwise differences to zero. Differences in survival times between treatment groups were also tested using a one-way ANOVA. To examine the relationship between monocyte markers (within Ly6c hi and lo) and survival, the

markers were included as a covariate in a series of one-way ANCOVAs. For each hypothesis of interest, the Holm-Bonferroni correction was applied to adjust for multiple testing and control the Type I error rate. For survival analysis, defined as time to a specific tumor diameter, the Kaplan-Meier log-rank analysis was used. For quantitative RT-PCR analysis, unpaired T test was used to compare data between groups. For chemotaxis experiments, a linear mixed effects model, i.e. a completely randomized, split-plot design with subsampling, was used to analyze the chemotaxis data. This model includes random effects for mouse nested within treatment and chemoattractant-by-mouse combination also nested within treatment, since each such combination was subsampled in duplicate. The model also includes fixed effects for treatment and chemoattractant and their interaction. Residual diagnostics indicated that variability in monocyte movement increased with the mean, as is the case with counting variables. Accordingly, the square root transformation was applied to the counts, resulting in better homogeneity of variance. The cut-off for statistical significance before adjusting was set at $p < 0.05$ throughout.

Murine monocytes (Orthotopic OS model): Statistical analyses were performed to compare monocyte cell surface receptor expression levels between groups using the non-parametric Mann-Whitney U-test due to the non-normal distribution of the data.

2.3. Results

Monocyte Studies

2.3.1 Study populations

Canine: Fourteen healthy control dogs and 18 dogs with OS were recruited for the study. The mean (+/-SD) age at time of OS diagnosis was 8.7 (+/- 2.1) years. All dogs with OS were purebred, with the most common pure breeds being Labrador Retriever (5 [28%]), Rottweiler (3 [17%]), Great Dane (3 [17%]), and Golden Retriever (2 [11%]). There were 8 (44%) spayed females, and 10 (56%) castrated males.

Human: Fourteen healthy human subjects and 15 humans with OS were recruited for the study.

Murine: Female C3H-HeN inbred mice were used to establish the SQ syngeneic OS model. All C3H-HeN mice were 8-10 weeks of age, weighed 40-45 grams, and purchased from Charles River Laboratories (Raleigh, NC). Mice were housed 4 to a cage in a temperature-controlled room with a 12:12-hour automated light/dark cycle, and fed a standardized commercial pelleted diet. All mice underwent a 14-day acclimatization period before starting the study. There were 11 mice with OS, and 7 normal control mice. The orthotopic syngeneic model was created using an injection of Cre recombinase expressing adenovirus to induce tumor formation, which occurs by deleting the floxed alleles (Rb and p53) in the cells that are infected with Cre. There were 9 mice with OS, and 8 normal control mice.

2.3.2 Flow cytometry

Canine monocytes: The primary flow cytometry canine monocyte gates were based on typical forward and side scatter characteristics. Once that forward versus side light scatter gate was established, we ensured that greater than 98% of the CD14+ cells were found within this gate. As CD14 expression on peripheral blood monocytes varies greatly, this ensured that we included the $CD14^{lo}$ monocytes for surface receptor analysis. Canine monocytes exhibited positive surface expression of CD14, CD16, CD32, CD62L, CCR2, CCR7, CD43, CX3CR1, CXCR2, with low levels of CD11c. Irrelevant isotype controls were used for each experiment—the isotype control binding of monocytes was <5%. The median percentages and ranges of positively staining cells for each antibody are listed in the legend accompanying Figure 3a. Comparison of monocyte surface receptors between untreated dogs with OS and healthy controls revealed a significant decrease in surface receptor expression of CD62L ($p < .00001$), CCR2 ($p = 0.0006$), CCR7 ($p = 0.0004$), CD43 ($p = 0.008$), CX3CR1 ($p = 0.002$), CXCR2 ($p = 0.0007$) in dogs with OS, and a significant increase in CD16 expression in dogs with OS ($P = 0.005$) (Fig. 3b). Fig 3b depicts representative dot plots with the percentage of cell surface receptor expression in monocytes of a healthy control versus an OS dog.

Figure 3: Monocyte surface marker expression is altered in dogs with OS

Flow cytometry plots illustrating cell surface receptor expression in peripheral blood monocytes from dogs with OS (n = 18) and healthy controls (n = 13). (A) Box-and-whisker plot depicting the % positive monocyte cell surface receptor expression of the different receptors (CD14, CD16, CD32, CD62L, CCR2, CCR7, CD43, CX3CR1, CXCR2), comparing expression between healthy controls and dogs with OS. The median percentages and ranges of positively staining cells for each antibody in healthy controls are as follows: CD14 (15%, 3–84%), CD16 (9%, 0.5–24%), CD32 (33%, 1–82%), CD62L (31%, 10–75%), CCR2 (58%, 2–94%), CCR7 (36%, 1–90%), CD43 (52%, 2–93%), CX3CR1 (9%, 0.2–87%), and CXCR2 (54%, 2–92%). The median percentages and ranges of positively staining cells for each antibody in dogs with OS are as follows: CD14 (29%, 2–82%), CD16 (24%, 3–76%), CD32 (28%, 4–52%), CD62L (11%, 3–36%), CCR2 (29%, 3–45%), CCR7 (8%, 0.1–41%), CD43 (28%, 3–47%), CX3CR1 (5%, 0.6–70%), and CXCR2 (23%, 0.2–52%). Significant differences are marked with an asterisk ($p < 0.05$). Chemokine receptors have significantly decreased expression, and CD16 expression is significantly increased in monocytes of dogs with OS. (B) Representative dot plots showing the percentage cell surface expression of CD14 and CCR2 in monocytes of a healthy control (upper panel) versus an OS dog (lower panel). There was no significant difference between CD14 expression in OS compared to control dogs. A portion of the CD14 positive monocytes in dogs with OS were noted to have increased forward scatter, denoting larger cell sizes. CCR2 expression is significantly decreased in dogs with OS ($p = 0.0006$). Representative dot plots for isotype controls are displayed for each dog.

A.

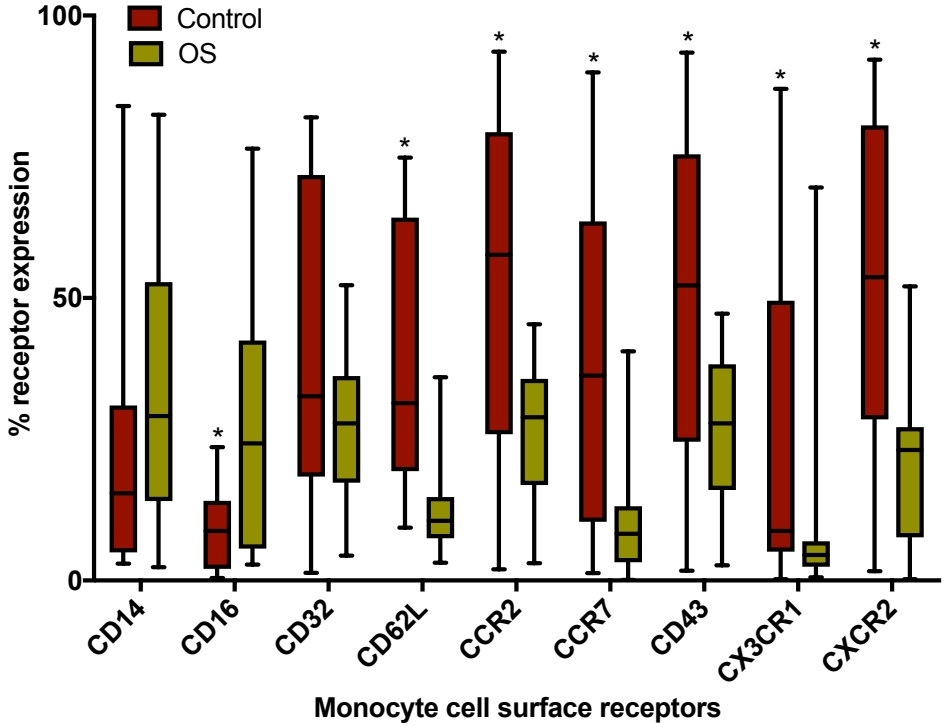
Control
OS
100
50
0
% receptor expression
CD14
CD16
CD32
CD62L
CCR2
CCR7
CD43
CX3CR1
CXCR2
Monocyte cell surface receptors

B.

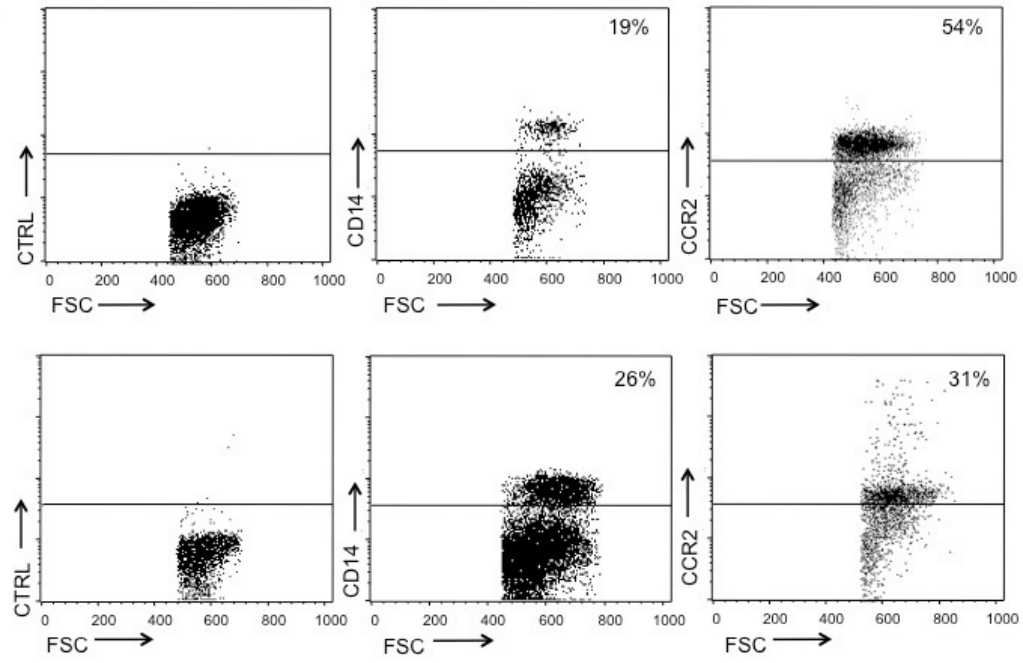
CTRL
CD14
CCR2
FSC
19%
54%
26%
31%
0
200
400
600
800
1000

A peripheral blood monocyte count of >400 cells/μl has been significantly associated with decreased disease- free interval in dogs with OS.[21] Others have reported associations between peripheral blood monocyte counts and outcomes in humans with OS.[10] Hence, we evaluated the flow cytometry data in conjunction with peripheral blood monocyte counts, using 400 cells/μl as a differentiation point between high and low monocyte counts according to previously reported findings.[21] There was no significant difference in the peripheral blood monocyte counts of dogs with OS (mean = 514.7 cells/μl, SD = 377.9 cells/μl) compared to healthy controls (mean = 331.9 cells/μl, SD = 192.6 cells/μl; p = 0.16). Comparison of receptor expression between dogs with high (>400 cells/μl) versus low (<400 cells/μl) monocyte counts revealed a dichotomy of CD14, CD16 expression in dogs with OS— CD14 expression is high (p = 0.01) and CD16 expression is low (p = 0.02) when monocyte counts are high (Table 7).

Table 7: Comparison of receptor expression between dogs with high (>400 cells/μl, n = 11) versus low (<400 cells/μl, n = 17) monocyte counts. In dogs with OS, when monocyte counts are high, there is a dichotomy of CD14, CD16 expression—CD14 is high (p = 0.01) and CD16 is low (p = 0.02).

		Control Dogs		Dogs with OSA	
Chemokine receptor	Monocyte counts	Median (% expression)	*P*-value	Median (% expression)	*P*-value
CD14	High	11.9	.90	37.5	.01
	Low	7.7		13.9	
CD16	High	2.8	.15	5.7	.02
	Low	11.3		37.3	

Human monocytes: Based on our findings reported above in canine monocytes - that monocyte chemokine receptors were significantly downregulated in dogs with OS compared

to normal controls, we compared monocyte surface receptors between human patients with OS and normal healthy human subjects to determine whether a similar effect could be observed in people. The gating strategy for human monocytes is the same as what we used for canine monocytes, and irrelevant isotype controls were used for each experiment—the isotype control binding of monocytes was <5%. Monocyte surface receptor expression was compared between groups for all CD14+ monocytes, as well as for the $CD14^{hi}$ and $CD14^{lo}$ monocyte subsets. Human patients with OS exhibited significantly decreased percentage of $CD14^{lo}$ monocytes compared to healthy controls ($p = 0.0004$) (Fig. 4). CCR2 expression in $CD14^{lo}$ monocytes was significantly higher in OS patients compared to healthy controls ($p = 0.0271$) (Fig. 4). CXCR2 expression in CD14+ monocytes and $CD14^{hi}$ monocytes was significantly decreased in OS patients compared to healthy controls ($p = 0.0093, 0.0324$ respectively) (Fig. 4). CD64 expression in CD14+ monocytes was significantly increased in OS patients compared to healthy controls ($p = 0.0271$) (Fig. 4). The CD11c expression in $CD14^{lo}$ monocytes trended towards a significant decrease in OS patients compared to healthy controls ($p = 0.0512$).

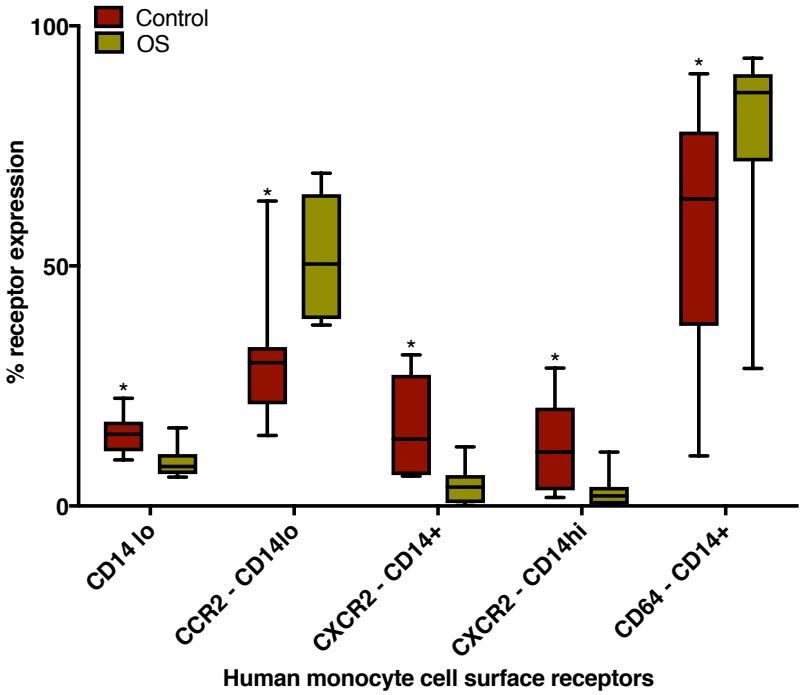

Figure 4: Monocyte surface marker expression is altered in humans with OS

Flow cytometry plots illustrating cell surface receptor expression in peripheral blood monocytes from human patients with OS (n = 14) and healthy controls (n = 14). Box-and-whisker plot depicting the % of $CD14^{lo}$ monocytes, %CCR2 expression in $CD14^{lo}$ monocytes, %CXCR2 expression in CD14+ and $CD14^{hi}$ monocytes, and %CD64 expression in CD14+ monocytes. The median percentages and ranges of positively staining cells for each antibody in healthy controls are as follows: $CD14^{lo}$ monocytes (15%, 10–22%), CCR2 in $CD14^{lo}$ monocytes (30%, 15–64%), CXCR2 in CD14b+ monocytes (14%, 6–31%), CXCR2 in $CD14^{hi}$ monocytes (11%, 2–29%), CD64 in CD14+ monocytes (64%, 10–88%). The median percentages and ranges of positively staining cells for each antibody in humans with OS are as follows: $CD14^{lo}$ monocytes (8%, 6–16%), CCR2 in $CD14^{lo}$ monocytes (50%, 38–69%), CXCR2 in CD14b+ monocytes (4%, 0.12–12%), CXCR2 in $CD14^{hi}$ monocytes (2%, 0.1–11%), CD64 in CD14+ monocytes (86%, 29–93%). Significant differences are marked with an asterisk ($p < 0.05$).

Murine monocytes: Based on our findings reported above in canine monocytes - that monocyte chemokine receptors were significantly downregulated in dogs with OS compared

to normal controls, we compared monocyte surface receptors between mice with OS and normal control mice to determine whether a similar effect could be observed in mice. We utilized both the syngeneic SQ OS model as well as the orthotopic OS model. In the SQ OS model, monocyte surface receptor expression was compared between groups for all CD11b+ monocytes, as well as for the $Ly6C^{hi}$ and $Ly6C^{lo}$ monocyte subsets. There was no significant difference in proportion of both $Ly6C^{hi}$ monocytes and $Ly6C^{lo}$ monocytes in normal control versus OS mice (Fig. 5a). When surface receptor expression was evaluated for all CD11b+ monocytes, CCR7 expression was significantly higher in monocytes of normal control mice compared to OS mice ($p = 0.0146$) (Fig. 5a). When surface receptor expression was evaluated in the $Ly6C^{hi}$ and $Ly6C^{lo}$ monocyte subsets, CCR7 expression was significantly higher in the $Ly6C^{lo}$ monocytes of normal control mice compared to OS mice ($p = 0.0004$) (Fig. 5a). In the mice with OS, CCR2 expression was significantly higher ($p = 0.001, 0.0039$ respectively) and CXCR4 expression was significantly lower ($p = 0.002, 0.0039$ respectively) in $Ly6C^{hi}$ monocytes compared to $Ly6C^{lo}$ monocytes (Fig. 5b). The expression pattern of CCR7 in the monocyte subsets was significantly different between normal control and OS mice. In normal control mice, CCR7 expression was higher in $Ly6C^{lo}$ monocytes compared to $Ly6C^{hi}$ monocytes, versus OS mice, where the opposite occurred - CCR7 expression is higher in $Ly6C^{hi}$ monocytes compared to $Ly6C^{lo}$ monocytes, and this variation in CCR7 expression pattern was significantly different between normal control and tumor control mice ($p = 0.0151$) (Fig. 5c).

Figure 5: Monocyte surface marker expression is altered in mice with OS (syngeneic SQ OS model)

Flow cytometry plots illustrating cell surface receptor expression in peripheral blood monocytes from mice with OS (n = 11) and healthy controls (n = 7). (A) Box-and-whisker plot depicting the % of $Ly6C^{hi}$ and $Ly6C^{lo}$ monocyte subsets, and % positive CCR7 cell surface receptor expression in all CD11b+ monocytes and in the $Ly6C^{lo}$ monocyte subset in OS versus normal control mice. (B) Box-and-whisker plot comparing % positive CCR2 and CXCR4 cell surface receptor expression between the $Ly6C^{lo}$ and $Ly6C^{hi}$ monocyte subsets in mice with OS. (C) Box-and-whisker plot demonstrating the difference in % positive CCR7 cell surface receptor expression between $Ly6C^{lo}$ and $Ly6C^{hi}$ monocyte subsets, and comparing the variation of these differences between OS mice and normal controls. The median percentages and ranges of positively staining cells for each antibody in healthy controls are as follows: $Ly6C^{hi}$ (19%, 8–29%), $Ly6C^{lo}$ (14%, 9–19%), CCR7 in CD11b+ monocytes (37%, 4–66%), CCR7 in $Ly6C^{hi}$ monocytes (35%, 2–64%), CCR7 in $Ly6C^{lo}$ monocytes (41%, 6–70%). The median percentages and ranges of positively staining cells for each antibody in mice with OS are as follows: $Ly6C^{hi}$ (18%, 9–32%), $Ly6C^{lo}$ (19%, 7–34%), CCR7 in CD11b+ monocytes (16%, 1–37%), CCR7 in $Ly6C^{hi}$ monocytes (15%, 2–62%), CCR7 in $Ly6C^{lo}$ monocytes (10%, 0.3–29%), CCR2 in $Ly6C^{hi}$ monocytes (99%, 96–100%), CCR2 in $Ly6C^{lo}$ monocytes (69%, 20–91%), CXCR4 in $Ly6C^{hi}$ monocytes (5%, 2–11%), CXCR4 in $Ly6C^{lo}$ monocytes (10%, 5–19%). Significant differences are marked with an asterisk ($p < 0.05$).

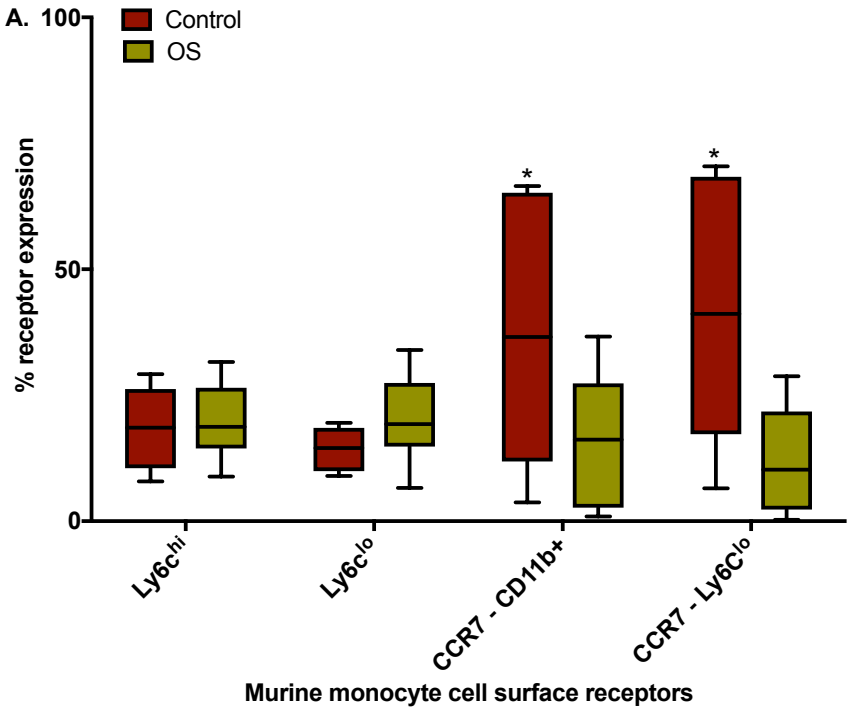
A.
100
50
0
Control
OS
% receptor expression
*
*
Ly6C^hi
Ly6C^lo
CCR7 - CD11b+
CCR7 - Ly6C^lo
Murine monocyte cell surface receptors

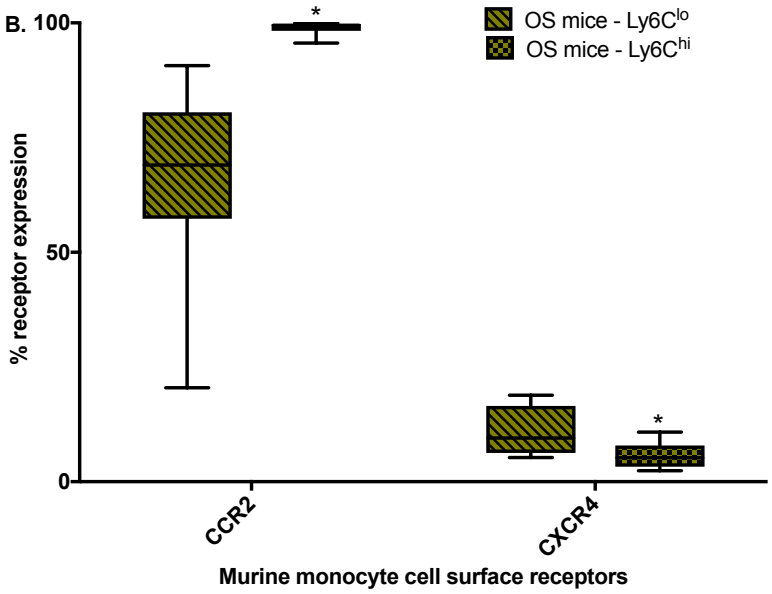
B.
100
50
0
OS mice - Ly6C^lo
OS mice - Ly6C^hi
% receptor expression
*
*
CCR2
CXCR4
Murine monocyte cell surface receptors

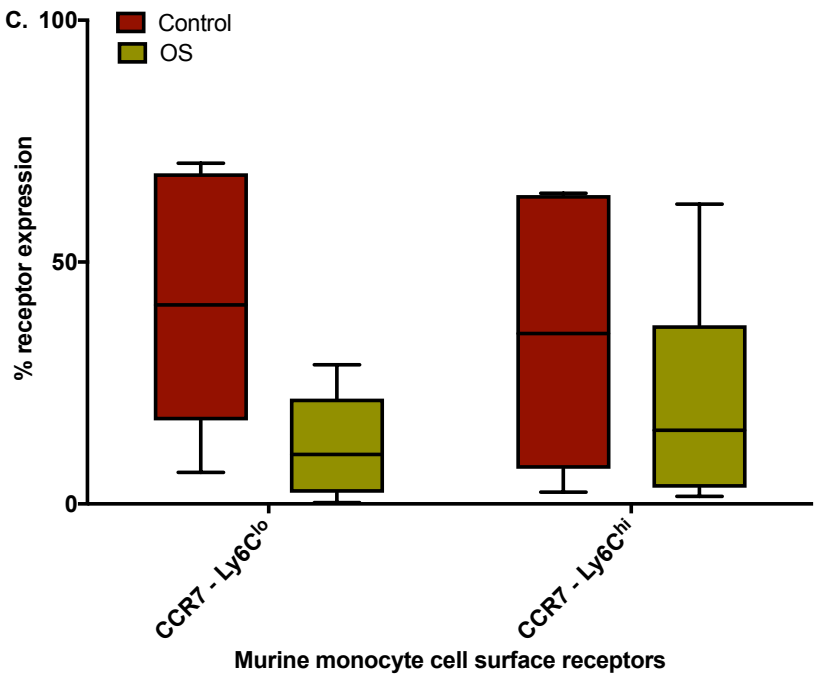
C.
100
50
0
Control
OS
% receptor expression
CCR7 - Ly6C^lo
CCR7 - Ly6C^hi
Murine monocyte cell surface receptors

Monocyte receptor expression was also compared between normal control and OS-bearing mice using the orthotopic OS model. In the orthotopic OS model, monocyte surface receptor expression was compared between groups for all CD11b+ monocytes, as well as for the $Ly6C^{hi}$ and $Ly6C^{lo}$ monocyte subsets. The percent of both $Ly6C^{hi}$ ($p = 0.0045$) and $Ly6C^{lo}$ ($p = 0.0238$) monocytes was significantly higher in OS mice compared to normal control mice (Fig. 6a). $Ly6C^{hi}$ monocyte CCR2 ($p = 0.0143$) expression was significantly higher in OS mice compared to normal controls (Fig. 6a). CXCR4 expression in $Ly6C^{hi}$ monocytes was significantly higher in normal control compared to OS mice ($p = 0.0143$) (Fig. 6a). CCR7 expression was significantly higher in OS mice compared to normal controls in all monocyte groups - $Ly6C^{hi}$ monocytes ($p = 0.0238$), $Ly6C^{lo}$ monocytes ($p = 0.0006$), and CD11b+ monocytes ($p = 0.0009$) (Fig. 6b). CX3CR1 expression in $Ly6C^{hi}$ ($p = 0.0006$) and CD11b+ ($p = 0.0108$) monocytes was significantly higher in normal control compared to OS mice. CD62L expression in $Ly6C^{hi}$ ($p = 0.0017$) and CD11b+ ($p = 0.0017$) monocytes was significantly lower in normal control versus OS mice (Fig. 6c).

Figure 6: Monocyte surface marker expression is altered in mice with OS (orthotopic OS model)

Flow cytometry plots illustrating cell surface receptor expression in peripheral blood monocytes from mice with OS (n = 9) and healthy controls (n = 8). (A) Box-and-whisker plot depicting the % of $Ly6C^{hi}$ and $Ly6C^{lo}$ monocyte subsets, and % positive CCR2 and CXCR4 cell surface receptor expression in the $Ly6C^{hi}$ monocyte subset in OS versus normal control mice. (B) Box-and-whisker plot depicting the % positive CCR7 cell surface receptor expression in the $Ly6C^{hi}$, $Ly6C^{lo}$ and CD11b+ monocyte subset in OS versus normal control mice. (C) Box-and-whisker plot depicting the % positive CX3CR1 and CD62L cell surface receptor expression in the $Ly6C^{hi}$ and CD11b+ monocyte subsets in OS versus normal control mice. The median percentages and ranges of positively staining cells for each antibody in healthy controls are as follows: $Ly6C^{hi}$ (8%, 0.83–23%), $Ly6C^{lo}$ (9%, 2–23%), CCR2 in $Ly6C^{hi}$ monocytes (98%, 90–99%), CXCR4 in $Ly6C^{hi}$ monocytes (13%, 10–37%), CCR7 in $Ly6C^{hi}$ monocytes (2%, 0.4–15%), CCR7 in $Ly6C^{lo}$ monocytes (2%, 0.3–12%), CCR7 in CD11b+ monocytes (3%, 0.3-10%), CX3CR1 in $Ly6C^{hi}$ monocytes (99%, 97–100%), CX3CR1 in CD11b+ monocytes (95%, 68–97%), CD62L in $Ly6C^{hi}$ monocytes (10%, 6–21%), CD62L in CD11b+ monocytes (17%, 6-39%). The median percentages and ranges of positively staining cells for each antibody in mice with OS are as follows: $Ly6C^{hi}$ (26%, 16–58%), $Ly6C^{lo}$ (15%, 11–23%), CCR2 in $Ly6C^{hi}$ monocytes (99.6%, 99.5–99.9%), CXCR4 in $Ly6C^{hi}$ monocytes (8%, 3–18%), CCR7 in $Ly6C^{hi}$ monocytes (10%, 2–21%), CCR7 in $Ly6C^{lo}$ monocytes (32%, 17–41%), CCR7 in CD11b+ monocytes (18%, 10-40%), CX3CR1 in $Ly6C^{hi}$ monocytes (79%, 44–95%), CX3CR1 in CD11b+ monocytes (67%, 56–93%), CD62L in $Ly6C^{hi}$ monocytes (79%, 52–91%), CD62L in CD11b+ monocytes (52%, 32-%).

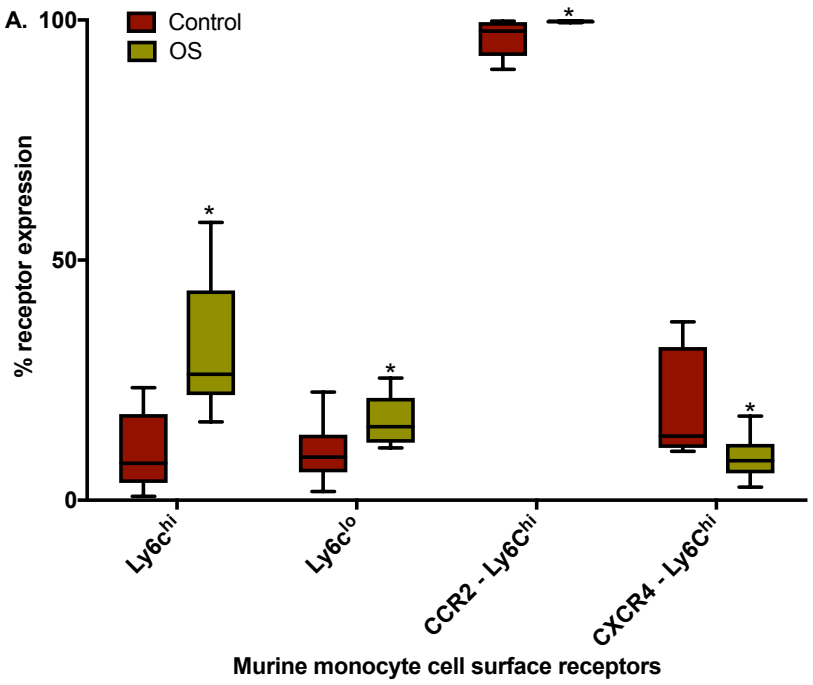
A.
100
50
0
Control
OS
% receptor expression
*
*
*
*
Ly6c^hi
Ly6c^lo
CCR2 - Ly6C^hi
CXCR4 - Ly6C^hi
Murine monocyte cell surface receptors

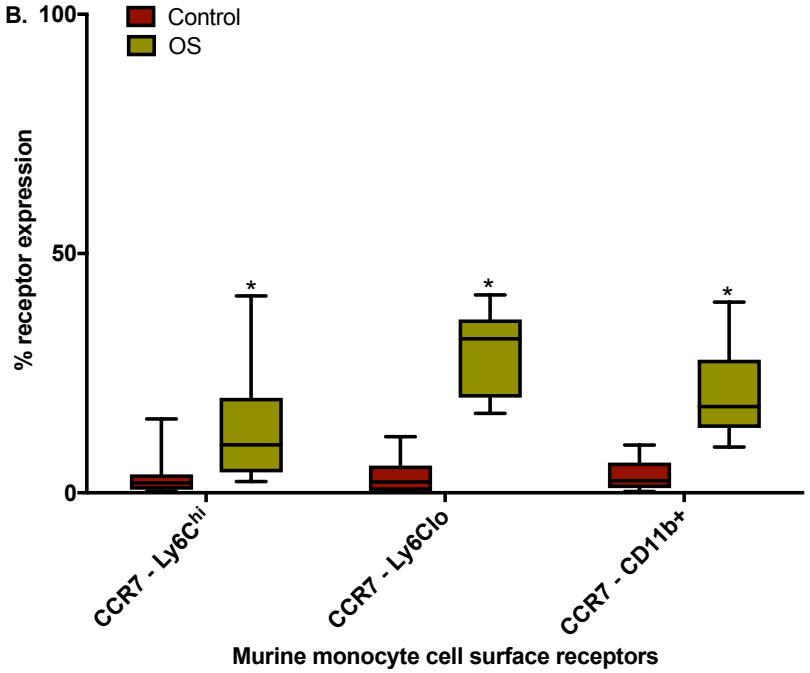
B.
100
50
0
Control
OS
% receptor expression
*
*
*
CCR7 - Ly6C^hi
CCR7 - Ly6Clo
CCR7 - CD11b+
Murine monocyte cell surface receptors

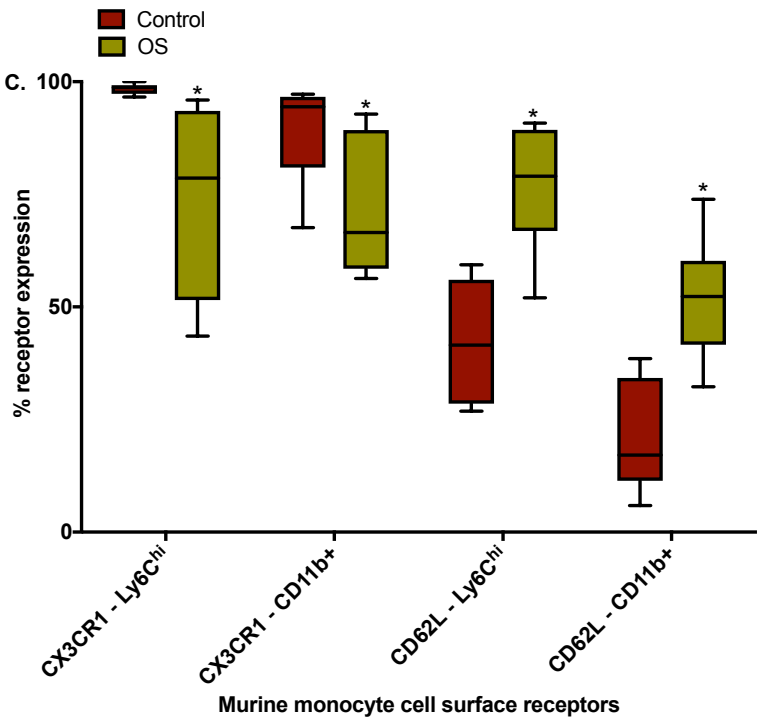
Control
OS
C.
100
50
0
% receptor expression
*
*
*
*
CX3CR1 - Ly6Chi
CX3CR1 - CD11b+
CD62L - Ly6Chi
CD62L - CD11b+
Murine monocyte cell surface receptors

2.3.3 Quantitative RT-PCR

Canine relative mRNA expression of monocyte IL-10, IL-12, TNF-α, and COX-2: TNFα, IL-10 and IL-12 are inflammatory mediators secreted by monocytes and macrophages, and differential levels of TNFα, IL-10 and IL-12 secretion have been described for the various human monocyte subsets,[22,23] reflecting subset-specific functional differences. COX-2 expression in monocytes reflects a proinflammatory state.[24,25] We compared relative mRNA expression of IL-10, IL-12, TNFα, and COX-2 in dogs with OS versus healthy controls to discern potential variation in cytokine secretion that might reflect functional differences. mRNA expression analysis of monocytes from untreated dogs with OS and healthy controls revealed no significant differences in relative mRNA expression levels of IL-10 ($p=0.44$), IL-12 ($p=0.41$), and TNF-α ($p=0.14$) between the 2 groups. The relative mRNA expression of COX-2 was decreased in dogs with OS compared to healthy controls, but the difference was not significant ($p = 0.08$).

2.3.4 Monocyte Chemotaxis

Canine monocytes: The results of our phenotypic analysis of monocytes between dogs with OS and healthy controls revealed marked decreases in chemokine receptor expression in dogs with OS (Fig. 3a). Therefore we asked whether monocyte chemotaxis might be altered by OS. As described in the methods, monocytes from OS and healthy dogs were assessed by the NeuroProbe ChemoTx® cell migration system. Comparison of monocyte chemotaxis between dogs with OS and healthy controls revealed significantly decreased chemotaxis in dogs with OS when CCL19 ($p = 0.018$), and when a mixture of all 4 chemoattractants ($p = 0.018$) was used (Fig. 7). With CCL2 or fMLP as chemoattractants,

there was also decreased monocyte chemotaxis in dogs with OS compared to healthy controls, but the difference did not reach significance (CCL2 p = 0.067; fMLP p = 0.067).

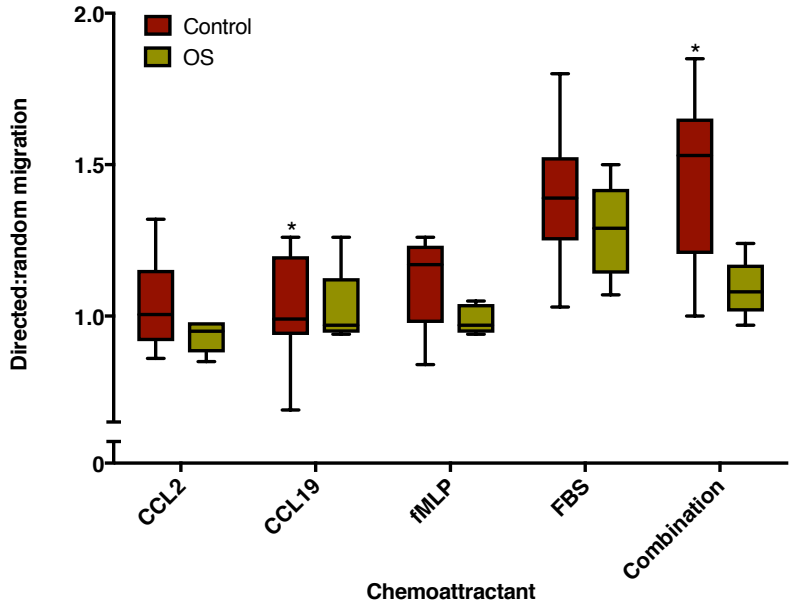

Figure 7: Monocyte chemotaxis is decreased in canine OS: Box-and-whisker plot comparing the mean levels of random: directed monocyte migration for the various chemokines used, either alone or in combination (CCL2, CCL19, FBS, fMLP) between healthy controls (n=14) and dogs with OS (n=5). Monocyte migration is significantly reduced in dogs with OS when CCL19 (p=0.018) or a combination of chemokines (p = 0.018) was used as chemoattractants. Decreased migration in dogs with OS was also observed with CCL2 or fMLP as chemoattractants, but the difference did not reach significance (CCL2 p = 0.067; fMLP p = 0.067).

Murine monocytes: As we had previously demonstrated decreased chemotaxis in monocytes from dogs with OS compared to monocytes from normal controls, we asked if murine OS may have a similar effect on monocytes. There was significant variation between experimental groups in the degree to which murine monocytes migrated in response to MCP (p = 0.0013) and SDF (p = 0.0022), whereas there was no difference in the degree to which

monocytes migrated in response to PBS ($p = 0.5399$) between experimental groups. There were no significant differences in monocyte chemotaxis between mice with OS and normal control mice ($p = 0.1409$ with MCP, $p = 0.9777$ with SDF).

2.3.5 Evaluation of IL-10, IFN-γ, TNF-α, and prostaglandin E_2 secretion from canine monocytes

Since mRNA levels might not consistently correspond with protein secretion, we analyzed monocyte secretion of the cytokines IL-10, IFN-γ, TNF-α, and PGE_2. Similar to our mRNA evaluation, we compared cytokine secretion from monocytes of dogs with OS versus healthy controls to assess for functional differences. Secretion of cytokines such as TNF-α, IL-10, IFN-γ, and PGE_2 have been noted to differ between human monocyte subsets, and can be affected by disease.[23-25] PGE_2 ELISA and the MILLIPLEX® assay revealed increased PGE_2 levels ($p = 0.04$) and increased TNF-α levels ($p = 0.02$) respectively in supernatants of cultured monocytes stimulated with LPS of untreated dogs with OS compared to normal controls (Fig. 8). The median concentrations and ranges of PGE_2 concentrations were 347.36 pg/ml, 103.4-1268.5 pg/ml for dogs with OS, and 136.23 pg/ml, 69.93-542.6 pg/ml for healthy controls. The median concentrations and ranges of TNF-α levels were 934.7 pg/ml, 644.3-2709 pg/ml for dogs with OS, and 267.2 pg/ml, 70.4-670.4 pg/ml for healthy controls. Levels of IL-10 and IFN-γ were low to undetectable in both groups.

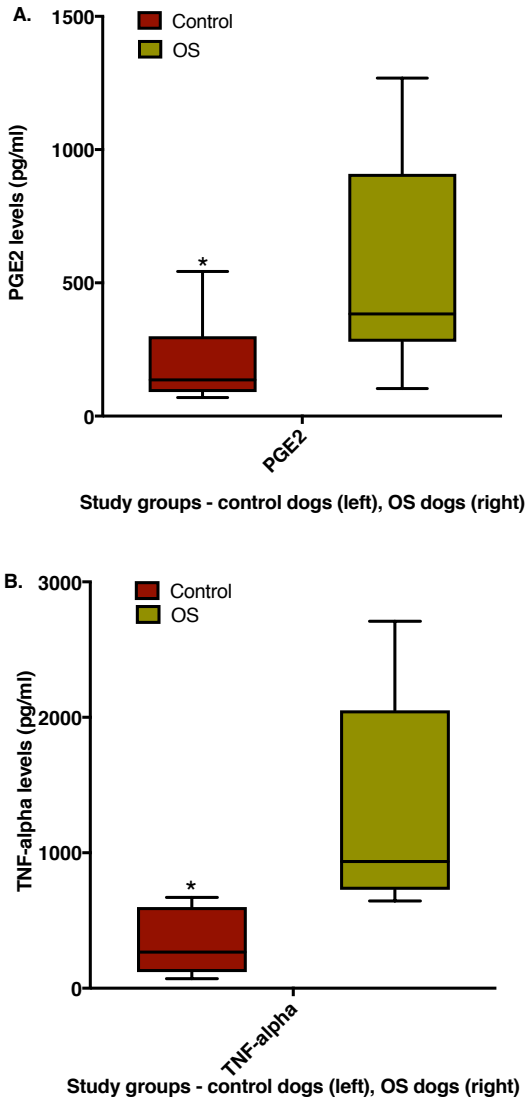

Figure 8: Monocyte PGE_2 and TNF-α secretion are increased in canine OS: Box-and-whisker plots displaying the levels of (A) PGE_2 (pg/ml) in monocyte culture supernatants of healthy controls (n=8) versus dogs with OS (n=7), and (B) TNF-α (pg/ml) in monocyte culture supernatants of healthy controls (n=5) versus dogs with OS (n=5). Monocytes from dogs with OS secreted significantly higher levels of PGE_2 ($p = 0.04$) and TNF-α ($p = 0.02$) compared to healthy control monocytes.

2.3.6 Survival Analysis

Canine: Since a peripheral canine monocyte count of >400 cells/μl has been significantly associated with decreased disease-free interval in dogs with OS,[21] we performed a Kaplan-Meier survival analysis comparing dogs with OS with high or low monocyte counts, using 400 cells/μl as a cut-off point. One dog died of unknown cause, and was assumed to have died from OS. We did not find a statistically significant difference in median survival between the 2 groups ($p = 0.15$). Our regression analysis revealed that increasing percentages of CCR2 expression on peripheral monocytes was significantly associated with increasing survival in dogs with OS ($p<0.0001$).

Murine: Unlike our findings in canine monocytes, we did not find any statistically significant correlation between murine survival and monocyte receptor expression.

Macrophage Studies

2.3.7 Study populations

Thirty-six healthy dogs over 1 year old and seventeen healthy humans 25 years or younger were recruited for the study. Canine owner and human volunteer participation written consent were obtained, and peripheral blood samples were collected for macrophage cultures.

2.3.8 Flow cytometry

Canine macrophages: Percent of CD80 expression was significantly higher in canine macrophages cultured with OS compared to macrophages cultured alone ($p < 0.0001$) (Fig. 9).

Human macrophages: Percent of CCR2 expression was significantly lower in human macrophages cultured with OS compared to macrophages cultured alone ($p < 0.0001$) (Fig. 10a). The mean fluorescence intensity (MFI) of CD86 expression was significantly higher in macrophages cultured with OS compared to macrophages cultured alone ($p = 0.0017$) (Fig. 10b).

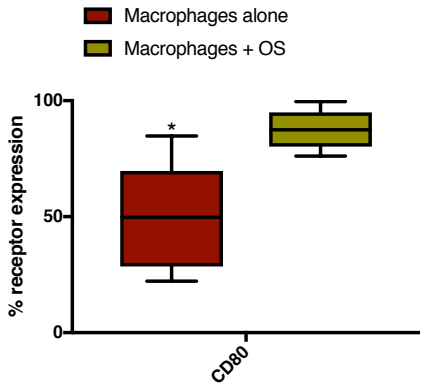

Figure 9: Macrophage receptor expression is altered in canine OS

Flow cytometry plot illustrating cell surface receptor expression in cultured primary canine macrophages from macrophages cultured alone (n = 9), and macrophages cultured with OS (n = 8). Box-and-whisker plot depicting the % positive CD80 cell surface receptor expression in macrophages cultured alone versus macrophages cultured with OS. The median percentage and range of CD80 positively staining cells in macrophages cultured alone were 50%, 22–85%. The median percentage and range of CD80 positively staining cells in macrophages cultured with OS were 87%, 76–100%.

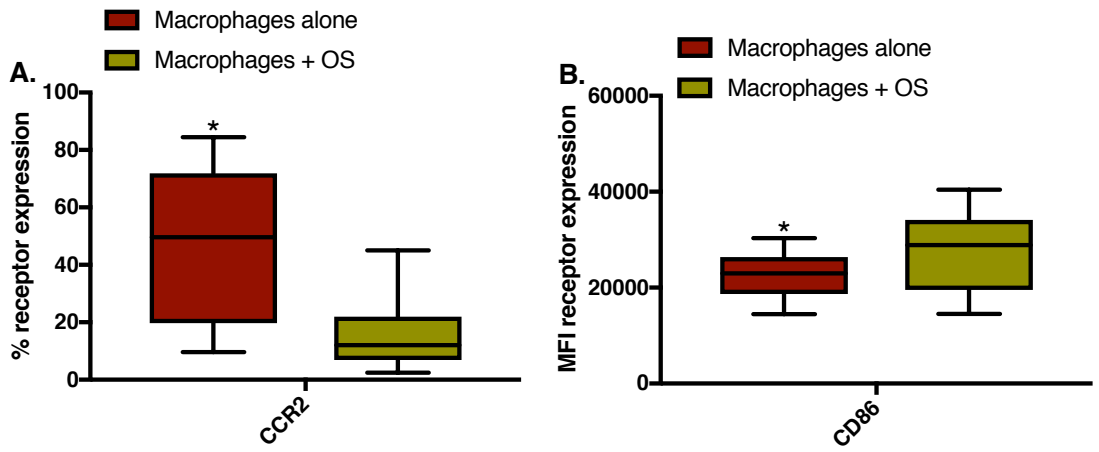

Figure 10: Macrophage receptor expression is altered in human OS

Flow cytometry plot illustrating cell surface receptor expression in cultured primary human macrophages from macrophages cultured alone (n = 7), and macrophages cultured with OS (n = 9). (A) Box-and-whisker plot depicting the % positive CCR2 cell surface receptor expression in macrophages cultured alone versus macrophages cultured with OS. The median percentage and range of CCR2 positively staining cells in macrophages cultured alone were 50%, 10–85%. The median percentage and range of CCR2 positively staining cells in macrophages cultured with OS were 12%, 3–45%. (B) Box-and-whisker plot depicting the MFI of CD86 cell surface receptor expression in macrophages cultured alone versus macrophages cultured with OS. The median MFI and range of CD86 positively staining cells in macrophages cultured alone were 22,951, 14,476–30,311. The median MFI and range of CD86 positively staining cells in macrophages cultured with OS were 28,887, 14,527–40,442.

2.3.9 Evaluation of cytokine secretion from canine and human macrophages

Canine macrophages: The MILLIPLEX® assay revealed increased MCP-1 levels ($p < 0.0001$) in culture supernatants of canine primary macrophages cultured with OS compared to macrophages cultured alone (Fig. 11). The results of the TGF-β ELISA did not yield significant differences between TGF-β in culture supernatants of macrophages cultured alone versus macrophages cultured with OS ($p > 0.99$). The median concentrations and ranges of

MCP-1 concentrations were 6369 pg/ml, 273-42,390 pg/ml for macrophages cultured alone, and 65,729 pg/ml, 33,778-86,963 pg/ml for macrophages cultured with OS.

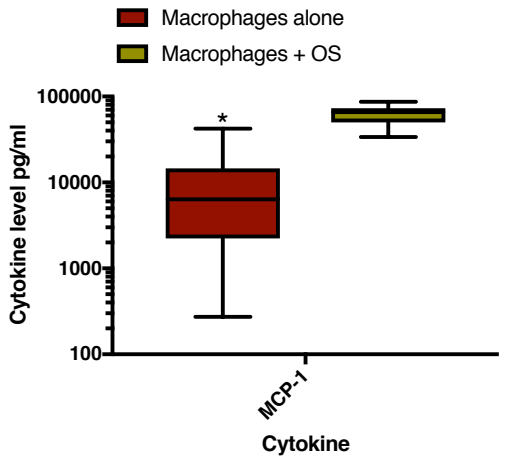

Figure 11: Macrophage MCP-1 secretion is increased in the presence of OS: Box-and-whisker plots displaying the levels of MCP-1 (pg/ml) in macrophage culture supernatants of macrophages cultured alone (n=11) versus macrophages cultured with OS (n=13). Macrophages cultured with OS secreted significantly higher levels of MCP-1 ($p < 0.0001$) compared to macrophages cultured alone.

Human macrophages: There were no significant differences in secretion of MCP-1, IFN-γ ($p=0.9912$), TNF-α ($p=0.9487$), IL-10 ($p=0.999$), IL-12p40 ($p>0.999$), IL-12p70 ($p>0.999$), or TGF-β ($p>0.999$) in culture supernatants of primary human macrophages cultured alone or cultured with OS.

2.3.10 Quantitative RT-PCR

Canine relative mRNA expression of macrophage IL-10, TNF-α, and Arginase: TNF-α, IL-10 and Arginase mRNA expression in human macrophages can aid in differentiating macrophages into M1 versus M2 macrophages. mRNA expression of IL-10 ($p = 0.00596$)

and TNF-α (p = 0.00024) were significantly increased in macrophages cultured with OS compared to macrophages cultured alone (Fig. 12).

Human relative mRNA expression of macrophage IL-10, TNF-α, and Arginase: There were no significant differences in TNF-α (p = 0.4179), IL-10 (p = 0.0672) and Arginase (p = 0.1645) mRNA expression in primary human macrophages cultured alone compared to macrophages cultured with OS.

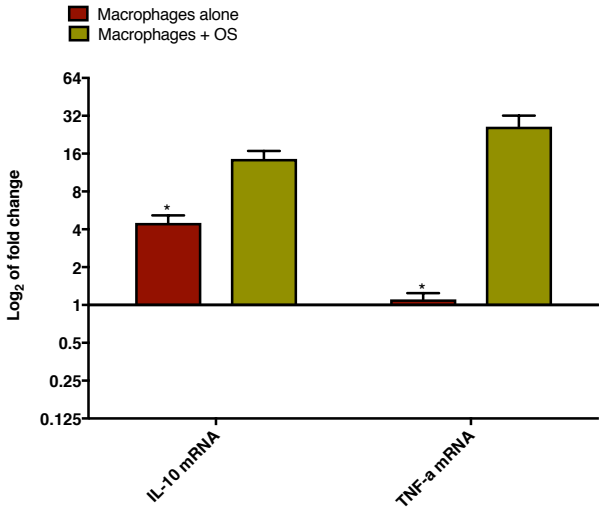

Figure 12: Macrophage IL-10 and TNF-α mRNA expression are increased in the presence of canine OS: Gene expression levels (Log_2 fold change) of IL-10 and TNF-α in canine macrophages cultured alone (n=12) compared to macrophages cultured with OS (n=14). Macrophages cultured with OS had significantly increased mRNA expression of IL-10 (p = 0.00596) and TNF-α (p = 0.00024).

2.4. Discussion

The goal of the studies in this chapter was to determine the effect of OS on monocytes across species – canine, human and murine. We sought to identify differences in

monocyte phenotype and chemotaxis, and macrophage differentiation in OS compared to controls.

Our hypothesis was that evasion of the immune response by OS is due in part to expansion of the non-classical / alternatively activated monocyte subtype, down-regulation of monocyte chemokine receptor expression and migratory function, and suppression of host immune responses as demonstrated by an immunosuppressive cytokine and mRNA signature in monocytes and macrophages. We demonstrated a significant decrease in canine monocyte chemokine receptors, increased PGE_2 and TNF-α secretion by canine monocytes, and decreased monocyte chemotaxis in dogs with OS. We demonstrated a lower proportion of $CD14^{lo}CD16^{hi}$ non-classical monocytes in human OS patients compared to healthy controls, and found that the chemokine receptor expression pattern in OS patients is variable, unlike the uniform decrease in chemokine receptor expression in canine monocytes in OS. We also found mixed monocyte receptor profiles in mice with syngeneic SQ OS and orthotopic OS, some of which were similar findings to canine and human OS patients. We demonstrated that human and canine macrophages cultured with OS exhibited an inflammatory phenotype that had concurrent IL-10 mRNA elevations, thus potentially rendering them inducers of a tumorigenic inflammatory response.

Monocytes display a variety of cell surface receptors, including leukocyte chemokine receptors. The main population of human monocytes (~90% of monocytes) are termed classical monocytes, and are characterized by high CD14 with no CD16 expression ($CD14^{++}CD16^{-}$ or $CD14^{+}CD16^{-}$), and the minor population of monocytes (~10% of monocytes) are subdivided into the intermediate and non-classical subsets. Intermediate

monocytes are characterized by high CD14 with low CD16 expression ($CD14^{++}CD16^{+}$ or $CD14^{+}CD16^{+}$), and non-classical monocytes are characterized by lower CD14 expression relative to the high CD16 expression ($CD14^{+}CD16^{++}$ or $CD14^{dim}CD16^{+}$).[26] CD62L, also known as L-selectin, is a cell adhesion molecule present on immune cells such as monocytes, lymphocytes, and NK cells. CD62L mediates the trafficking of these cells to sites of inflammation and peripheral lymphoid tissue by binding to glycoproteins.[27,28] CCR2, a chemokine receptor for MCP-1, is especially prominent in mediating monocyte migration.[29] Similarly, CCR7 regulates migration of leukocytes to secondary lymphoid organs via binding of its ligands CCL19 and CCL21.[28] CD43 can be found on a variety of immune cells including lymphocytes, granulocytes, monocytes, macrophages, and NK cells, and it plays a role in cell adhesion and migration.[30,31] CX3CR1, and CXCR2, both G protein- coupled chemokine receptors, mediate lymphocyte, monocyte and granulocyte migration.[28] There are few reports describing the effect of OS on monocyte surface receptor expression in dogs. For example, down-regulation of MHC class II and CD80 in canine myeloid cells when exposed to tumor cell lines including OS in vitro has been observed.[32] In humans, the prevalence of an immunosuppressive phenotype in peripheral blood monocytes of OS patients has been observed.[10] Monocytes make up approximately 2-4% of murine leukocytes.[33] Similar to human monocytes, murine monocytes are divided into inflammatory and alternative subpopulations, with the inflammatory monocytes exhibiting high Ly6C expression and alternative monocytes exhibiting low or negative Ly6C expression. $Ly6C^{hi}$ inflammatory monocytes are recruited to inflammatory foci including sites of bacterial infection, where they then carry out defensive microbicidal functions.[34] Alternative $Ly6C^{lo}$ monocytes

typically patrol the endothelium, and are ready to extravasate and migrate to tissue sites of infection, providing a rapid first line of innate immune defense against pathogens prior to the subsequent and more robust recruitment of Ly6C^{hi} inflammatory monocytes to these sites.[35] As early as 2-8 hours post extravasation, alternative Ly6C^{lo} monocytes then cease the production of inflammatory cytokines and upregulate genes involved in tissue repair and remodeling such as arginase, Fizz and mannose receptor (CD206).[35]

We assessed the expression of monocyte surface receptors using flow cytometry, and demonstrated that peripheral blood monocytes from dogs with OS exhibited significantly decreased chemokine receptor expression, namely of CD62L, CCR2, CCR7, CD43, CX3CR1, and CXCR2. This pronounced down-regulation of monocyte chemokine receptors of dogs with OS suggests a peripheral sequestration of monocytes, inhibited from migrating to sites of need such as the primary tumor or metastatic lesions. Two of the chemokine receptors, CCR2 and CXCR2, had significantly higher expression on monocytes of healthy controls with low monocyte counts compared to monocytes of dogs with OS that had high or low monocyte counts. This supports our theory that the decreased expression of chemokine receptors in dogs with OS reflects a peripheral sequestration. There was no difference in the mean peripheral monocyte counts between dogs with OS and healthy controls, which could indicate that this parameter is not as sensitive for detecting a peripheral sequestration compared to analyzing the relationship between chemokine receptors and monocyte counts in both groups of dogs. Alternatively, the lack of difference in mean monocyte counts could also refute our theory of peripheral monocyte sequestration in OS. We found a strong positive correlation between expression of chemokine receptors in healthy controls, whereas

the correlation was less robust in dogs with OS, suggesting a disturbance in the regulation of these chemokine receptors.

The pattern of monocyte cell surface receptor expression in human patients with OS compared to healthy controls did not parallel what we observed in the dog. Human patients with OS had significantly decreased proportion of $CD14^{lo}$ monocytes compared to healthy controls. These $CD14^{lo}$ human monocytes had concurrently high CD16 expression, representing the non-classical subset. Also, these $CD14^{lo}$ human monocytes in OS patients had significantly higher expression of CCR2 compared to healthy controls. High CCR2 expression is more commonly associated with the classical / inflammatory monocyte subtype,[23] and in the context of cancer, CCL2 is an important tumor-derived factor responsible for inducing chemotaxis in monocytes. CCL2 is the ligand that binds to its cognate receptor CCR2, and the CCL2-CCR2 signaling axis has been shown to promote tumor growth and metastasis.[36] It is interesting that higher CCR2 expression is found in the $CD14^{lo}$ human non-classical monocytes in our study. The non-classical monocytes have a patrolling role in the endothelium compared to the classical monocytes that respond to inflammatory stimuli, and their prevalence in our human OS patients could support our hypothesis that OS suppresses the immune response by promoting non-classical monocyte subsets versus classical monocytes that can differentiate into M1 inflammatory macrophages capable of anti-tumor activity. We hypothesize that the increased CCR2 expression on these monocytes in our OS patients represents upregulation of the chemokine receptor by the tumor, promoting monocyte migration to enhance tumorigenesis and metastasis. A future study to further evaluate this hypothesis will be to determine levels of CCL2 in the peripheral

circulation of human OS patients compared to healthy controls. Similar to our findings of decreased monocyte chemokine receptor expression in OS dogs including CXCR2, human OS patients also exhibited decreased CXCR2 expression in CD14+ monocytes and $CD14^{hi}$ monocytes compared to healthy controls. Such lower expression of CXCR2 in monocytes, specifically classical monocytes, may reflect an inhibition of chemotaxis in the subset that can differentiate into anti-tumor M1 macrophages. A follow-up study to assess the migratory capability of classical monocytes of human OS patients compared to healthy control monocytes will determine whether human monocytes have decreased chemotactic ability, such as that found in monocytes of OS dogs. CD64 expression was significantly higher in all monocytes (CD14+) of human OS patients compared to healthy controls. Increased CD64 expression has been documented in patients with lupus nephritis and in septic patients.[37,38] The increase in CD64 expression in monocytes of OS patients could potentially reflect an activation of peripheral monocytes in response to the tumor, but the role of such activation is undetermined. The variation observed in monocyte chemokine receptor expression in human OS patients does not follow the pattern of receptor expression in monocyte subsets, supporting the observation in tumor-bearing mice that peripheral monocytes do not fall into defined subsets.[39]

In our murine studies using the SQ syngeneic OS model, the higher CCR7 expression observed in monocytes from normal control mice compared to mice with OS parallels our previous finding of increased chemokine receptor expression, including CCR7, in monocytes from normal control dogs compared to dogs with untreated OS.[40] We also observed higher CCR2 and lower CXCR4 expression in the $Ly6C^{hi}$ monocytes of tumor-bearing mice

compared to their Ly6C^{lo} monocytes. In tumor-bearing animals, the CCR2-CCL2 axis is important for Ly6C^{hi} monocyte recruitment to the tumor, Ly6C^{hi} monocytes being generally considered as precursors of tumor-associated macrophages (TAM).[41] The higher CCR2 expression in the Ly6C^{hi} monocytes of tumor-bearing mice may represent tumor-driven upregulation of CCR2 expression to facilitate Ly6C^{hi} monocyte migration towards the tumor. CXCR4 over-expression by tumors has been extensively studied, with CXCR4 implicated in the promotion of angiogenesis and metastasis.[42] CXCR4 is normally expressed on monocytes, and a study reported that Ly6C^{hi} murine monocytes in the peripheral circulation uniformly exhibited low CXCR4 expression.[43] Furthermore, CXCR4 monocyte expression regulated monocyte homing and margination to tissue reservoirs such as the lung in response to the CXCL12 ligand.[43] Potentially, CXCR4 expression on the Ly6C^{lo} monocytes of tumor-bearing mice could represent another mechanism by which the tumor recruits monocytes. Interestingly, the findings in the SQ syngeneic model were not reflected in the orthotopic model – when comparisons were made between monocytes from OS-bearing and normal control mice, CCR7 expression was significantly higher in OS-bearing mice, which is opposite of what we found in the SQ syngeneic model. OS mice in the orthotopic model also had higher proportions of both Ly6C^{hi} and Ly6C^{lo} monocytes. The expression pattern of chemokine receptors was varied in the orthotopic model – CXCR4 and CX3CR1 expression had higher expression in normal control mice, reflecting our findings in canine monocytes, whereas CCR2 and CD62L expression were higher in OS-bearing mice, with CCR2 reflecting our findings in human monocytes. Even though the monocyte receptor expression pattern was not uniformly similar across species, our studies have helped identify receptors

that are dysregulated across species, specifically CCR2, CCR7, CXCR2, and CX3CR1, thereby increasing the specificity of follow-up studies focusing on these receptors in monocytes.

A retrospective study of dogs with OS found that dogs with peripheral monocyte counts above 400 cells/μl had a significantly shorter disease-free interval.[21] Similarly, in human OS patients, a low peripheral lymphocyte-to-monocyte ratio (≤3.43) was associated with poorer prognosis for survival and disease-free interval.[44] One possible explanation is that higher monocyte counts reflect a peripheral sequestration of monocytes in dogs that had more rapid tumor progression, and our findings of suppressed expression of multiple monocyte chemokine receptors in dogs with OS suggest such an association. We did not detect a significant overall difference in peripheral monocyte counts of dogs with OS versus healthy controls in our study population. Our Kaplan-Meier survival analysis comparing dogs with OS with high (>400 cells/μl) versus low (<400 cells/μl) monocyte counts did not reveal significant differences in survival between groups. However, we did find that increasing percentages of CCR2 expression on monocytes of dogs with OS was significantly associated with increasing survival, which, in conjunction with our chemotaxis data, suggests that suppression of chemokine receptors and chemotaxis is a form of tumor-mediated monocyte dysfunction.

Additionally, we found that dogs with OS with a peripheral monocyte count of >400 cells/μl exhibited a dichotomy of CD14, CD16 expression on monocytes— CD14 expression was high and CD16 expression was low, when compared to dogs with monocyte counts <400 cells/μl. Human monocytes have been classified into subsets, with different phenotypes and

functions. Earlier classification schemes split human monocytes into $CD14^{hi}CD16^-$ "inflammatory, classical" and $CD14^{low}CD16^+$ "resident, nonclassical" monocytes.[45,46] Recent studies have shown that the CD16+ monocytes can be further characterized into intermediate and non- classical subsets, with the intermediate subset expressing higher CD14 and lower CD16 levels, and the nonclassical subset conversely expressing lower CD14 and higher CD16 levels.[23] The function of these monocyte subsets has not been fully defined, but the intermediate subset appears to produce proinflammatory cytokines such as TNF-a, IL-1b, IL-6, express high levels of MHC II antigen processing and presentation genes, and are potent stimulators of T cells.[23] There are no corresponding studies differentiating canine monocytes into subsets. Based upon human classification, our data suggest that there is an increase in intermediate monocytes in dogs with OS with monocyte counts >400 cells/μl. Potentially, these intermediate monocytes, with their proinflammatory and immunostimulatory capacity, are effective antitumor monocytes that are sequestered in the periphery in OS.

Monocyte migration can be affected by neoplasia. Peripheral monocyte migration is inhibited by lactate concentrations common in tumor microenvironments, and this loss of migratory ability is not because of a reduction in cell viability.[47] Chemokine receptors such as CCR5 are down-regulated in monocytes and macrophages in human patients with head and neck squamous cell carcinoma, leading to dysregulation of chemotactic receptor-ligand signaling and decreased monocyte/macrophage migratory ability.[48] Based on findings by other investigators and our demonstration of profound down-regulation of monocyte chemokine receptors in dogs with OS, we hypothesized that OS inhibits monocyte chemotaxis as an immunosuppressive strategy. Using an in vitro migration assay, we

demonstrated decreased monocyte chemotaxis in dogs with OS compared to healthy controls. This difference was significant when CCL19 was used as a chemoattractant, and when supraphysiologic combinations of chemoattractants were used—a combination of FBS, CCL2, CCL19, and fMLP. CCL19 is a ligand for the chemokine receptor CCR7, and is a known monocyte chemoattractant.[49] 30 There was also decreased monocyte migration in dogs with OS when other known chemokines such as CCL2 or fMLP were used, and even though the differences were not significant, the proximity of the P-value (.067) to significance (.05) suggests that use of these chemokines deserves further evaluation. CCL2 is also known as monocyte chemotactic protein, binds CCR2, and together with fMLP, which binds to G protein-coupled receptors, is used as chemoattractants for monocytes. The significant down-regulation of CCR2 and CCR7 on monocytes of dogs with OS demonstrated by our flow cytometry data supports the observation that monocyte migration is decreased in dogs with OS. The primary disadvantage of our method for assessing migration was the high level of random migration observed, potentially because of excessive stimulation of monocytes by the cell sorting process. As a result, we included supraphysiologic combinations of chemoattractants to counter this potential issue. In our murine studies, we did not observe a similar decrease in monocyte chemotaxis from tumor-bearing mice compared to normal control mice.

There could be a multi-faceted explanation for the down-regulation of monocyte chemokine receptors in dogs with OS. Similar to our findings, the loss of CX3CR1 expression in human monocytes increased glioma growth.[50] However, in contrast to our observations, this tumor-promoting effect is not because of loss of migratory capability. In

fact, the absence of CX3CR1 was associated with an increase in monocyte infiltration into the tumor microenvironment, where the monocytes were theorized to differentiate into tumor-associated macrophages for promotion of tumor growth. Evaluation of the relationship between monocyte chemokine receptor expression and the infiltration of monocytes/macrophages in the tumor microenvironment in OS is needed to explore whether this phenomenon occurs in dogs.

The higher PGE_2 levels that we observed in monocyte culture supernatants of dogs with OS are consistent with our hypothesis that OS suppresses monocyte chemotaxis and the host immune response. PGE_2 is a main metabolite resulting from the conversion of arachidonic acid by cyclooxygenases (COX-1 and COX- 2), and increased levels of COX-2 and PGE_2 have been observed in various tumors.[51-54] PGE_2 secretion from human carcinoma cell lines inhibits monocyte chemotaxis by down-regulating cell surface expression of chemokine and adhesion receptors CCR5 and Mac-1, respectively.[55] Our finding of increased PGE_2 secretion from monocytes of dogs with OS correlates with our observation that monocyte chemotaxis is inhibited in OS. Increased PGE_2 levels have been shown to effect global immunosuppression, contributing to immunopathology in many cancers.[56] For example, PGE_2 disables the innate immune response by inhibiting neutrophils, monocytes and macrophages, and disrupts the cross-talk between dendritic cells and T cells that is essential for activation of the adaptive immune response. PGE_2 also skews T helper cells toward a type 2 pro-tumorigenic instead of a type 1 antitumor response, and promotes the accumulation of T regulatory and myeloid-derived suppressor cells, which can be utilized by the tumor to suppress an effective antitumor response.[56] A recent study in human OS showed

inhibition of human OS cells by decreasing PGE_2 levels via microRNA modulation, demonstrating the role of PGE_2 in tumor promotion.[57] Specifically in OS of dogs, PGE_2 is increased in both canine OS cell lines and in naturally occurring tumors,[58] COX-2, microsomal PGE_2 synthase-1, and PGE_2 receptor are demonstrated to be increased in OS lesions using immunohistochemistry staining,[59] and OS cells from dogs secrete PGE_2.[60] Our findings of increased PGE_2 in dogs with OS are in accordance with these previous reports, and emphasize the ability of PGE_2 to induce immunopathology in OS.

We did not find significant differences in relative mRNA expression of IL-10, IL-12, TNF-α, and COX-2 in monocytes from OS compared to healthy dogs. There was a decreasing trend in COX-2 expression in dogs with OS, but the difference from healthy controls was not significant. This is contrary to what we expected, given the higher PGE_2 secretion from monocytes of dogs with OS, and the overexpression of COX-2 that has been reported in OS of dogs.[59,61] Potentially, there might be other enzymes such as microsomal PGE_2 synthase-1 that could be concurrently influencing the level of PGE_2 secretion. However, as the difference in COX-2 expression between OS and healthy dogs was not statistically significant, whether COX-2 expression in monocytes of dogs with OS is truly decreased needs to be further evaluated, as other influences such as miRNA activity can affect mRNA transcription. Because of potential disparities between mRNA and protein expression, we evaluated monocyte secretion of TNF-α, IFN-γ, and IL-10, using IFN-γ as representative of IL-12 activity. There were low to undetectable levels of IFN-γ and IL-10 from both groups, and higher levels of TNF-α secreted from monocytes of dogs with OS.

This was an unexpected finding, as TNF-α is a proinflammatory cytokine. However, TNF-α induces a number of other changes, particularly in the context of the tumor microenvironment. TNF-α induces the up-regulation of IL-34 expression in OS cell lines, and IL-34 has been associated with progression of disease and promotion of angiogenesis in OS.[62] TNF-α has also been shown to increase the production of PGE_2 as a mechanism for effecting bone resorption.[63] Potentially, the increase in TNF-α in monocytes of dogs with OS reflects tumor-driven mechanisms for OS promotion rather than induction of a proinflammatory monocyte response. Other immunomodulatory cytokines such as TGF-β are utilized by OS for tumor promotion. TGF-β, generally known to dampen immune responses and promote tumor growth, is secreted by OS cells from dogs,[64] and has also been implicated in the pathogenesis of human OS.[65] Collectively, these findings indicate a complex microenvironment that promotes immune dysfunction and tumor growth.

One potential limitation of our canine study is the use of clinical dogs and random source healthy controls, instead of purpose-bred dogs which provide a genetically uniform study population. However, one strong advantage of using nonpurpose-bred dogs is the genetic diversity that accurately reflects that of the general pet population. This diversity, together with the exposure to shared environmental variables with humans, contributes to the unique canine model of spontaneously occurring OS that bears striking similarities to the human disease. As such, we conducted a parallel study in human OS patients to increase the relevance of the common findings across species. Such a canine model of spontaneous

disease is extremely valuable for studying the disease to improve outcomes for both humans and dogs.

For our macrophage studies, we utilized an *ex-vivo* / *in-vitro* method of culturing primary macrophages from healthy canine and human volunteers. In both human and canine macrophages, the presence of OS significantly increases the expression of the co-stimulatory markers CD80 and CD86, suggesting a polarization trend towards M1 macrophages. The surface receptor expression of CCR2 in human macrophages was also decreased in the presence of OS, which also suggests the polarization towards an M2 macrophage in OS. Interestingly, we demonstrated increased MCP-1 (CCL2) cytokine secretion by canine macrophages cultured with OS. We also demonstrated increased TNF-α and IL-10 mRNA expression in canine macrophages cultured with OS. The expression of CCL2 is increased by inflammatory stimuli, inducing IL-10 production, and binding with its cognate receptor CCR2, influences macrophage polarization to an M2 phenotype.[66] Cancer induced inflammation creates a microenvironment of chronic low grade inflammation that promotes tumorigenesis and metastasis, and suppresses an effective anti-tumor immune response.[41] We hypothesize that the presence of OS cells stimulates the polarization of macrophages towards an M1-like phenotype that can effectively maintain a chronic environment of smoldering inflammation, but is not an M1 phenotype that is functionally effective against the tumor. The increased cell surface expression of the macrophage co-stimulatory markers CD80 and CD86, the decreased expression of CCR2 in the presence of OS, and the increased mRNA expression of TNF-α in macrophages cultured with OS support the hypothesis of M1-like polarization induced by OS. TNF-α is one of the major inflammatory cytokines implicated in

maintenance of tumor-induced inflammation, however, it is also involved in anti-tumor inflammatory responses.[41] The increased mRNA expression of IL-10, a major inhibitor of inflammation and a hallmark cytokine of M2 macrophages, in macrophages cultured with OS suggests the induction of macrophages that have a functional inflammatory phenotype, but are inhibited from an appropriate anti-tumor inflammatory response by the prevalence of IL-10. The increased secretion of CCL2 by macrophages cultured with OS could be a mechanism whereby IL-10 mRNA expression is increased in these macrophages, as CCL2 can increase macrophage IL-10 production.[66] However, in spite of the tumor-promoting properties of chronic inflammation, an inflammatory response, if appropriately stimulated and maintained, can be an effective anti-tumor response.[41] Macrophages can be induced to polarize into an M1 phenotype with the ability to kill tumor cells,[41,67] thus finding the appropriate stimulus to re-educate tumor associated macrophages to induce a sustained anti-tumor response represents a key to breaking the development of metastasis in OS and other cancers.

In conclusion, this chapter demonstrated that monocyte chemokine receptors are markedly downregulated in dogs with OS compared to healthy controls, and the expression pattern of CXCR2 in human monocytes, CX3CR1 in murine monocytes parallel the observation in canine monocytes of inhibited chemokine receptor expression in OS. Monocytes from dogs with OS exhibit decreased chemotactic capacity and secrete higher levels of PGE_2 and TNF-α. Our findings strongly suggest that OS in dogs evades the immune system by suppressing chemokine receptor expression and increasing PGE_2 secretion in monocytes, thus inhibiting their migration, leading to sequestration in the periphery.

Increased PGE_2 levels could also promote immunosuppression, as PGE_2 can exert a multitude of immunopathologic effects such as interfering with lymphocyte proliferation and the antitumor cytotoxicity of T cells, inhibit NK cell, dendritic cell, neutrophil, monocyte and macrophage effector functions. Increased TNF-α secretion could be a tumor- promoting mechanism through manipulation of the tumor microenvironment and elevating PGE_2 production. The lower proportion of $CD14^{lo}CD16^{hi}$ non-classical monocytes in human OS patients compared to healthy controls supports our hypothesis of OS-induced immunosuppression, as non-classical monocytes, unlike classical monocytes, do not mount a robust inflammatory response. Through our cross-species evaluation of monocyte surface receptors in OS, we have identified receptors that are dysregulated across species, specifically CCR2, CCR7, CXCR2, and CX3CR1, thereby increasing the specificity and relevance of follow-up studies focusing on these receptors in monocytes. We demonstrated that human and canine macrophages cultured with OS exhibited an inflammatory phenotype that had concurrent IL-10 mRNA elevations, thus potentially rendering them inducers of a tumorigenic inflammatory response. Understanding the mechanisms by which OS causes dysregulation of the immune response will provide insight into developing novel immunotherapeutics to reverse tumor-induced immunopathology and reduce metastatic disease in OS.

REFERENCES

1. Friebele JC, Peck J, Pan X, et al. Osteosarcoma: A Meta-Analysis and Review of the Literature. *Am J Orthop (Belle Mead NJ)* 2015;44:547-553.

2. Selmic LE, Burton JH, Thamm DH, et al. Comparison of carboplatin and doxorubicin-based chemotherapy protocols in 470 dogs after amputation for treatment of appendicular osteosarcoma. *J Vet Intern Med* 2014;28:554-563.

3. Alvarez FJ, Kisseberth W, Hosoya K, et al. Postoperative adjuvant combination therapy with doxorubicin and noncytotoxic suramin in dogs with appendicular osteosarcoma. *J Am Anim Hosp Assoc* 2014;50:12-18.

4. Meazza C, Scanagatta P. Metastatic osteosarcoma: a challenging multidisciplinary treatment. *Expert Rev Anticancer Ther* 2016.

5. da Silveira Nogueira Lima JP, Georgieva M, Haaland B, et al. A systematic review and network meta-analysis of immunotherapy and targeted therapy for advanced melanoma. *Cancer Med* 2017.

6. Malhotra J, Jabbour SK, Aisner J. Current state of immunotherapy for non-small cell lung cancer. *Transl Lung Cancer Res* 2017;6:196-211.

7. Wycislo KL, Fan TM. The immunotherapy of canine osteosarcoma: a historical and systematic review. *J Vet Intern Med* 2015;29:759-769.

8. Wan J, Zhang X, Liu T, et al. Strategies and developments of immunotherapies in osteosarcoma. *Oncol Lett* 2016;11:511-520.

9. Mason NJ, Gnanandarajah JS, Engiles JB, et al. Immunotherapy with a HER2-Targeting Listeria Induces HER2-Specific Immunity and Demonstrates Potential Therapeutic Effects in a Phase I Trial in Canine Osteosarcoma. *Clin Cancer Res* 2016;22:4380-4390.

10. Hingorani P, Maas ML, Gustafson MP, et al. Increased CTLA-4(+) T cells and an increased ratio of monocytes with loss of class II (CD14(+) HLA-DR(lo/neg)) found in aggressive pediatric sarcoma patients. *J Immunother Cancer* 2015;3:35.

11. Pahl JH, Kwappenberg KM, Varypataki EM, et al. Macrophages inhibit human osteosarcoma cell growth after activation with the bacterial cell wall derivative liposomal muramyl tripeptide in combination with interferon-gamma. *J Exp Clin Cancer Res* 2014;33:27.

12. Xiao Q, Zhang X, Wu Y, et al. Inhibition of macrophage polarization prohibits growth of human osteosarcoma. *Tumour Biol* 2014;35:7611-7616.

13. Sottnik JL, U'Ren LW, Thamm DH, et al. Chronic bacterial osteomyelitis suppression of tumor growth requires innate immune responses. *Cancer Immunol Immunother* 2010;59:367-378.

14. Buddingh EP, Kuijjer ML, Duim RA, et al. Tumor-infiltrating macrophages are associated with metastasis suppression in high-grade osteosarcoma: a rationale for treatment with macrophage activating agents. *Clin Cancer Res* 2011;17:2110-2119.

15. Gustafson MP, Lin Y, New KC, et al. Systemic immune suppression in glioblastoma: the interplay between CD14+HLA-DRlo/neg monocytes, tumor factors, and dexamethasone. *Neuro Oncol* 2010;12:631-644.

16. Lin Y, Gustafson MP, Bulur PA, et al. Immunosuppressive CD14+HLA-DR(low)/- monocytes in B-cell non-Hodgkin lymphoma. *Blood* 2011;117:872-881.

17. Vuk-Pavlovic S, Bulur PA, Lin Y, et al. Immunosuppressive CD14+HLA-DRlow/- monocytes in prostate cancer. *Prostate* 2010;70:443-455.

18. Walkley CR, Qudsi R, Sankaran VG, et al. Conditional mouse osteosarcoma, dependent on p53 loss and potentiated by loss of Rb, mimics the human disease. *Genes Dev* 2008;22:1662-1676.

19. Sanchez-Robert E, Altet L, Alberola J, et al. Longitudinal analysis of cytokine gene expression and parasite load in PBMC in Leishmania infantum experimentally infected dogs. *Vet Immunol Immunopathol* 2008;125:168-175.

20. Clemente M, Sanchez-Archidona AR, Sardon D, et al. Different role of COX-2 and angiogenesis in canine inflammatory and non-inflammatory mammary cancer. *Vet J* 2013;197:427-432.

21. Sottnik JL, Rao S, Lafferty MH, et al. Association of blood monocyte and lymphocyte count and disease-free interval in dogs with osteosarcoma. *J Vet Intern Med* 2010;24:1439-1444.

22. Smedman C, Ernemar T, Gudmundsdotter L, et al. FluoroSpot analysis of TLR-activated monocytes reveals several distinct cytokine secreting subpopulations. *Scand J Immunol* 2011.

23. Wong KL, Yeap WH, Tai JJ, et al. The three human monocyte subsets: implications for health and disease. *Immunol Res* 2012;53:41-57.

24. Ma X, You X, Zeng Y, et al. Mycoplasma fermentans MALP-2 induces heme oxygenase-1 expression via mitogen-activated protein kinases and Nrf2 pathways to modulate cyclooxygenase 2 expression in human monocytes. *Clin Vaccine Immunol* 2013;20:827-834.

25. Beyan H, Goodier MR, Nawroly NS, et al. Altered monocyte cyclooxygenase response to lipopolysaccharide in type 1 diabetes. *Diabetes* 2006;55:3439-3445.

26. Ziegler-Heitbrock L, Ancuta P, Crowe S, et al. Nomenclature of monocytes and dendritic cells in blood. *Blood* 2010;116:e74-80.

27. Ivetic A. Signals regulating L-selectin-dependent leucocyte adhesion and transmigration. *Int J Biochem Cell Biol* 2013;45:550-555.

28. Thomas S, Baumgart DC. Targeting leukocyte migration and adhesion in Crohn's disease and ulcerative colitis. *Inflammopharmacology* 2012;20:1-18.

29. Yadav A, Saini V, Arora S. MCP-1: chemoattractant with a role beyond immunity: a review. *Clin Chim Acta* 2010;411:1570-1579.

30. Steiniger B, Stehling O, Scriba A, et al. Monocytes in the rat: phenotype and function during acute allograft rejection. *Immunol Rev* 2001;184:38-44.

31. Axelsson B, Perlmann P. Persistent superphosphorylation of leukosialin (CD43) in activated T cells and in tumour cell lines. *Scand J Immunol* 1989;30:539-547.

32. Wasserman J, Diese L, VanGundy Z, et al. Suppression of canine myeloid cells by soluble factors from cultured canine tumor cells. *Vet Immunol Immunopathol* 2012;145:420-430.

33. Italiani P, Boraschi D. From Monocytes to M1/M2 Macrophages: Phenotypical vs. Functional Differentiation. *Front Immunol* 2014;5:514.

34. Shi C, Pamer EG. Monocyte recruitment during infection and inflammation. *Nat Rev Immunol* 2011;11:762-774.

35. Auffray C, Fogg D, Garfa M, et al. Monitoring of blood vessels and tissues by a population of monocytes with patrolling behavior. *Science* 2007;317:666-670.

36. Lim SY, Yuzhalin AE, Gordon-Weeks AN, et al. Targeting the CCL2-CCR2 signaling axis in cancer metastasis. *Oncotarget* 2016;7:28697-28710.

37. Li Y, Lee PY, Sobel ES, et al. Increased expression of FcgammaRI/CD64 on circulating monocytes parallels ongoing inflammation and nephritis in lupus. *Arthritis Res Ther* 2009;11:R6.

38. Groselj-Grenc M, Ihan A, Derganc M. Neutrophil and monocyte CD64 and CD163 expression in critically ill neonates and children with sepsis: comparison of fluorescence intensities and calculated indexes. *Mediators Inflamm* 2008;2008:202646.

39. Caso R, Silvera R, Carrio R, et al. Blood monocytes from mammary tumor-bearing mice: early targets of tumor-induced immune suppression? *Int J Oncol* 2010;37:891-900.

40. Tuohy JL, Lascelles BD, Griffith EH, et al. Association of Canine Osteosarcoma and Monocyte Phenotype and Chemotactic Function. *J Vet Intern Med* 2016;30:1167-1178.

41. Mantovani A, Allavena P, Sica A, et al. Cancer-related inflammation. *Nature* 2008;454:436-444.

42. Owen JL, Mohamadzadeh M. Macrophages and chemokines as mediators of angiogenesis. *Front Physiol* 2013;4:159.

43. Chong SZ, Evrard M, Devi S, et al. CXCR4 identifies transitional bone marrow premonocytes that replenish the mature monocyte pool for peripheral responses. *J Exp Med* 2016;213:2293-2314.

44. Liu T, Fang XC, Ding Z, et al. Pre-operative lymphocyte-to-monocyte ratio as a predictor of overall survival in patients suffering from osteosarcoma. *FEBS Open Bio* 2015;5:682-687.

45. Gordon S, Taylor PR. Monocyte and macrophage heterogeneity. *Nat Rev Immunol* 2005;5:953-964.

46. Varol C, Yona S, Jung S. Origins and tissue-context-dependent fates of blood monocytes. *Immunol Cell Biol* 2009;87:30-38.

47. Goetze K, Walenta S, Ksiazkiewicz M, et al. Lactate enhances motility of tumor cells and inhibits monocyte migration and cytokine release. *Int J Oncol* 2011;39:453-463.

48. Chakraborty K, Bose A, Chakraborty T, et al. Restoration of dysregulated CC chemokine signaling for monocyte/macrophage chemotaxis in head and neck squamous cell carcinoma patients by neem leaf glycoprotein maximizes tumor cell cytotoxicity. *Cell Mol Immunol* 2010;7:396-408.

49. Frascaroli G, Varani S, Moepps B, et al. Human cytomegalovirus subverts the functions of monocytes, impairing chemokine-mediated migration and leukocyte recruitment. *J Virol* 2006;80:7578-7589.

50. Feng X, Szulzewsky F, Yerevanian A, et al. Loss of CX3CR1 increases accumulation of inflammatory monocytes and promotes gliomagenesis. *Oncotarget* 2015.

51. Eberhart CE, Coffey RJ, Radhika A, et al. Up-regulation of cyclooxygenase 2 gene expression in human colorectal adenomas and adenocarcinomas. *Gastroenterology* 1994;107:1183-1188.

52. Wolff H, Saukkonen K, Anttila S, et al. Expression of cyclooxygenase-2 in human lung carcinoma. *Cancer Res* 1998;58:4997-5001.

53. Pugh S, Thomas GA. Patients with adenomatous polyps and carcinomas have increased colonic mucosal prostaglandin E2. *Gut* 1994;35:675-678.

54. Rigas B, Goldman IS, Levine L. Altered eicosanoid levels in human colon cancer. *J Lab Clin Med* 1993;122:518-523.

55. Zeidler R, Csanady M, Gires O, et al. Tumor cell-derived prostaglandin E2 inhibits monocyte function by interfering with CCR5 and Mac-1. *FASEB J* 2000;14:661-668.

56. Kalinski P. Regulation of immune responses by prostaglandin E2. *J Immunol* 2012;188:21-28.

57. Xu H, Mei Q, Shi L, et al. Tumor-suppressing effects of miR451 in human osteosarcoma. *Cell Biochem Biophys* 2014;69:163-168.

58. Mohammed SI, Coffman K, Glickman NW, et al. Prostaglandin E2 concentrations in naturally occurring canine cancer. *Prostaglandins Leukot Essent Fatty Acids* 2001;64:1-4.

59. Millanta F, Asproni P, Cancedda S, et al. Immunohistochemical expression of COX-2, mPGES and EP2 receptor in normal and reactive canine bone and in canine osteosarcoma. *J Comp Pathol* 2012;147:153-160.

60. Shor S, Fadl-Alla BA, Pondenis HC, et al. Expression of nociceptive ligands in canine osteosarcoma. *J Vet Intern Med* 2015;29:268-275.

61. Mullins MN, Lana SE, Dernell WS, et al. Cyclooxygenase-2 expression in canine appendicular osteosarcomas. *J Vet Intern Med* 2004;18:859-865.

62. Segaliny AI, Mohamadi A, Dizier B, et al. Interleukin-34 promotes tumor progression and metastatic process in osteosarcoma through induction of angiogenesis and macrophage recruitment. *Int J Cancer* 2015;137:73-85.

63. Zhang W, Dziak R. Tumor necrosis factor alpha stimulates arachidonic acid metabolism in human osteoblastic osteosarcomal cells. *Prostaglandins Leukot Essent Fatty Acids* 1996;54:427-431.

64. Portela RF, Fadl-Alla BA, Pondenis HC, et al. Pro-tumorigenic effects of transforming growth factor beta 1 in canine osteosarcoma. *J Vet Intern Med* 2014;28:894-904.

65. Xu S, Yang S, Sun G, et al. Transforming growth factor-beta polymorphisms and serum level in the development of osteosarcoma. *DNA Cell Biol* 2014;33:802-806.

66. Sierra-Filardi E, Nieto C, Dominguez-Soto A, et al. CCL2 shapes macrophage polarization by GM-CSF and M-CSF: identification of CCL2/CCR2-dependent gene expression profile. *J Immunol* 2014;192:3858-3867.

67. Mantovani A, Bottazzi B, Colotta F, et al. The origin and function of tumor-associated macrophages. *Immunol Today* 1992;13:265-270.

CHAPTER 3

A cross-species evaluation of the effects of *Staphylococcus aureus* on OS in monocytes and macrophages

3.1 Introduction

The concept of enhancing the immune system for anti-cancer therapy is not a new one. In the early 1900's, William B. Coley, a surgeon in New York, noted concurrent tumor regression in some patients with a bacterial infection. Erysipelas infections, caused primarily by group A *Streptococci*, were most commonly associated with the patients whose tumors regressed. Coley developed vaccine concoctions of bacterial organisms, most commonly heat-killed *Streptococcus* combined with *Serratia marcescens*, and administered what became known as Coley's Toxins to hundreds of patients, some of whom reportedly experienced tumor regression.[1] Since Coley's trials with his vaccine, the multi-dimensional effects of streptococcal exotoxin have been explored as immune stimulators creating an anti-tumor response.[2] The immune reaction caused by local *Streptococci* infection in the dermis of a typical Erysipelas patient is characterized by an innate local inflammatory response orchestrated by monocytes, macrophages, neutrophils and dendritic cells.[2] For example, TNF-α and IL-1β are secreted by monocytes and macrophages in response to *Streptococcus*, and these cytokines can trigger a downstream T-cell adaptive response.[2,3] Furthermore, the lipotechoic acid of the streptococcal cell wall can be a T-cell mitogen.[2] There also is the hypothesis that an Erysipelas infection can lead to inappropriate accumulation of translocated gastrointestinal endotoxin and subsequent initiation of an innate inflammatory response with its accompanying cytokine cascade.[2] A fundamental factor influencing the effectiveness of an

anti-tumor response in the presence of a bacterial infection is tumor immunogenicity, which is the ability of a tumor to be recognized by the immune system, resulting in an immune response. Murine models have been used to demonstrate the importance of tumor immunogenicity in the success of treating tumors with bacterial endotoxin.[4] Mice inoculated with immunogenic tumor strains can experience complete tumor regression that requires a T-cell adaptive response, whereas mice inoculated with non-immunogenic tumors only experienced transient hemorrhagic necrosis of their tumors with subsequent tumor regrowth.[4,5] Given the observation that a history of infection with *Mycobacterium tuberculosis* enhances the sensitivity of laboratory animals to endotoxin, an interesting hypothesis has been submitted – that combination therapy with Bacille-Calmette-Guerin (BCG) vaccination and Coley's vaccine is needed to reproduce the therapeutic effectiveness of the vaccine.[2]

Since the time of Coley's observations and clinical experimentation with his vaccine, observations have been made in OS that support the immunogenic potential of the tumor – in clinical dogs with OS, increased survival times have been observed in patients with surgical site infections after surgery to remove the primary tumor.[6-8] Similar observations have been made in human OS patients.[9,10] The effects of infection on OS have been evaluated using murine models. A study utilizing a syngeneic subcutaneous model of murine OS and bacterial osteomyelitis demonstrated induction of anti-OS activity in tumor-bearing mice with concurrent bacterial osteomyelitis, and also demonstrated the importance of monocytes and macrophages in shaping the anti-tumor response.[11] Additionally, studies have showed potential efficacy of liposomal encapsulated muramyl tripeptide phosphatidyl ethanolamine

(L-MTP-PE), a synthetic derivative of muramyl dipeptide (MDP), a bacterial cell wall component in both gram-positive and gram-negative bacterial cell walls, against OS.[12-15] The clinical observations of improved survival in OS with infection, together with the potential therapeutic efficacy of L-MTP-PE, provide strong support to the hypothesis that OS is an immunogenic tumor that can be targeted by an immune response upregulated by a bacterial agent. This chapter describes how *in vivo* infection or *ex vivo* exposure to a bacterial agent (*Staphylococcus aureus*) influenced the phenotype of monocytes and macrophage differentiation in the presence of OS. Comparisons were made between the dog, human, and mouse, wherever possible. Our hypothesis was that infection will reverse the phenotypic changes in monocytes associated with OS, and that *S. aureus* will induce an inflammatory macrophage phenotype (M1-like) in the presence of OS.

3.2 Materials and Methods

Monocyte Studies

3.2.1 Patient enrollment and sample preparation – canine

Canine monocyte samples: Client-owned dogs diagnosed with OS that were determined to have a surgical site infection associated with primary tumor removal were enrolled into the study. The criteria for determining a surgical wound infection include a positive culture, or in the absence of a positive culture, clinical signs of an infection (limb swelling, wound drainage, radiographic evidence). Enrolled patients were required to have an active infection at time of blood collection for the study. Due to the low incidence of these clinical cases, recruitment forms were sent to participating institutions in North America. An

institution with an eligible patient collected peripheral blood samples to be shipped overnight on ice to North Carolina State University (NCSU) together with requested information about the patient. Client-owned dogs diagnosed with OS that received standard-of-care therapy (limb amputation for primary tumor removal followed by adjuvant chemotherapy) were also enrolled into the study to serve as treated controls. Peripheral blood mononuclear cells (PBMCs) were isolated as described in Chapter 2 (2.2.2).

3.2.2 Murine model of OS + osteomyelitis

OS induction: A SQ syngeneic OS model was established in C3H-HeN mice with a subcutaneous injection of 2 x 10^8 DLM8 murine OS cells suspended in 30 µl HBSS into the right flank region. Tumor growth at the widest diameter was measured 2-3 times weekly using calipers, and mice were euthanized when their individual tumors measured 18 mm in diameter.

Osteomyelitis establishment: *Staphylococcus aureus* (XEN36) with stable expression of the luciferin and luciferase genes (Perkin Elmer, Waltham, MA) was used for inducing bacterial osteomyelitis. Bacteria were grown to log phase in LB Broth, then stored in frozen aliquots at -80°C. Bacterial osteomyelitis was induced in the distal femur of the mice, using a technique modified from what was previously reported.[11] The XEN36 *S. aureus* were cultured in sterile LB broth in a shaking incubator at 37°C and 180 rpm for 5-6 hours to achieve log growth. The *S. aureus* were then counted using a SmartSpec™ Plus spectrophotometer and diluted using LB broth to a concentration of 1 x 10^8 CFUs/ml, and 1 ml of the diluted bacteria was placed in each well of a 24-well culture plate. One 12 mm segment of 6-0 Silk suture was placed in each well, and incubated in a shaking incubator for

36 hours at 37°C and 100 rpm, with media changes performed every 12 hours. The suture were then imaged using an IVIS® Lumina imaging system and the Living Image® version 4.2 software with a 30-second exposure time and medium sensitivity binning to confirm bacterial adherence to the suture. Mice were anesthetized using an intraperitoneal injection of ketamine (150 mg/kg) and xylazine (10 mg/kg) for suture implantation. The distal femur was clipped and prepped aseptically using chlorhexidine gluconate scrub and sterile saline. A 1 mm skin incision was made on the lateral aspect of the left distal femur with a #10 surgical blade to facilitate accurate placement of the needle. A 25-gauge Monoject™ needle was inserted transversely through the distal femur in a lateromedial direction, after which a piece of suture with adherent bacteria was threaded into the tip of the needle, and the tip of the needle crushed using a needle holder to increase the security of the suture within the needle tip. The needle was then withdrawn, effectively pulling the suture through the distal femur. The ends of the suture on the medial and lateral aspects of the distal femur were cut flush with the skin, and the medial skin incision was apposed using tissue adhesive. The mice were administered a subcutaneous dose of buprenorphine (0.05 mg/kg) during recovery from anesthesia. *In vivo* luciferase imaging was used to monitor luminescence indicative of *S. aureus*. The distal femora of all mice were imaged in the immediate post-operative period to confirm positive emission of luminescence from the implanted suture. The IVIS® Lumina imaging system and the Living Image® version 4.2 software with a 60-second exposure time, and high sensitivity binning was used for *in vivo* imaging. Subsequently, the mice were anesthetized with isoflurane for imaging 1-2 times weekly to assess the presence of

luminescence in the distal femora. At time of euthanasia, the left distal femur was aseptically harvested, placed in 25 mls of LB broth, and cultured at 37°C. When the LB broth exhibited gross evidence of organism growth, the broth was plated onto a blood agar plate. The resultant bacterial colonies were visually examined to determine whether they were pure cultures. The bacterial colonies were imaged using the IVIS® Lumina imaging system and the Living Image® version 4.2 software with a 5-second exposure time and medium sensitivity binning to confirm an osteomyelitis with luminescent XEN36 *S. aureus*.

3.2.3 Flow cytometry (FACS)

Cell staining for flow cytometry, gating strategies and analysis were performed as described in Chapter 2 (2.2.4). The antibodies used were the same as those listed in 2.2.4.

3.2.4 Total RNA extraction, reverse transcription, and quantitative RT-PCR

Murine tumors: Tumor samples were collected at euthanasia, placed in RNALater® and stored at -80°C for subsequent PCR analysis. Thawed tumor samples were homogenized in Tri-Reagent (Zymo Research) using Zirconia grinding beads (BioSpec) oscillating at 30-second intervals in the Mini Bead Beater Mill (Cole-Parmer). The Direct Zol RNA Miniprep™ kit (Zymo Research) was used to extract total RNA from tumor samples according to the manufacturer's protocol. The concentration and quality of the extracted RNA was determined using a NanoDrop 2000c spectrophotometer as well as the Agilent Bioanalyzer, and the RNA samples were stored at -80°C until processing. Immediately prior to RT reactions, DNase treatment was applied to all RNA samples using the Ambion® TURBO DNA-*free*™ kit. cDNA was synthesized from 1000 ng RNA per sample using the

QuantaBio qScript™ cDNA synthesis kit according to manufacturer's directions, and the RT reactions were carried out in a GeneAmp®PCR System 9700 thermal cycler. mRNA gene expression was determined with SYBR Green qPCR using the QuantaBio PerfeCTa® SYBR Green FastMix® per manufacturer's directions, and reactions cycled in a Roche Lightcycler 480. All samples were run in triplicate. Primers for detection of mRNA expression levels of Arginase, Fizz, IL-6, TNF-α, CD206, β-actin, and GAPDH (Table 1) were selected based on previous reports and purchased from Life Technologies, Inc.[16] The qPCR cycling conditions were as follows: denaturation at 95°C for 1 minute, followed by 95°C for 5 seconds, 60°C for 15 seconds, 72°C for 10 seconds, for a total of 45 cycles. The PCR product was sequenced by GENEWIZ® DNA sequencing services, and the sequences were subjected to alignment searches in the NCBI database to confirm matches with the gene of interest. Expression of the target genes was normalized to expression of the housekeeping genes GAPDH and β-actin. The $2^{-\Delta\Delta CT}$ method was used to calculate the normalized relative mRNA expression of the target genes.

Table 1: **Quantitative RT-PCR primers to detect mRNA expression levels of inflammatory and macrophage markers in murine OS tissue**

Target	(5' – 3')
Arginase (F)	CAGAAGAATGGAAGAGTCAG
Arginase (R)	CAGATATGCAGGGAGTCACC
Fizz (F)	GGTCCCAGTGCATATGGATGAGACCATAGA
Fizz (R)	CACCTCTTCACTCGAGGGACAGTTGGCAGC
IL-6 (F)	GAGGATACCACTCCCAACAGACC
IL-6 (R)	AAGTGCATCATCGTTGTTCATACA
TNF-α (F)	CCTGTAGCCCACGTCGTAGC
TNF-α (R)	AGCAATGACTCCAAAGTAGACC
CD206 (F)	CTCTGTTCAGCTATTGGACGC
CD206 (R)	CGGAATTTCTGGGATTCAGCTTC

3.2.5 Chemotaxis assay

Murine monocyte chemotaxis assays were performed as previously described in Chapter 2 (2.2.6).

Macrophage Studies

Volunteer enrollment for macrophage studies was carried out as described in Chapter 2 (2.2.9), and primary macrophages were cultured from canine and human samples as described in Chapter 2 (2.2.10).

For experimental groups that required addition of live *S. aureus* to the macrophage-OS co-culture, antibiotic-free culture media was used to establish primary macrophage

cultures, and at 48 hours, *S. aureus* was added using the following method. A frozen aliquot of XEN36 *S. aureus* was thawed and a 100 µl added to 25 mls LB broth in an Erlenmeyer flask. The flask was placed in a 37°C shaker at 200 rpm until an O.D. of 0.8 was reached. The bacteria were then washed twice with 25 mls PBS and pelleted by centrifugation at 8000 rpm for 10 minutes. The pelleted bacteria were resuspended in antibiotic-free media and diluted 1:10 for addition of 1 ml (resulting in approximately 2 x 10^7 cfu/ml *S. aureus* to achieve a MOI of 1:50) to each well of a 12-well culture plate containing primary macrophages. The plates were incubated for 30 minutes for macrophage phagocytosis of bacteria at 37°C, 5% CO_2, after which the media containing XEN36 *S. aureus* was removed from the wells, taking care to not disturb the adherent layer of primary macrophages. The wells were washed twice with HBSS with calcium and magnesium, followed by the addition of media containing 50 µg/ml concentration of Gentamicin to kill the extracellular bacteria. The plates were incubated for 60 minutes at 37°C, 5% CO_2, after which the media was removed and plated onto blood agar plates to confirm the absence of extracellular bacteria. The cells were washed twice with HBSS with calcium and magnesium. Media containing 10 µg/ml concentration of Gentamicin was added to the wells, and the plates cultured for an additional 48 hours at 37°C, 5% CO_2. Two wells were used for each plate to measure the number of phagocytosed bacteria – 1 ml 0.1% Triton X was added to each well to lyse the macrophages, and the Triton X solution plated on blood agar plates for counting number of bacteria phagocytosed. Intracellular bacterial counts were determined to be within a logarithmic difference between samples.

Macrophage flow cytometry experiments, culture supernatant cytokine level measurements, quantitative RT-PCR experiments were performed as described in Chapter 2 (2.2.11-2.2.14). Statistical analyses were performed as described in Chapter 2 (2.2.15).

3.3. Results

Monocyte Studies

3.3.1 Study populations

Canine: Nine dogs with OS and a concurrent surgical site infection were recruited for the study.

Murine: Female C3H-HeN inbred mice were used to establish the SQ syngeneic OS model. All C3H-HeN mice were 8-10 weeks of age, weighed 40-45 grams, and purchased from Charles River Laboratories (Raleigh, NC). Mice were housed 4 to a cage in a temperature-controlled room with a 12:12-hour automated light/dark cycle, and fed a standardized commercial pelleted diet. All mice underwent a 14-day acclimatization period before starting the study. There were 13 mice with OS and osteomyelitis. Bacterial osteomyelitis was successfully induced in mice, as indicated by positive luciferase imaging of the distal femur, and / or positive bacterial cultures of the bacterial implantation site in the distal femur post euthanasia. All bacterial cultures were positive for luminescence, confirming the identity of XEN 36 *Staphylococcus aureus*. (Fig. 1).

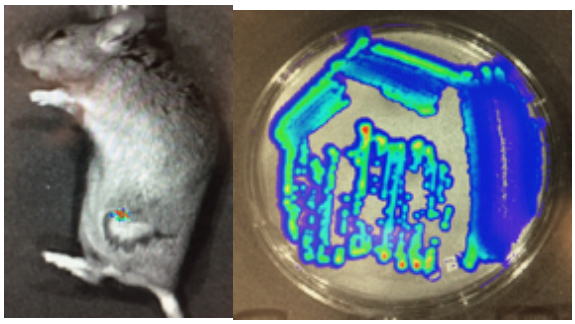

Figure 1. Induction of bacterial osteomyelitis. Mice were inoculated with luciferase positive XEN36 *S. aureus* as described in the methods. (A.) Osteomyelitis was confirmed following femoral inoculation using luminescence live imaging in anesthetized mice. (B.) Following euthanasia, the femur was asceptically harvested and cultured as described in the methods. Luciferase positive bacterial cultures confirmed the presence of pure luminescent *XEN36 S. aureus*.

3.3.2 Flow cytometry

Canine monocytes: The primary flow cytometry canine monocyte gates were based on typical forward and side scatter characteristics. Once that forward versus side light scatter gate was established, we ensured that greater than 98% of the CD14+ cells were found within this gate. As CD14 expression on peripheral blood monocytes varies greatly, this ensured that we included the $CD14^{lo}$ monocytes for surface receptor analysis. Canine monocytes exhibited positive surface expression of CD14, CD16, CD62L, CCR2, CCR7, CD43, CX3CR1, CXCR2. Irrelevant isotype controls were used for each experiment—the isotype control binding of monocytes was <5%. The median percentages and ranges of positively staining cells for each antibody are listed in the legend accompanying Figure 2, and data from the OS dogs with an infection were compared to the data previously presented in Chapter 2, Figure 1a. Comparison of monocyte surface receptors between healthy controls, untreated dogs with OS, dogs with OS that had a concurrent surgical site infection revealed a

significant increase in surface receptor expression of CD14 between controls and infected OS dogs ($p<0.0001$), and between untreated OS dogs and infected OS dogs ($p<0.0001$); a significant increase in CD16 expression in untreated OS dogs compared to controls (see Chapter 2, Figure 1a), and in OS dogs with infection compared to untreated OS dogs and controls ($p<0.0001$, $p=0.0007$ respectively); a significant decrease in CCR2 expression in untreated OS dogs compared to controls (see Chapter 2, Figure 1a), and a significant increase in OS dogs with infection compared to untreated OS dogs ($p<0.0001$); a significant decrease in CCR7 expression in untreated OS dogs compared to controls (see Chapter 2, Figure 1a), and a significant increase in OS dogs with infection compared to untreated OS dogs ($p=0.0012$); a significant decrease in CX3CR1 expression in untreated OS dogs compared to controls (see Chapter 2, Figure 1a), and a significant increase in OS dogs with infection compared to untreated OS dogs and controls ($p=0.0002$, $p=0.044$ respectively); a significant decrease in CXCR2 expression in untreated OS dogs compared to controls (see Chapter 2, Figure 1a), and a significant increase in OS dogs with infection compared to untreated OS dogs ($p=0.0023$). Even though there were no significant differences in CD62L and CD43 expression in OS dogs with infection compared to untreated OS dogs and controls, expression of CD62L and CD43 displayed an increased trend in infected OS dogs compared to untreated OS dogs. The treatment control group of OS dogs that received standard-of-care therapy (amputation + chemotherapy) exhibited significantly decreased expression of monocyte chemokine receptors compared to normal controls, and the degree of receptor downregulation was similar to that in untreated OS dogs (Supplemental Figure 1). These data suggest that the upregulation of monocyte chemokine receptors in OS dogs with an infection

is associated with the presence of an infection rather than removal of the primary tumor or adjuvant chemotherapy.

Figure 2: Monocyte surface marker expression is altered in dogs with OS, and in dogs with OS + infection

Flow cytometry plots illustrating cell surface receptor expression in peripheral blood monocytes from dogs with OS (n = 18), healthy controls (n = 13), and dogs with OS and an infection (n = 9). (A) Box-and-whisker plot depicting the % positive monocyte cell surface receptor expression of the different receptors (CD14, CD16, CD62L, CCR2, CCR7, CD43, CX3CR1, CXCR2), comparing expression between healthy controls, dogs with OS, and dogs with OS + infection. The median percentages and ranges of positively staining cells for each antibody in healthy controls are as follows: CD14 (15%, 3–84%), CD16 (9%, 0.5–24%), CD62L (31%, 10–75%), CCR2 (58%, 2–94%), CCR7 (36%, 1–90%), CD43 (52%, 2–93%), CX3CR1 (9%, 0.2–87%), and CXCR2 (54%, 2–92%). The median percentages and ranges of positively staining cells for each antibody in dogs with OS are as follows: CD14 (29%, 2–82%), CD16 (24%, 3–76%), CD62L (11%, 3–36%), CCR2 (29%, 3–45%), CCR7 (8%, 0.1–41%), CD43 (28%, 3–47%), CX3CR1 (5%, 0.6–70%), and CXCR2 (23%, 0.2–52%). The median percentages and ranges of positively staining cells for each antibody in dogs with OS plus an infection are as follows: CD14 (78%, 12–99%), CD16 (64%, 32–79%), CD62L (21%, 3–57%), CCR2 (68%, 50–87%), CCR7 (41%, 6–90%), CD43 (37%, 9–63%), CX3CR1 (56%, 16–86%), and CXCR2 (57%, 23–65%).Significant differences are marked with an asterisk ($p < 0.05$).

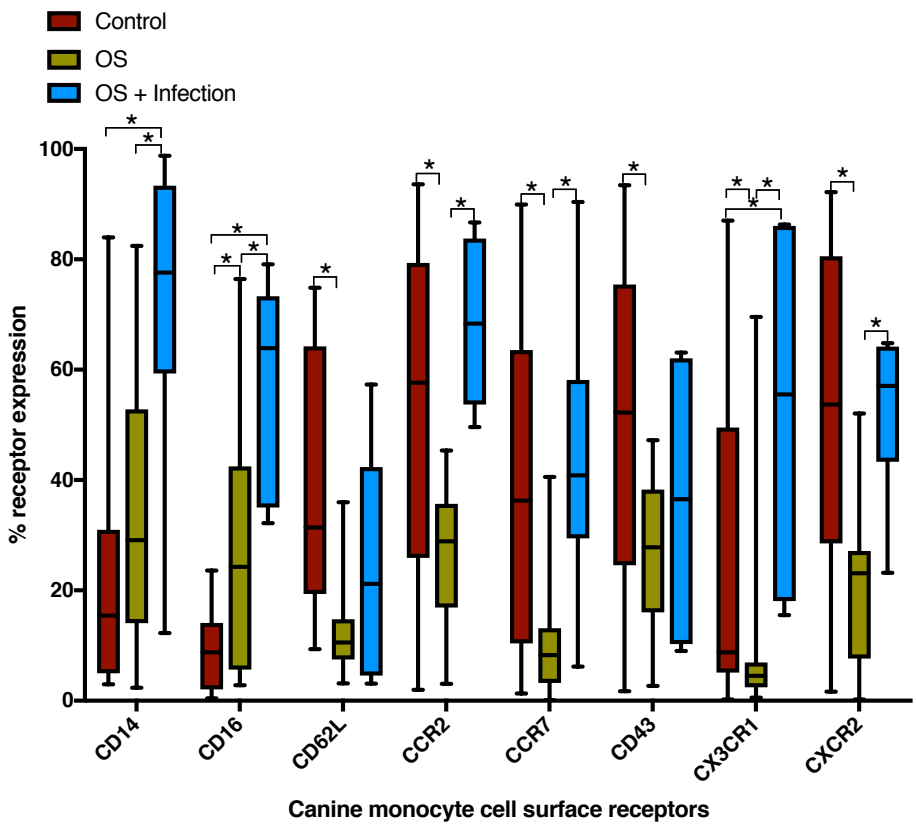
Control
OS
OS + Infection
% receptor expression
100
80
60
40
20
0
CD14
CD16
CD62L
CCR2
CCR7
CD43
CX3CR1
CXCR2
Canine monocyte cell surface receptors

Murine monocytes: Based on our findings reported above in canine monocytes - that monocyte chemokine receptors were significantly downregulated in dogs with OS compared to normal controls, and OS dogs with infection display increased monocyte receptor expression compared to untreated OS dogs, we compared monocyte surface receptors between mice with OS, mice with OS and osteomyelitis, and normal control mice to determine whether a similar effect could be observed in mice. The median percentages and ranges of positively staining cells for each antibody are listed in the legend accompanying Figure 3, and data from the osteomyelitis mice were compared to the data previously presented in Chapter 2, Figure 5. Osteomyelitis mice exhibited a significantly greater proportion of $Ly6C^{lo}$ monocytes compared normal control mice ($p = 0002$), tumor control mice ($p = 0.0184$). Next, when surface receptor expression was evaluated for all monocytes, CCR7 expression was significantly higher in monocytes of normal control mice compared to tumor control mice ($p = 0.0146$) and osteomyelitis mice ($p = 0.0012$). When surface receptor expression was evaluated between the monocyte subsets, CCR7 expression was significantly higher in the $Ly6C^{lo}$ monocytes of normal control mice compared to tumor control mice ($p = 0.0004$) and osteomyelitis mice ($p < 0.0001$) (Fig. 3).

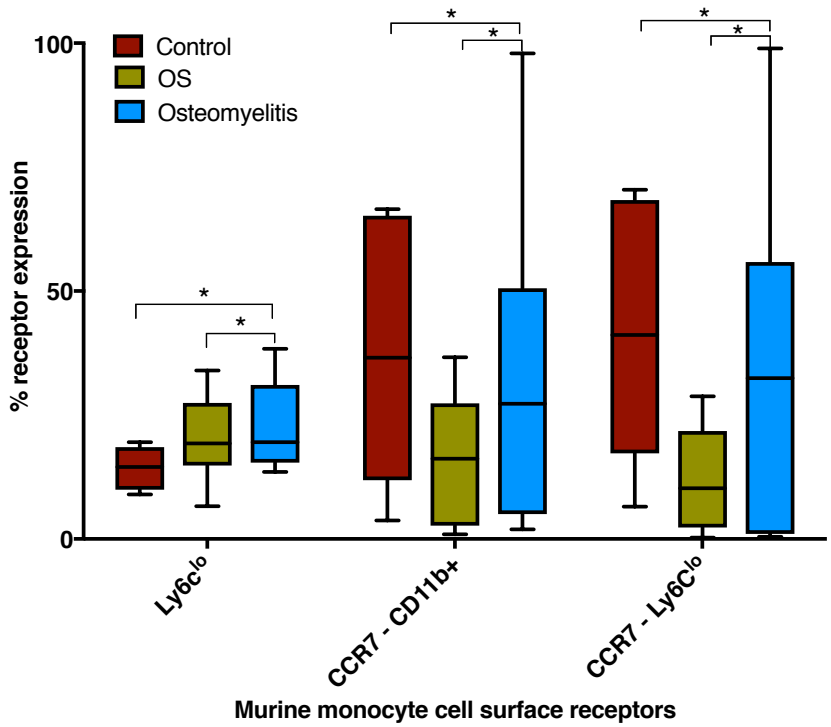

Figure 3: Monocyte surface marker expression is altered in mice with OS, and in mice with OS + osteomyelitis

Flow cytometry plots illustrating cell surface receptor expression in peripheral blood monocytes from mice with OS (n = 11), mice with OS and osteomyelitis (n=13), and healthy controls (n = 7). Box-and-whisker plot depicting the % of Ly6C^{lo} monocyte subset, and % positive CCR7 cell surface receptor expression in all CD11b+ monocytes and in the Ly6C^{lo} monocyte subset in OS versus normal control mice. The median percentages and ranges of positively staining cells for each antibody in healthy controls are as follows: Ly6C^{lo} (14%, 9–19%), CCR7 in CD11b+ monocytes (37%, 4–66%), CCR7 in Ly6C^{lo} monocytes (41%, 6–70%). The median percentages and ranges of positively staining cells for each antibody in mice with OS are as follows: Ly6C^{lo} (19%, 7–34%), CCR7 in CD11b+ monocytes (16%, 1–37%), CCR7 in Ly6C^{lo} monocytes (10%, 0.3–29%). The median percentages and ranges of positively staining cells for each antibody in mice with OS + osteomyelitis are as follows: Ly6C^{lo} (20%, 15–38%), CCR7 in CD11b+ monocytes (27%, 2–98%), CCR7 in Ly6C^{lo} monocytes (32%, 0.4–98%). Significant differences are marked with an asterisk ($p < 0.05$).

3.3.3 Quantitative RT-PCR

Murine relative tumor mRNA expression: IL-6, and TNF-α are markers of inflammation, and together with arginase, Fizz, and CD206, can be used to differentiate between polarized macrophage subsets in mice.[16] In order to investigate the effects of osteomyelitis on the expression of the above markers within tumor tissue, we compared the relative mRNA expression of IL-6, TNF-α, arginase, Fizz, and CD206 in tumor tissue from osteomyelitis mice to tumor control mice. There were no significant differences in relative mRNA expression of all markers of interest in tumor tissue of experimental groups compared to tumor control tissue. The p-values for the markers of interest were as follows: IL-6 ($p = 0.4396$), TNF-α ($p = 0.0675$), arginase ($p = 0.8616$), Fizz ($p = 0.4007$), CD206 ($p = 0.5868$).

3.3.4 Monocyte Chemotaxis

As we had previously demonstrated decreased chemotaxis in monocytes from dogs with OS compared to monocytes from normal controls, we asked if murine OS may have a similar effect on monocytes. Our hypothesis was that osteomyelitis might enhance monocyte chemotaxis in mice with OS.[17] Contrary to our hypothesis, when MCP was used as a chemoattractant, monocytes from osteomyelitis mice exhibited significantly decreased chemotaxis compared to monocytes from tumor control ($p = 0.0043$).

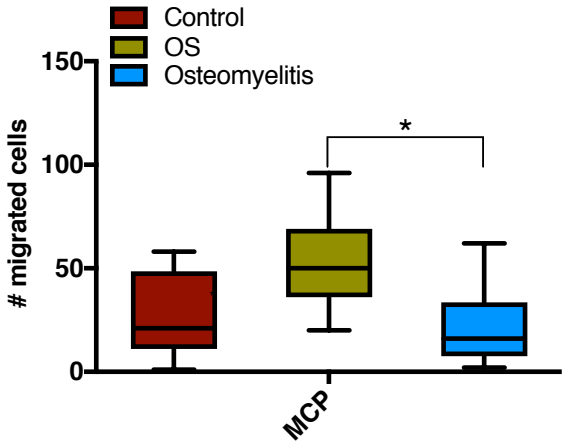

Figure 4: Monocyte chemotaxis is decreased in mice with OS + osteomyelitis Box-and-whisker plot comparing the mean numbers of migrated monocytes in response to MCP between normal control mice, mice with OS, mice with OS + osteomyelitis.

Murine monocytes: As we had previously demonstrated decreased chemotaxis in monocytes from dogs with OS compared to monocytes from normal controls, we asked if murine OS may have a similar effect on monocytes. There was significant variation between experimental groups in the degree to which murine monocytes migrated in response to MCP ($p = 0.0013$) and SDF ($p = 0.0022$), whereas there was no difference in the degree to which monocytes migrated in response to PBS ($p = 0.5399$) between experimental groups. Monocytes from OS + osteomyelitis mice exhibited significantly decreased chemotaxis compared to monocytes from tumor control ($p = 0.0043$).

3.3.5 Survival Analysis

In order to evaluate the effects of osteomyelitis on survival in OS, we performed a Kaplan-Meier survival analysis comparing survival between osteomyelitis mice and tumor control mice. Median survival for osteomyelitis mice was 24 days, and for tumor control

mice was 25 days. We did not find a statistically significant difference in median survival between experimental groups ($p = 0.53$). Our previous work had demonstrated that increasing percentages of CCR2 expression on canine peripheral monocytes was significantly associated with increasing survival in dogs with OS.[17] However, the current study did not find any statistically significant correlation between murine survival and monocyte receptor expression.

Macrophage Studies

3.3.6 Study populations

The same study population was recruited for this portion of the study as described in Chapter 2 (2.3.7). Thirty-six healthy dogs over 1 year old and seventeen healthy humans 25 years or younger were recruited for the study. Canine owner and human volunteer participation written consent were obtained, and peripheral blood samples were collected for macrophage cultures.

3.3.7 Flow cytometry

Canine macrophages: Percent of CD80 expression was significantly higher in canine macrophages cultured with OS and *S. aureus* compared to macrophages cultured alone ($p < 0.0001$) (Fig. 5). The percent CD80 expression was also significantly higher in canine macrophages cultured with OS compared to macrophages cultured alone (see Chapter 2, 2.3.8), and there was no difference between CD80 expression in macrophages cultured with OS and macrophages cultured with OS + *S. aureus*.

Human macrophages: Percent of CCR2 expression was significantly lower in human macrophages cultured with OS + *S. aureus* compared to macrophages cultured alone ($p < 0.0001$) (Fig. 6a). Percent of CCR2 expression was also significantly lower in human macrophages cultured with OS compared to macrophages cultured alone (see Chapter 2, 2.3.8), and there was no difference in CCR2 expression between macrophages cultured with OS and macrophages cultured with OS + *S. aureus*. The mean fluorescence intensity (MFI) of CD86 expression was significantly higher in macrophages cultured with OS + *S. aureus* compared to macrophages cultured alone ($p<0.0001$), and compared to macrophages cultured with OS ($p = 0.0168$) (Fig. 6b). We had previously reported the mean fluorescence intensity (MFI) of CD86 expression was significantly higher in macrophages cultured with OS compared to macrophages cultured alone ($p = 0.0017$) (See Chapter 2, 2.3.8).

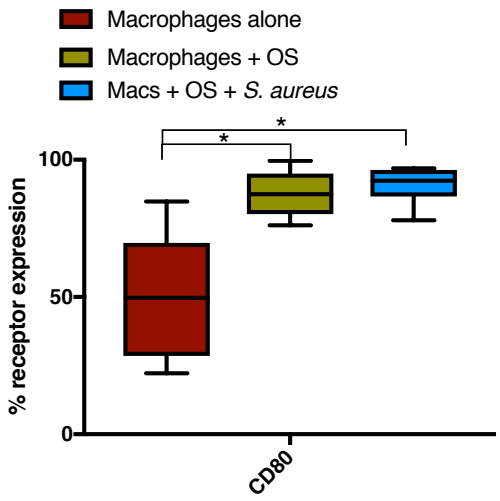

Figure 5: Canine macrophage receptor expression is altered in the presence of OS and *S. aureus*
Flow cytometry plot illustrating cell surface receptor expression in cultured primary canine macrophages from macrophages cultured alone (n = 9), macrophages cultured with OS (n = 8), and macrophages cultured with OS + *S. aureus* (n = 6). Box-and-whisker plot depicting the % positive CD80 cell surface receptor expression in macrophages cultured alone compared to macrophages cultured with OS and macrophages cultured with OS + *S. aureus*. The median percentage and range of CD80 positively staining cells in macrophages cultured alone were 50%, 22–85%. The median percentage and range of CD80 positively staining cells in macrophages cultured with OS were 87%, 76–100%. The median percentage and range of CD80 positively staining cells in macrophages cultured with OS and *S. aureus* were 92%, 78–97%.

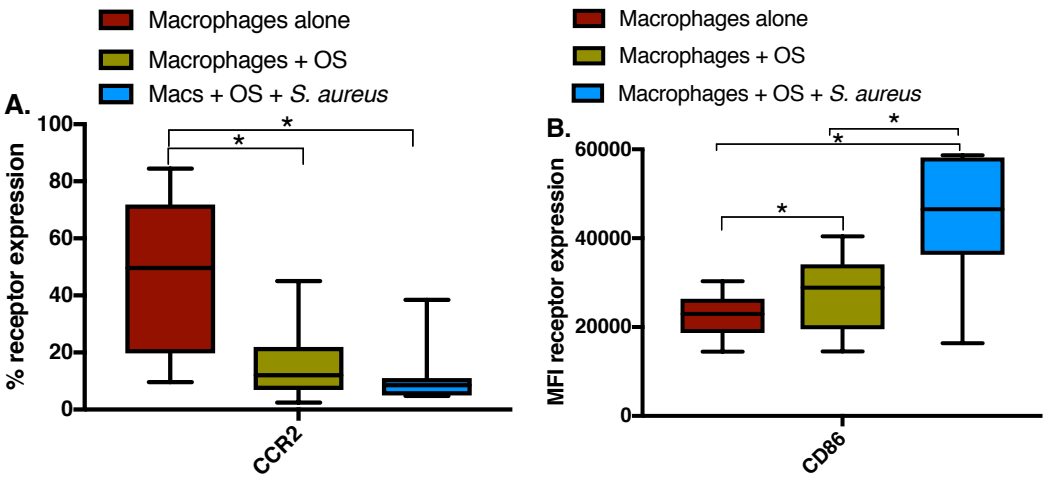

Figure 6: Human macrophage receptor expression is altered in the presence of OS and *S. aureus*

Flow cytometry plot illustrating cell surface receptor expression in cultured primary human macrophages from macrophages cultured alone (n = 7), macrophages cultured with OS (n = 9), macrophages cultured with OS + *S. aureus* (n = 7). (A) Box-and-whisker plot depicting the % positive CCR2 cell surface receptor expression in macrophages cultured alone versus macrophages cultured with OS. The median percentage and range of CCR2 positively staining cells in macrophages cultured alone were 50%, 10–85%. The median percentage and range of CCR2 positively staining cells in macrophages cultured with OS were 12%, 3–45%. The median percentage and range of CCR2 positively staining cells in macrophages cultured with OS + *S. aureus* were 9%, 5–38%. (B) Box-and-whisker plot depicting the MFI of CD86 cell surface receptor expression in macrophages cultured alone versus macrophages cultured with OS. The median MFI and range of CD86 positively staining cells in macrophages cultured alone were 22,951, 14,476–30,311. The median MFI and range of CD86 positively staining cells in macrophages cultured with OS were 28,887, 14,527–40,442. The median MFI and range of CD86 positively staining cells in macrophages cultured with OS + *S. aureus* were 46,529, 16,390–58,690.

3.3.8 Evaluation of cytokine secretion from canine and human macrophages

Canine macrophages: The MILLIPLEX® assay revealed increased MCP-1 levels ($p=0.0467$) in culture supernatants of canine primary macrophages cultured with OS compared to macrophages cultured with OS + *S. aureus* (Fig. 7a). When compared to macrophages cultured alone, macrophages cultured with OS + *S. aureus* expressed significantly increased levels of MCP-1 ($p<0.0001$) (Fig. 7a). We had previously noted increased MCP-1 levels ($p <0.0001$) in culture supernatants of canine primary macrophages cultured with OS compared to macrophages cultured alone (See Chapter 2, 2.3.9). TNF-α levels from macrophages cultured with OS + *S. aureus* were significantly higher compared to levels from macrophages cultured alone ($p<0.0001$) and from macrophages cultured with OS ($p=0.0004$) (Fig. 7b). The median concentrations and ranges of MCP-1 concentrations were 6369 pg/ml, 273-42,390 pg/ml for macrophages cultured alone; 65,729 pg/ml, 33,778-86,963 pg/ml for macrophages cultured with OS; 47,830 pg/ml, 29,739-93,803 pg/ml for macrophages cultured with OS + *S. aureus*. The median concentrations and ranges of TNF-α concentrations were 6.33 pg/ml, 2-83 pg/ml for macrophages cultured alone; 3310 pg/ml, 1114-8089 pg/ml for macrophages cultured with OS; 18,261 pg/ml, 7655-36,525 pg/ml for macrophages cultured with OS + *S. aureus*.

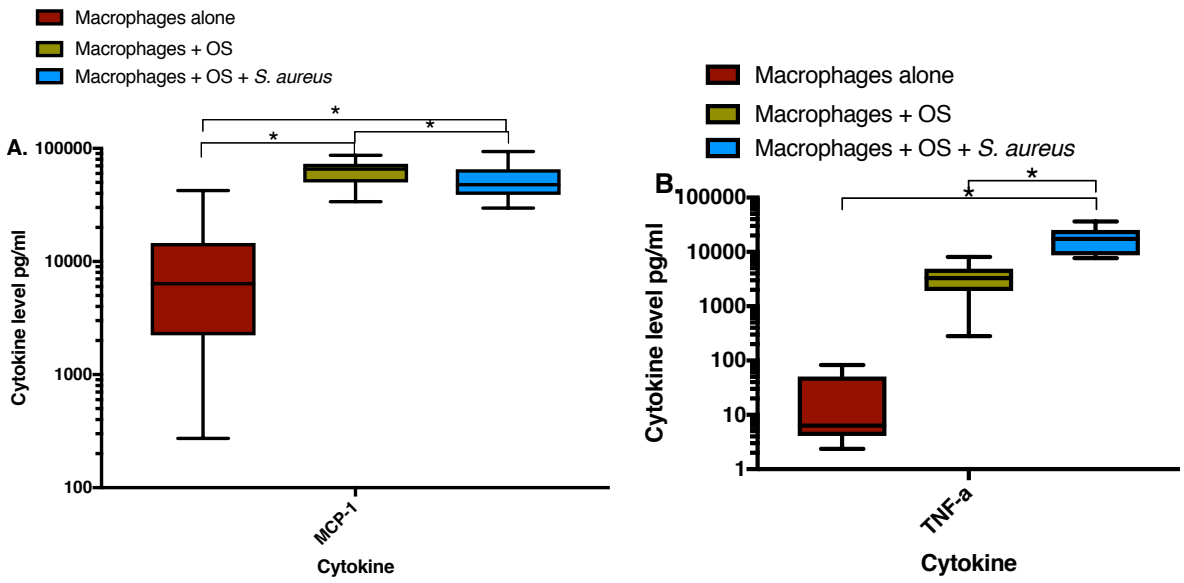

Figure 7: Canine macrophage MCP-1 and TNF-α secretion are altered by the presence of OS and *S. aureus* Box-and-whisker plots displaying the levels of (A) MCP-1 (pg/ml) and (B) TNF-α (pg/ml) in macrophage culture supernatants of macrophages cultured alone (n = 11), macrophages cultured with OS (n = 13), and macrophages cultured with OS + *S. aureus* (n = 12). Macrophages cultured with OS secreted significantly higher levels of MCP-1 compared to macrophages cultured alone ($p < 0.0001$), and to macrophages cultured with OS + *S. aureus* ($p = 0.0467$). Macrophages cultured with OS + *S. aureus* secreted significantly higher levels of MCP-1 compared to macrophages cultured alone ($p<0.0001$). Macrophages cultured with OS + *S. aureus* secreted significantly higher levels of TNF-α compared to macrophages cultured alone ($p<0.0001$), and macrophages cultured with OS ($p = 0.0004$).

The results of the TGF-β ELISA showed significantly decreased TGF-β in culture supernatants of canine macrophages cultured with OS + *S. aureus* compared to macrophages cultured alone ($p = 0.0375$), and to macrophages cultured with OS ($p = 0.0034$) (Fig. 8). The median concentrations and ranges of TGF-β concentrations were 1381 pg/ml, 1117-3286 pg/ml for macrophages cultured alone; 1656 pg/ml, 1147-2349 pg/ml for macrophages

cultured with OS; 1039 pg/ml, 978-1291 pg/ml for macrophages cultured with OS + *S. aureus*.

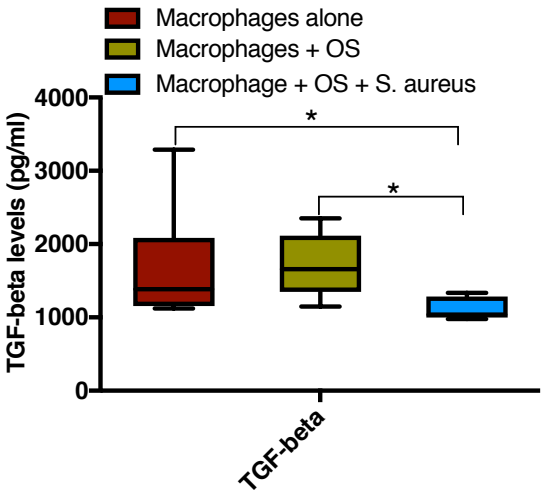

Figure 8: Canine macrophage TGF-β secretion is altered by the presence of OS and *S. aureus*
Box-and-whisker plots displaying the levels of TGF-β (pg/ml) in macrophage culture supernatants of macrophages cultured alone (n = 11), macrophages cultured with OS (n = 11), and macrophages cultured with OS + *S. aureus* (n = 8). Macrophages cultured with OS + *S. aureus* secreted significantly lower levels of TGF-β compared to macrophages cultured alone (p = 0.0375), and to macrophages cultured with OS (p = 0.0034).

Human macrophages: The MILLIPLEX® assay revealed increased IFN-γ (p<0.0001) (Fig. 8a), TNF-α (p<0.0001) (Fig. 8b) and MCP-1 (p<0.0001) (Fig. 8c) levels in culture supernatants of human primary macrophages cultured with OS + *S. aureus* compared to macrophages cultured alone and macrophages cultured with OS. The median concentrations and ranges of IFN-γ concentrations were 10 pg/ml, 10-72 pg/ml for macrophages cultured alone; 109 pg/ml, 10-1240 pg/ml for macrophages cultured with OS; 14,845 pg/ml, 658-88,155 pg/ml for macrophages cultured with OS + *S. aureus*. The median concentrations and

ranges of MCP-1 concentrations were 1324 pg/ml, 606-74,400 pg/ml for macrophages cultured alone; 86,250 pg/ml, 37,390-127,130 pg/ml for macrophages cultured with OS; 102,540 pg/ml, 85,610-140,370 pg/ml for macrophages cultured with OS + *S. aureus*. The median concentrations and ranges of TNF-α concentrations were 31 pg/ml, 19-2299 pg/ml for macrophages cultured alone; 1435 pg/ml, 368-6272 pg/ml for macrophages cultured with OS; 38,260 pg/ml, 4640-85,700 pg/ml for macrophages cultured with OS + *S. aureus*.

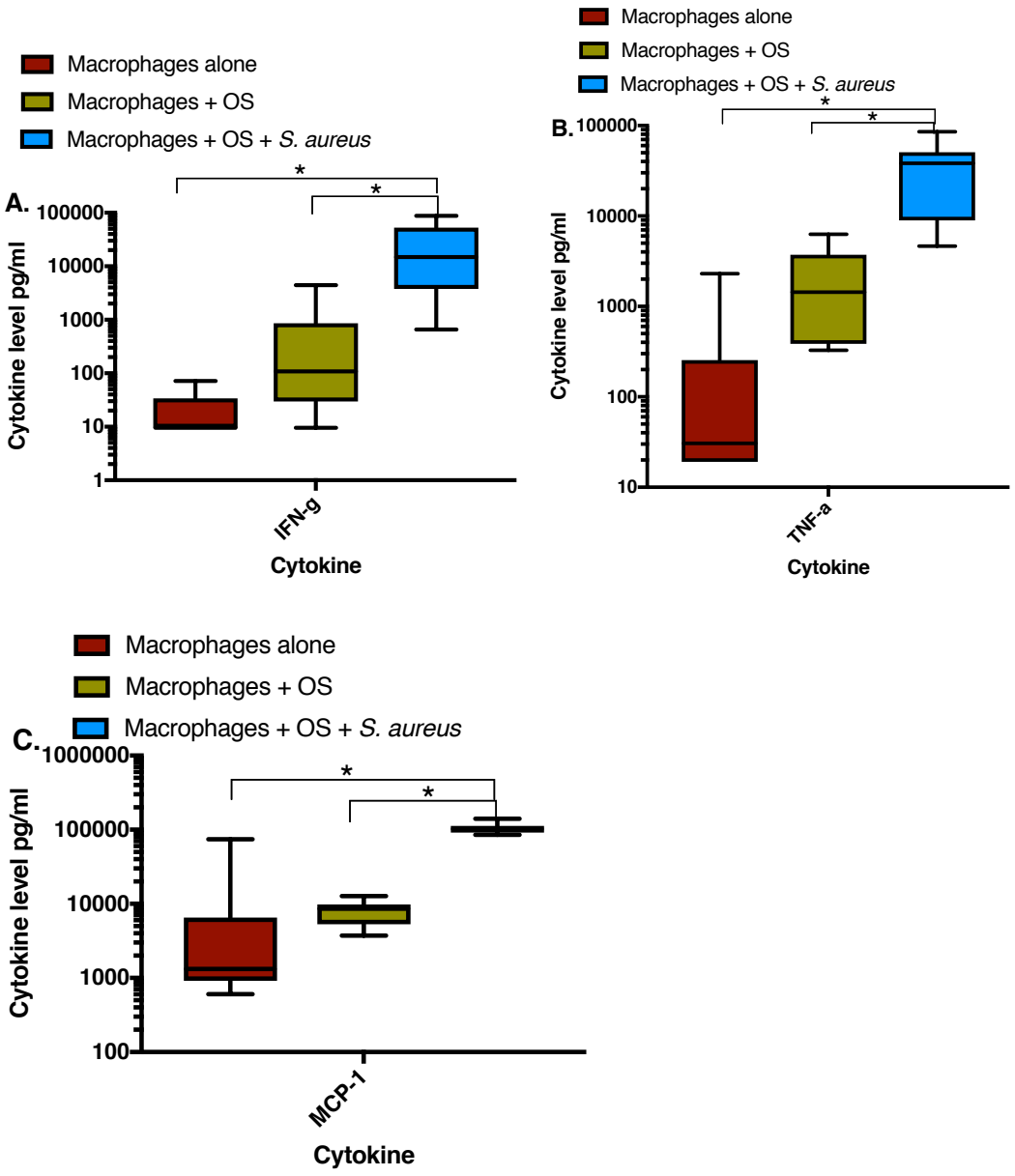

Figure 9: Human macrophage IFN-γ, TNF-α and MCP-1 secretion are altered by the presence of OS and *S. aureus* Box-and-whisker plots displaying the levels of (A) IFN-γ, (B) TNF-α and (C) MCP-1 (pg/ml) in macrophage culture supernatants of macrophages cultured alone (n = 10), macrophages cultured with OS (n = 9), and macrophages cultured with OS + *S. aureus* (n = 9). Macrophages cultured with OS + *S. aureus* secreted significantly higher levels of IFN-γ, TNF-α and MCP-1 compared to macrophages cultured alone ($p<0.0001$ for all 3 cytokines), and to macrophages cultured with OS ($p<0.0001$ for all 3 cytokines).

The results of the TGF-β ELISA showed a similar trend in human macrophages as observed in canine macrophages - TGF-β in culture supernatants of human macrophages cultured with OS + *S. aureus* was significantly decreased compared to macrophages cultured alone ($p = 0.0466$), and to macrophages cultured with OS ($p = 0.0033$) (Fig. 10). The median concentrations and ranges of TGF-β concentrations were 1836 pg/ml, 689-2482 pg/ml for macrophages cultured alone; 2016 pg/ml, 1175-3226 pg/ml for macrophages cultured with OS; 1148 pg/ml, 954-1404 pg/ml for macrophages cultured with OS + *S. aureus*.

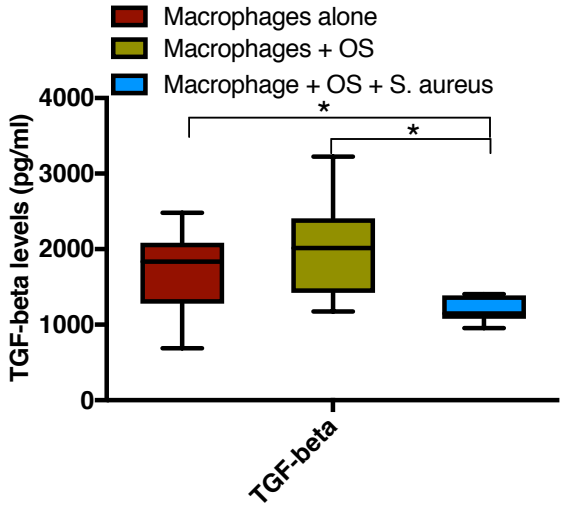

Figure 10: Human macrophage TGF-β secretion is altered by the presence of OS and *S. aureus*
Box-and-whisker plots displaying the levels of TGF-β (pg/ml) in macrophage culture supernatants of macrophages cultured alone (n = 10), macrophages cultured with OS (n = 10), and macrophages cultured with OS + *S. aureus* (n = 9). Macrophages cultured with OS + *S. aureus* secreted significantly lower levels of TGF-β compared to macrophages cultured alone ($p = 0.0466$), and to macrophages cultured with OS ($p = 0.0033$).

3.3.9 Quantitative RT-PCR

Canine relative mRNA expression of macrophage IL-10, TNF-α, and Arginase: TNF-α, IL-10 and Arginase mRNA expression in human macrophages can aid in differentiating macrophages into M1 versus M2 macrophages. mRNA expression of IL-10 ($p = 0.0041$) and TNF-α ($p = 0.0008$) were significantly increased in macrophages cultured with OS + *S. aureus* compared to macrophages cultured alone (Fig. 11a). As previously noted in Chapter 2, 2.3.10), mRNA expression of IL-10 ($p = 0.00596$) and TNF-α ($p = 0.00024$) were significantly increased in macrophages cultured with OS compared to macrophages cultured alone. There were no significant differences in IL-10 or TNF-α mRNA expression between macrophages cultured with OS and macrophages cultured with OS + *S. aureus*.

Human relative mRNA expression of macrophage IL-10, TNF-α, and Arginase: mRNA expression of IL-10 ($p = 0.00758$) and TNF-α ($p = 0.00758$) were significantly increased in macrophages cultured with OS + *S. aureus* compared to macrophages cultured alone (Fig. 11b). TNF-α ($p = 0.01078$) and IL-10 ($p = 0.00804$) mRNA were significantly increased in macrophages cultured with OS + *S. aureus* compared to macrophages cultured with OS (Fig. 11b).

Figure 11: Canine and human macrophage mRNA expression of IL-10 and TNF-α in the presence of OS and *S. aureus* Bar graphs displaying the level of mRNA expression of IL-10 and TNF-α in (a) - canine macrophages cultured alone (n = 12), macrophages cultured with OS (n = 14), and macrophages cultured with OS + *S. aureus* (n = 10); in (b) – human macrophages cultured alone (n = 5), macrophages cultured with OS (n = 8), and macrophages cultured with OS + *S. aureus* (n = 9). IL-10 and TNF-α mRNA expression were both increased with the addition of OS and of *S. aureus* to macrophage cultures compared to macrophages cultured alone.

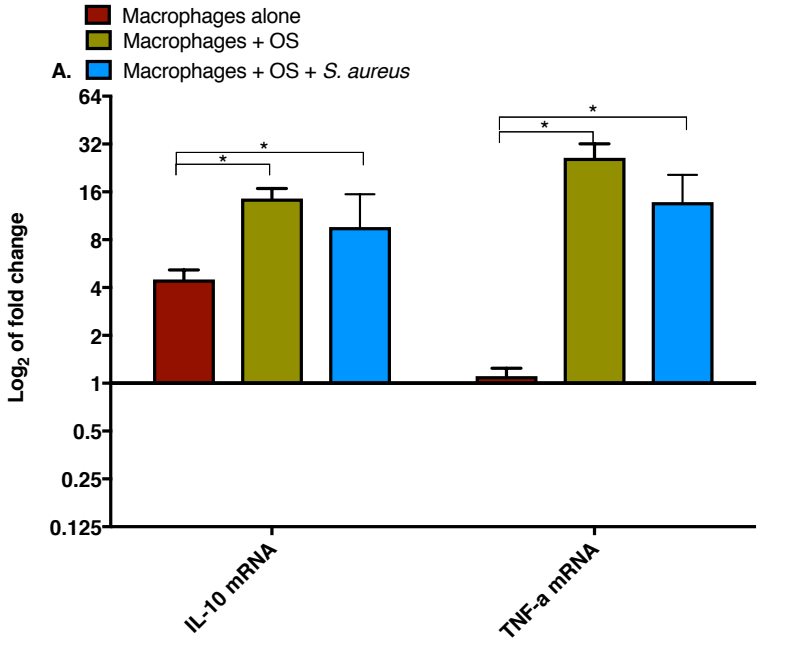
Macrophages alone
Macrophages + OS
A. Macrophages + OS + S. aureus
Log2 of fold change
64
32
16
8
4
2
1
0.5
0.25
0.125
*
*
*
*
IL-10 mRNA
TNF-a mRNA

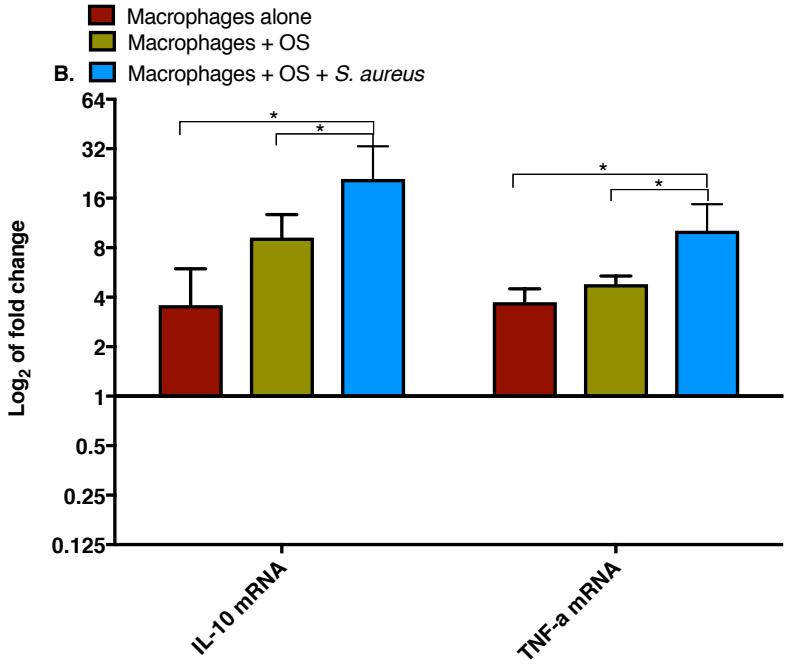
Macrophages alone
Macrophages + OS
B. Macrophages + OS + S. aureus
Log2 of fold change
64
32
16
8
4
2
1
0.5
0.25
0.125
*
*
*
*
IL-10 mRNA
TNF-a mRNA

3.4. Discussion

The goal of the studies in this chapter was to determine the effect of *in vivo* infection or *in vitro* exposure to a bacterial agent (*Staphylococcus aureus*) on the phenotype of monocytes and macrophage differentiation in the presence of OS. Our hypothesis was that infection will reverse the phenotypic changes in monocytes associated with OS, and that *S. aureus* will induce an inflammatory macrophage phenotype (M1-like) in the presence of OS. We demonstrated a significant increase in the proportion of CD14+ monocytes and in CD16 monocyte expression in dogs with OS and a concurrent surgical site infection compared to dogs with untreated OS and controls. We also demonstrated a reversal of the inhibitory effect of OS on canine monocyte chemokine receptors as noted in Chapter 2 – OS dogs with an infection had increased expression of CCR2, CCR7, CX3CR1, and CXCR2 monocyte receptors compared to untreated OS dogs. We observed some parallel findings in OS mice with osteomyelitis – these mice exhibited higher CCR7 monocyte expression compared to mice with OS, but the CCR7 expression in osteomyelitis mice was still lower than normal control mice. We demonstrated that monocytes from mice with osteomyelitis exhibited significantly decreased chemotactic ability compared to monocytes from OS-bearing mice. In our macrophage studies, we demonstrated that human macrophages cultured with OS and *S. aureus* exhibited an inflammatory phenotype with increased CD86 receptor expression, increased IFN-γ, TNF-α and MCP-1 cytokine secretion, decreased TGF-β cytokine secretion, and increased mRNA expression of TNF-α and IL-10 compared to macrophages cultured with OS and to baseline macrophages. Canine macrophages exhibited a similar trend when cultured with OS and *S. aureus* – we observed increased CD80 receptor expression,

increased TNF-α cytokine secretion, decreased TGF-β cytokine secretion, and increased mRNA expression of TNF-α and IL-10 (discussed in more detail below).

We had previously reported a decrease in canine monocyte chemokine receptors in dogs with OS, with a corresponding decrease in monocyte chemotactic ability in these dogs, compared to healthy controls (Chapter 2). Interestingly, we observed an increase in monocyte chemokine receptor expression in dogs with OS and a concurrent surgical site infection. We hypothesized that evasion of the immune response by OS is due partly to the down-regulation of monocyte chemokine receptor expression and migratory function. Our findings in OS dogs with an infection suggest that infection serves to reverse the immunosuppressive effects of OS, in part, by upregulating monocyte chemokine receptor expression. Due to the limitations of sample acquisition and obtaining patient follow-up information from distant collaborators, we did not have adequate samples to perform monocyte chemotaxis assays, and were unable to acquire survival data from infected dogs with OS.

Our murine monocyte flow cytometric analysis revealed a higher proportion of $Ly6C^{lo}$ peripheral monocytes in mice with osteomyelitis compared to tumor-bearing mice and normal controls, which was an unexpected finding. Monocytes are a heterogeneous population of mononuclear leukocytes primarily found in the peripheral circulation, making up approximately 2-4% of murine leukocytes.[18] Murine monocytes are divided into inflammatory and alternative subpopulations, with the inflammatory monocytes exhibiting high Ly6C expression and alternative monocytes exhibiting low or negative Ly6C expression. $Ly6C^{hi}$ inflammatory monocytes are recruited to inflammatory foci including sites of bacterial infection, where they then carry out defensive microbicidal functions.[19]

Thus in our study, we expected the mice with osteomyelitis to exhibit higher proportions of $Ly6C^{hi}$ inflammatory monocytes, which was previously reported.[11] Alternative $Ly6C^{lo}$ monocytes typically patrol the endothelium, and are ready to extravasate and migrate to tissue sites of infection, providing a rapid first line of innate immune defense against pathogens prior to the subsequent and more robust recruitment of $Ly6C^{hi}$ inflammatory monocytes to these sites.[20] As early as 2-8 hours post extravasation, alternative $Ly6C^{lo}$ monocytes then cease the production of inflammatory cytokines and upregulate genes involved in tissue repair and remodeling such as arginase, Fizz and mannose receptor (CD206).[20] The predominance of $Ly6C^{lo}$ monocytes in the mice with osteomyelitis in our study suggests that the intensity of infection in these mice was low, as these mice were potentially resolving their infections, thus increasing the need for $Ly6C^{lo}$ monocytes promoting tissue repair. Even though all femora in the osteomyelitis group cultured positive for XEN36 *S. aureus* at time of euthanasia, >50% of the mice stopped exhibiting *in vivo* luminescence in the last 5 days prior to euthanasia. This suggests that the intensity of the infection may not have been robust enough to elicit a strong inflammatory reaction against the tumor. A murine study had reported that the tumor inhibitory effects of bacteria is dependent on the concentration of bacteria administered, with intermediate bacterial loads associated with more durable tumor control.[21] The higher CCR7 expression observed in monocytes from osteomyelitis mice parallels our finding of increased chemokine receptor expression, including CCR7, in monocytes from OS dogs with infections compared to dogs with untreated OS (Chapter 2). The decreased monocyte chemotaxis exhibited by mice with

osteomyelitis compared to tumor-bearing mice suggests a low-intensity of infection in these mice, resulting in decreased monocyte chemotaxis.

Both human and canine macrophages upregulated CD86 and CD80 expression respectively when cultured with *S. aureus* in the presence of OS. CD80 and CD86, also known as B7-1 and B7-2 respectively, are categorized as co-stimulatory molecules possessing dual specificity for CD28 and CTLA-4.[22] Binding of CD80 and CD86 to CD28 is a major signal for T cell activation and the interaction is critical for stimulating an effective adaptive response.[23] Conversely, binding to CTLA-4 induces peripheral T cell tolerance to regulate the immune response via physiological negative feedback.[23] Upregulation of the costimulatory molecules indicates the presence of an inflammatory response in macrophages. In the presence of OS, both canine and human macrophages significantly upregulated CD80 and CD86 expression, which we hypothesized can maintain a chronic low-grade inflammatory environment conducive to tumor growth and metastasis. With the addition of *S. aureus* to the macrophage-OS co-cultures, we demonstrated significantly increased expression of CD86 in human macrophages compared to the level of CD86 expression in macrophages cultured with OS. In canine macrophages, there was a slight increase in CD80 expression with the addition of *S. aureus* compared to macrophages cultured with OS, but this increase was not significant. Canine and human macrophages co-cultured with OS also exhibited an inflammatory cytokine profile when exposed to *S. aureus*, and these human macrophages had a corresponding significant increase in TNF-α mRNA expression. The canine macrophages also displayed an increase in TNF-α mRNA expression, but the increase was not significant when compared to the mRNA levels in macrophages cultured with OS.

TNF-α is one of the dominant cytokines in an inflammatory cytokine response to bacteria, and especially to endotoxin from Gram negative bacteria. A murine study reported that *Salmonella enterica* colonization of colon carcinoma lesions leading to tumor necrosis and growth inhibition was mediated in large part by TNF-α.[24] The significant upregulation of TNF-α secretion after exposure to *S. aureus* from human and canine macrophages co-cultured with OS suggests an inflammatory response in these macrophages that exceeded the level of tumor-induced inflammation that potentially has anti-tumor effects. In human macrophages, another inflammatory cytokine, IFN-γ, was also significantly increased with bacterial exposure when these macrophages were co-cultured with OS. Conversely, canine and human macrophages co-cultured with OS exhibited decreased secretion of the immunosuppressive cytokine, TGF-β, when exposed to *S. aureus*. Both human and canine macrophages co-cultured with OS displayed an increase in IL-10 mRNA expression when exposed to *S. aureus,* which is expected in an inflammatory response, since IL-10 is a key physiologic regulator of inflammation to limit collateral damage caused by excessive inflammation.[25] Il-10 has widespread immunosuppressive effects on both the innate and adaptive arms of the immune system. IL-10 downregulates the expression of the co-stimulatory molecules (CD80/CD86) and inflammatory cytokine secretion in monocytes and macrophages, inhibits dendritic cell migration to lymph nodes, and can act directly on T cells by inhibiting CD4-T cell proliferation.[26] These data suggest that in the presence of bacteria, macrophages can upregulate their inflammatory response to a higher intensity than the

inflammation caused by OS, to the degree that the response could potentially be inhibitory to tumor progression.

Bacteria-based anti-tumor therapies have been investigated over time, most notably by William Coley, and with OS being an immunogenic tumor, understanding of the mechanistic interplay between the tumor and the immune system in response to bacteria will help advance our progression towards positively manipulating the anti-tumor immune response. A recent study reports the therapeutic efficacy of bacteria against murine colon carcinoma and fibrosarcoma, and utilized the novel combination of *in vivo* experiments and mathematical modeling to conclude that intermediate doses of bacteria and low doses of TNF-α did not cause excessive morbidity and resulted in optimal tumor control.[21] Our findings in canine monocytes of an upregulation of chemokine receptors in OS dogs with an infection, and the inflammatory profile of human and canine macrophages cultured with OS and *S. aureus* support our hypothesis that infection or the presence of bacteria induces an inflammatory response that can have anti-tumor activity. Further work is needed to elucidate the optimal stimuli and signaling mechanisms for triggering a reliable anti-tumor immune response.

REFERENCES

1. McCarthy EF. The toxins of William B. Coley and the treatment of bone and soft tissue sarcomas. *Iowa Orthop J* 2006;26:154-158.

2. Wiemann B, Starnes CO. Coley's toxins, tumor necrosis factor and cancer research: a historical perspective. *Pharmacol Ther* 1994;64:529-564.

3. Hackett SP, Stevens DL. Streptococcal toxic shock syndrome: synthesis of tumor necrosis factor and interleukin-1 by monocytes stimulated with pyrogenic exotoxin A and streptolysin O. *J Infect Dis* 1992;165:879-885.

4. Berendt MJ, North RJ, Kirstein DP. The immunological basis of endotoxin-induced tumor regression. Requirement for a pre-existing state of concomitant anti-tumor immunity. *J Exp Med* 1978;148:1560-1569.

5. Berendt MJ, North RJ, Kirstein DP. The immunological basis of endotoxin-induced tumor regression. Requirement for T-cell-mediated immunity. *J Exp Med* 1978;148:1550-1559.

6. Thrall DE, Withrow SJ, Powers BE, et al. Radiotherapy prior to cortical allograft limb sparing in dogs with osteosarcoma: a dose response assay. *Int J Radiat Oncol Biol Phys* 1990;18:1351-1357.

7. Lascelles BD, Dernell WS, Correa MT, et al. Improved survival associated with postoperative wound infection in dogs treated with limb-salvage surgery for osteosarcoma. *Ann Surg Oncol* 2005;12:1073-1083.

8. Culp WT, Olea-Popelka F, Sefton J, et al. Evaluation of outcome and prognostic factors for dogs living greater than one year after diagnosis of osteosarcoma: 90 cases (1997-2008). *J Am Vet Med Assoc* 2014;245:1141-1146.

9. Jeys LM, Grimer RJ, Carter SR, et al. Post operative infection and increased survival in osteosarcoma patients: are they associated? *Ann Surg Oncol* 2007;14:2887-2895.

10. Chen YU, Xu SF, Xu M, et al. Postoperative infection and survival in osteosarcoma patients: Reconsideration of immunotherapy for osteosarcoma. *Mol Clin Oncol* 2015;3:495-500.

11. Sottnik JL, U'Ren LW, Thamm DH, et al. Chronic bacterial osteomyelitis suppression of tumor growth requires innate immune responses. *Cancer Immunol Immunother* 2010;59:367-378.

12. MacEwen EG, Kurzman ID, Rosenthal RC, et al. Therapy for osteosarcoma in dogs with intravenous injection of liposome-encapsulated muramyl tripeptide. *J Natl Cancer Inst* 1989;81:935-938.

13. Kurzman ID, Shi F, Vail DM, et al. In vitro and in vivo enhancement of canine pulmonary alveolar macrophage cytotoxic activity against canine osteosarcoma cells. *Cancer Biother Radiopharm* 1999;14:121-128.

14. Kurzman ID, MacEwen EG, Rosenthal RC, et al. Adjuvant therapy for osteosarcoma in dogs: results of randomized clinical trials using combined liposome-encapsulated muramyl tripeptide and cisplatin. *Clin Cancer Res* 1995;1:1595-1601.

15. Meyers PA, Schwartz CL, Krailo MD, et al. Osteosarcoma: the addition of muramyl tripeptide to chemotherapy improves overall survival--a report from the Children's Oncology Group. *J Clin Oncol* 2008;26:633-638.

16. Davis MJ, Tsang TM, Qiu Y, et al. Macrophage M1/M2 polarization dynamically adapts to changes in cytokine microenvironments in Cryptococcus neoformans infection. *MBio* 2013;4:e00264-00213.

17. Tuohy JL, Lascelles BD, Griffith EH, et al. Association of Canine Osteosarcoma and Monocyte Phenotype and Chemotactic Function. *J Vet Intern Med* 2016;30:1167-1178.

18. Italiani P, Boraschi D. From Monocytes to M1/M2 Macrophages: Phenotypical vs. Functional Differentiation. *Front Immunol* 2014;5:514.

19. Shi C, Pamer EG. Monocyte recruitment during infection and inflammation. *Nat Rev Immunol* 2011;11:762-774.

20. Auffray C, Fogg D, Garfa M, et al. Monitoring of blood vessels and tissues by a population of monocytes with patrolling behavior. *Science* 2007;317:666-670.

21. Hatzikirou H, Lopez Alfonso JC, Leschner S, et al. Therapeutic Potential of Bacteria against Solid Tumors. *Cancer Res* 2017;77:1553-1563.

22. Greenwald RJ, Freeman GJ, Sharpe AH. The B7 family revisited. *Annu Rev Immunol* 2005;23:515-548.

23. Sharpe AH, Freeman GJ. The B7-CD28 superfamily. *Nat Rev Immunol* 2002;2:116-126.

24. Leschner S, Westphal K, Dietrich N, et al. Tumor invasion of Salmonella enterica serovar Typhimurium is accompanied by strong hemorrhage promoted by TNF-alpha. *PLoS One* 2009;4:e6692.

25. Siewe L, Bollati-Fogolin M, Wickenhauser C, et al. Interleukin-10 derived from macrophages and/or neutrophils regulates the inflammatory response to LPS but not the response to CpG DNA. *Eur J Immunol* 2006;36:3248-3255.

26. Couper KN, Blount DG, Riley EM. IL-10: the master regulator of immunity to infection. *J Immunol* 2008;180:5771-5777.

SUPPLEMENTARY INFORMATION

Supplemental Figure 1: Monocyte surface marker expression is downregulated in treated OS dogs without an infection

Flow cytometry plots illustrating cell surface receptor expression in peripheral blood monocytes from dogs with OS (n = 18), healthy controls (n = 13), dogs with OS and an infection (n = 9), and treated OS dogs without an infection (n = 6). Box-and-whisker plot depicting the % positive monocyte cell surface receptor expression of the different receptors (CCR2, CCR7, CD43, CX3CR1, CXCR2), comparing expression between healthy controls, dogs with OS, dogs with OS + infection, treated dogs with OS without an infection. The median percentages and ranges of positively staining cells for each antibody in healthy controls are as follows: CCR2 (58%, 2–94%), CCR7 (36%, 1–90%), CD43 (52%, 2–93%), CX3CR1 (9%, 0.2–87%), and CXCR2 (54%, 2–92%). The median percentages and ranges of positively staining cells for each antibody in dogs with OS are as follows: CCR2 (29%, 3–45%), CCR7 (8%, 0.1–41%), CD43 (28%, 3–47%), CX3CR1 (5%, 0.6–70%), and CXCR2 (23%, 0.2–52%). The median percentages and ranges of positively staining cells for each antibody in treated OS dogs without an infection are as follows: CCR2 (21%, 1–75%), CCR7 (5%, 0.7–65%), CD43 (13%, 0.2–75%), CX3CR1 (4%, 1–11%), and CXCR2 (24%, 1–74%). The median percentages and ranges of positively staining cells for each antibody in dogs with OS plus an infection are as follows: CD14 (78%, 12–99%), CD16 (64%, 32–79%), CD62L (21%, 3–57%), CCR2 (68%, 50–87%), CCR7 (41%, 6–90%), CD43 (37%, 9–63%), CX3CR1 (56%, 16–86%), and CXCR2 (57%, 23–65%). Significant differences are marked with an asterisk ($p < 0.05$). Data from treated OS dogs were compared to the data previously presented in Chapter 2, Figure 1a and currently presented in Chapter 3, Figure 2. Comparison of monocyte surface receptors between healthy controls, untreated dogs with OS, dogs with OS that had a concurrent surgical site infection and treated OS dogs revealed a significant decrease in CCR2 expression in untreated OS dogs (see Chapter 2, Figure 1a) and treated OS dogs ($p = 0.034$) compared to normal controls, and a significant increase in OS dogs with infection compared to untreated OS dogs (see Chapter 3, Figure 2) and treated OS dogs ($p = 0.001$); a significant decrease in CCR7 expression in untreated OS dogs (see Chapter 2, Figure 1a) and treated OS dogs ($p = 0.00652$) compared to normal controls, and a significant increase in OS dogs with infection compared to untreated OS dogs (see Chapter 3, Figure 2); a significant decrease in CX3CR1 expression in untreated OS dogs (see Chapter 2, Figure 1a) and treated OS dogs ($p = 0.0251$) compared to controls, and a significant increase in OS dogs with infection compared to untreated OS

dogs, normal controls (see Chapter 3, Figure 2), and trending towards significant increase compared treated OS dogs ($p = 0.05$) ; a significant decrease in CXCR2 expression in untreated OS dogs (see Chapter 2, Figure 1a) and treated OS dogs ($p = 0.0226$) compared to controls, and a significant increase in OS dogs with infection compared to untreated OS dogs (see Chapter 3, Figure 2).

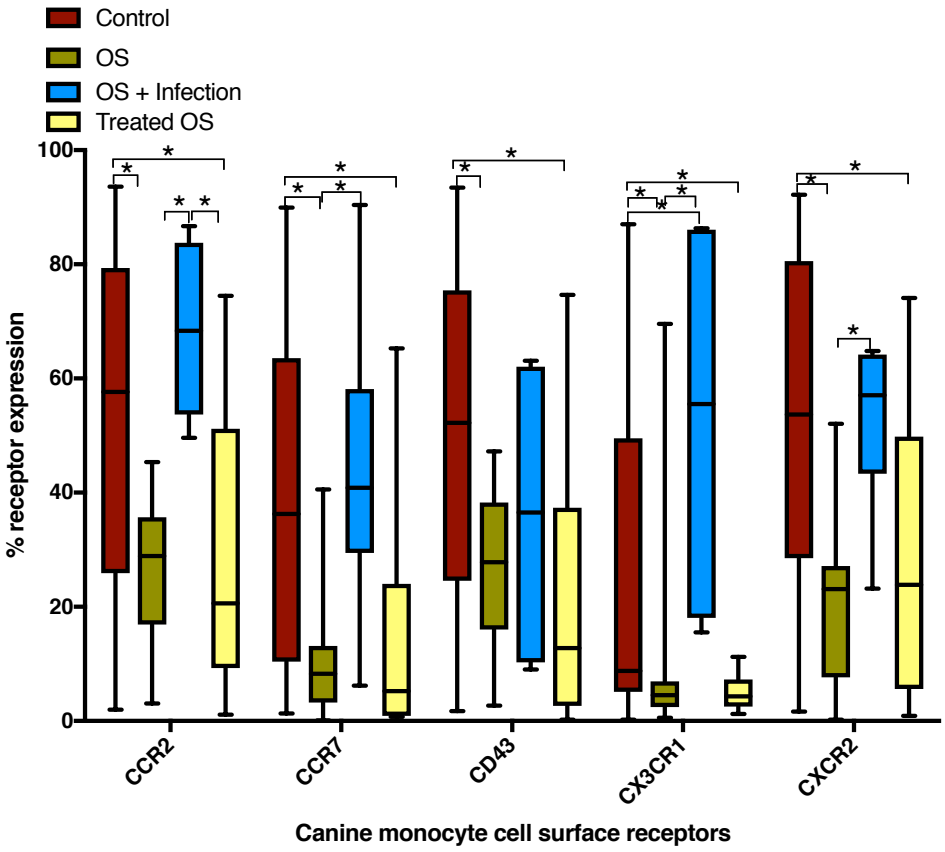
Control
OS
OS + Infection
Treated OS
% receptor expression
100
80
60
40
20
0
CCR2
CCR7
CD43
CX3CR1
CXCR2
Canine monocyte cell surface receptors

CHAPTER 4

A preliminary study on the effect of nanoparticle hyperthermia therapy on murine osteosarcoma.

4.1 Introduction

Osteosarcoma (OS), a malignant primary tumor of bone, is a devastating disease for both human and canine patients. It is the most common primary bone tumor in the dog, as well as in children and adolescents, and arises from mesenchymal cells that produce osteoid.[1,2] Despite successful removal of the primary tumor and administration of neoadjuvant / adjuvant chemotherapy, metastatic disease continues to be the primary cause of death for dogs and humans, with stagnation in survival times for both species over the past 30 years. The 5-year disease-free interval for human patients with non-metastatic OS remains around 70%, with only 20-30% long-term survival in patients with metastases, and the median survival in dogs with OS remains between 10-12 months despite various permutations of chemotherapeutic regimens.[2-5] Advancements in OS therapy are clearly needed to improve survival.

Hyperthermia therapy is well documented as an anti-tumor treatment, especially as a method of debulking primary tumors via irreversible thermal damage.[6-8] As is the goal of any treatment, hyperthermia therapy aims to deliver a therapeutic dose of heat to tumor tissue with minimal damage to surrounding normal tissue, and utilizing nanoparticles is a way of accomplishing this goal. Nanoparticle-assisted hyperthermia therapy involves localized administration of nanoparticles within a tumor followed by irradiation with an external energy source such as near-infrared lasers and alternating magnetic fields to induce tumor

hyperthermia. The tumor hyperthermia not only causes localized tumor necrosis, it also induces apoptotic signals that result in upregulation of tumor specific antigens (TSA) and heat shock proteins (HSP).[9] The TSA and HSP released from the tumor in response to heat stress are subsequently recognized by antigen presenting cells (APC), which in turn activate T-cells, in theory, promoting a vigorous anti-tumor response.[9] Nanoparticle-assisted hyperthermia therapy thus has the potential to eliminate the primary tumor, and to also target metastatic disease, especially if combined with immunomodulating therapies that help upregulate the immune response.

Magnetic nanoparticles are reported as vehicles for generating hyperthermia.[10-12] Magnetic cationic liposomes (MCL) are an efficient method of inducing intracellular hyperthermia, as these MCLs are shown to accumulate with a 10-fold higher affinity for tumor cells than neutrally charged magnetic liposomes due to the electrostatic attraction between MCLs and negatively charged cell membranes.[13] After deposition of the MCLs into the tumor, an alternating magnetic field (AMF) is applied, resulting in rapid oscillation of the MCLs, causing the MCLs to generate heat. A number of reports have documented the efficacy of MCL-hyperthermia therapy in rodent models against various tumors such as melanoma, mammary cell carcinoma, glioma, and OS.[10,14-16] MCL-hyperthermia therapy thus warrants investigation as a novel therapeutic option for OS.

To this end, we sought to evaluate the efficacy of MCL-hyperthermia therapy using a syngeneic murine model of OS. Normal healthy mice, mice with untreated OS, and mice with OS injected with MCLs without receiving hyperthermia therapy served as controls. Tumor burden, monocyte cell surface receptor expression and chemotaxis, and tumor mRNA

signatures were used for comparison between experimental groups. Our previous work demonstrated that cell surface chemokine receptors and chemotaxis were downregulated in monocytes from dogs with OS compared to normal controls (see Chapter 2). We posited that these findings represent ways in which OS causes dysregulation of the immune response. Thus, we also sought to determine whether the previously observed effects of OS on canine monocyte receptor expression and chemotaxis occur in murine OS. The objectives of our study were (1) to compare survival between experimental groups, (2) to compare monocyte surface receptor expression and monocyte chemotaxis between experimental groups, and (3) to compare tumor mRNA signatures between experimental groups. Our hypotheses were that MCL-hyperthermia therapy leads to longer survival in OS-bearing mice; that MCL-hyperthermia therapy will reverse the effects of OS on monocyte receptor expression and chemotaxis, and induce an inflammatory tumor mRNA signature.

4.2 Materials and Methods

4.2.1 Animals

Female C3H-HeN inbred mice were used for all experiments. All mice were 8-10 weeks of age, weighed 40-45 grams, and purchased from Charles River Laboratories (Raleigh, NC). Mice were housed 4 to a cage in a temperature-controlled room with a 12:12-hour automated light/dark cycle, and fed a standardized commercial pelleted diet. All mice underwent a 14-day acclimatization period before starting the study. All mice were randomly assigned to the following experimental groups – mice with OS that received MCL-hyperthermia treatment, mice with OS, mice with OS injected with MCLs without

hyperthermia therapy, normal control mice. All murine experiments were approved by the Institutional Animal Care and Use Committee, and all procedures were performed in an AAALAC-approved facility.

4.2.2 Murine model of OS

OS induction: A SQ syngeneic OS model was established in C3H-HeN mice with a subcutaneous injection of 2 x 10^8 DLM8 murine OS cells suspended in 30 µl HBSS into the right flank region. Tumor growth at the widest diameter was measured 2-3 times weekly using calipers, and mice were euthanized when their individual tumors measured 18 mm in diameter.

4.2.3 Magnetite Cationic Liposomes and MCL-Hyperthermia therapy

Magnetite particles were synthesized by Kaio Therapy, LLC, using a proprietary process, and MCLs were prepared using a previously described protocol with slight modifications.[13] MCL-hyperthermia therapy was administered to mice once their tumors reached 8-12 mm in diameter. On day 1 of treatment, 300 µl of MCLs were injected intratumorally over 30 minutes using a 25-gauge needle and an infusion pump. Hyperthermia therapy induced by an AMF was administered once daily for 30 minutes from days 2-4, for a total of 3 treatments. The AMF with a frequency of 100 kHz was created using Kaio Therapy's maganetic field generator designed and produced by TriE Medical Inc. (Research Triangle Park, NC). The mice were anesthetized by an intraperitoneal injection of ketamine (100 mg/kg) and xylazine (10 mg/kg), and placed under the coil with the tumor positioned within the center-field of the coil. Anesthetic parameters were monitored every 5 minutes; skin temperatures overlying the tumor and 10 mm away from the tumor were

measured using a Optocon FTC optical sensor (Optocon AG, Dresden, Germany), with a goal of reaching 43°C over the tumor, and maintaining normal surface temperature (21-23°C) 10 mm away from the tumor. Briefly, 24 hours after MCL injection, the tumors were subsequently heated by exposure to the AMF, while adjacent tissue and core body temperature remained constant. The therapeutic heating protocol was designed to maximize production of inducible heat shock proteins within cancer cells which can then bind with cancer antigens. Once released during necrosis of the tumor, the HSP:cancer antigen complexes become potent antigen specific immune stimulators.

4.2.4 Histopathologic evaluation

At time of euthanasia, tumor samples and any suspected metastatic or grossly abnormal lesions in internal organs observed at necropsy were placed in 10% neutral buffered formalin. Following fixation and paraffin embedding, 5 μm histologic sections were made and stained with hematoxylin and eosin using standard techniques. Sections from presumed metastatic lesions were reviewed by a board certified veterinary pathologist to confirm the lesions were metastases from the primary injection site. The injection site masses were also assessed for presence of black granular material (MCLs), areas of necrosis and local tissue reaction to heat treatment.

4.2.5 Flow cytometry (FACS)

Cell staining for flow cytometry, gating strategies and analysis were performed as described in Chapter 2 (2.2.4). The antibodies used were the same as those listed in 2.2.4.

4.2.6 Total RNA extraction, reverse transcription, and quantitative RT-PCR

RNA extraction from murine tumors, reverse transcription, and quantitative RT-PCR were performed as described in Chapter 3 (3.2.4).

4.2.7 Chemotaxis assay

Murine monocyte chemotaxis assays were performed as previously described in Chapter 2 (2.2.6).

4.2.8 Statistical analysis

Statistical analyses were performed as previously described in Chapter 2 (2.2.15)

4.3. Results

4.3.1 Experimental groups

The mice were divided into the following 4 experimental groups: healthy mice (normal control), OS-bearing mice (tumor control), OS-bearing mice treated with MCL-hyperthermia therapy (hyperthermia), OS-bearing mice injected with MCL without subsequent hyperthermia therapy (vehicle control). Anesthesia and procedures were well tolerated by all mice, and apart from 1 mouse with a thermal wound as a result of the MCL-hyperthermia therapy, all mice did not exhibit significant signs of pain post-procedure.

4.3.2 MCL-hyperthermia therapy

The complete course of MCL-Hyperthermia therapy was administered to 6 of 9 total mice. Three mice did not receive all 3 hyperthermia treatments due to the absence of gross tumor after 1-2 treatments. These 3 mice exhibited wounds at the tumor site that were suggestive of thermal necrotic injury, 1 mouse was euthanized immediately upon

development of the wound one day post hyperthermia treatment due to the severity of the injury, the other 2 mice were euthanized 12 days following the last hyperthermia treatment to standardize the time of euthanasia in treated mice without gross tumors.

4.3.3 Flow cytometry

Based on our findings reported above in canine monocytes - that monocyte chemokine receptors were significantly downregulated in dogs with OS compared to normal controls, and OS dogs with infection display increased monocyte receptor expression compared to untreated OS dogs, we compared monocyte surface receptors between mice with OS, mice with OS treated with MCL-hyperthermia therapy, vehicle control, and normal control mice to determine whether a similar effect could be observed in mice. The median percentages and ranges of positively staining cells for each antibody are listed in the legend accompanying Figure 1, and data from the hyperthermia and vehicle control mice were compared to the data previously presented in Chapter 2, Figure 5. When surface receptor expression was evaluated for all CD11b+ monocytes, CCR7 expression was significantly higher in monocytes of normal control mice compared to OS-bearing mice ($p = 0.0146$), hyperthermia mice ($p = 0.0002$), vehicle control mice ($p = 0.0282$) (Fig. 1a). When surface receptor expression was evaluated between the monocyte subsets, CCR7 expression was significantly higher in the $Ly6C^{lo}$ monocytes of normal control mice compared to OS-bearing mice ($p = 0.0004$), hyperthermia mice ($p < 0.0001$), and vehicle control mice ($p = 0.0029$) (Fig. 1a). In the hyperthermia mice, similar to the observations in OS-bearing mice (Chapter 2, Fig. 5b), CCR2 expression was significantly higher ($p = 0.0039$) and CXCR4 expression

was significantly lower ($p = 0.0039$) in $Ly6C^{hi}$ monocytes compared to $Ly6C^{lo}$ monocytes (Fig. 1b).

Figure 1: Monocyte surface marker expression is altered in mice with OS, and in OS mice treated with MCL-hyperthermia therapy

Flow cytometry plots illustrating cell surface receptor expression in peripheral blood monocytes from mice with OS (n = 11), hyperthermia mice (n=9), vehicle control mice (n = 6), and healthy controls (n = 7). (A) Box-and-whisker plot depicting the % positive CCR7 cell surface receptor expression in all CD11b+ monocytes and in the $Ly6C^{lo}$ monocyte subset in the experimental groups. (B) Box-and-whisker plot comparing % positive CCR2 and CXCR4 cell surface receptor expression between the $Ly6C^{lo}$ and $Ly6C^{hi}$ monocyte subsets in hyperthermia mice. The median percentages and ranges of positively staining cells for each antibody in healthy controls are as follows: CCR7 in CD11b+ monocytes (37%, 4–66%), CCR7 in $Ly6C^{lo}$ monocytes (41%, 6–70%). The median percentages and ranges of positively staining cells for each antibody in mice with OS are as follows: CCR7 in CD11b+ monocytes (16%, 1–37%), CCR7 in $Ly6C^{lo}$ monocytes (10%, 0.3–29%). The median percentages and ranges of positively staining cells for each antibody in mice with OS treated with MCL-hyperthermia are as follows: CCR7 in CD11b+ monocytes (3%, 2–25%), CCR7 in $Ly6C^{lo}$ monocytes (4%, 0.1–29%), CCR2 in $Ly6C^{hi}$ monocytes (96%, 81–100%), CCR2 in $Ly6C^{lo}$ monocytes (62%, 15–73%), CXCR4 in $Ly6C^{hi}$ monocytes (8%, 7–18%), CXCR4 in $Ly6C^{lo}$ monocytes (23%, 15–41%). The median percentages and ranges of positively staining cells for each antibody in vehicle control mice are as follows: CCR7 in CD11b+ monocytes (13%, 6–27%), CCR7 in $Ly6C^{lo}$ monocytes (13%, 3–22%), CCR2 in $Ly6C^{hi}$ monocytes (99%, 95–100%), CCR2 in $Ly6C^{lo}$ monocytes (70%, 49–93%), CXCR4 in $Ly6C^{hi}$ monocytes (8%, 2–28%), CXCR4 in $Ly6C^{lo}$ monocytes (16%, 5–32%). Significant differences are marked with an asterisk ($p < 0.05$).

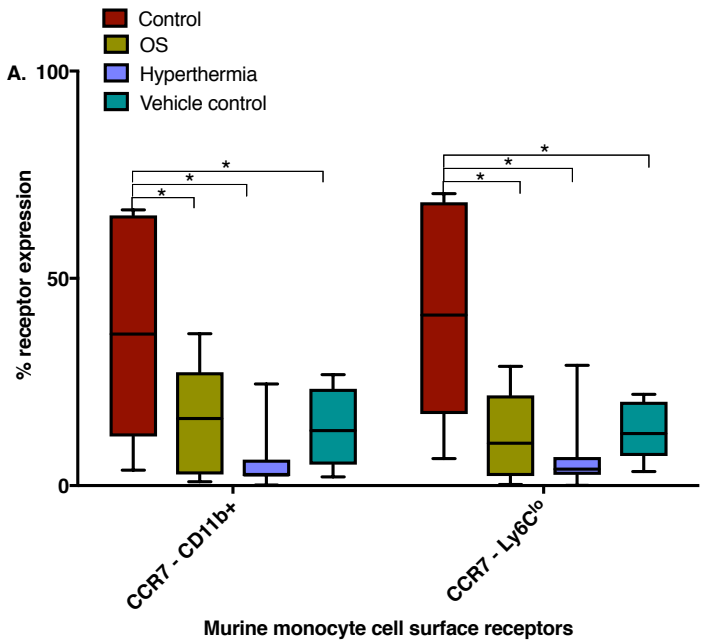
A.
Control
OS
Hyperthermia
Vehicle control
100
50
0
% receptor expression
*
*
*
*
*
*
CCR7 - CD11b+
CCR7 - Ly6C^lo
Murine monocyte cell surface receptors

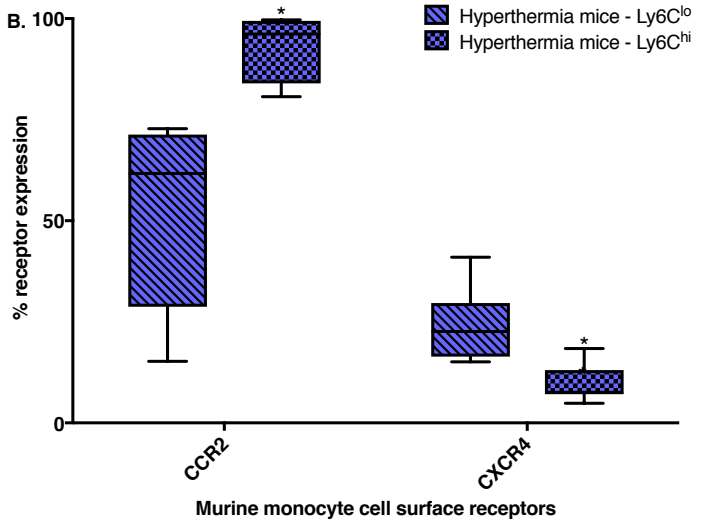
B.
Hyperthermia mice - Ly6C^lo
Hyperthermia mice - Ly6C^hi
100
50
0
% receptor expression
*
*
CCR2
CXCR4
Murine monocyte cell surface receptors

4.3.4 Quantitative RT-PCR

Murine relative tumor mRNA expression: IL-6, and TNF-α are markers of inflammation, and together with arginase, Fizz, and CD206, can be used to differentiate between polarized macrophage subsets in mice.[17] In order to investigate the effects of osteomyelitis on the expression of the above markers within tumor tissue, we compared the relative mRNA expression of IL-6, TNF-α, arginase, Fizz, and CD206 in tumor tissue from hyperthermia and vehicle control mice to OS-bearing mice. Similar to our findings in Chapter 3 (3.3.3), there were no significant differences in relative mRNA expression of all markers of interest in tumor tissue of experimental groups compared to tumor control tissue. The p-values for hyperthermia and vehicle control mice when compared to OS-bearing mice were as follows respectively: IL-6 ($p = 0.5120$, $p = 0.6761$), TNF-α ($p = 0.3488$, $p = 0.1539$), arginase ($p = 0.2994$, $p = 0.1462$), Fizz ($p = 0.0916$, $p = 0.9726$), CD206 ($p = 0.0513$, $p = 0.7262$).

4.3.5 Monocyte Chemotaxis

We had previously demonstrated decreased chemotaxis in monocytes from dogs with OS compared to monocytes from normal controls (Chapter 2, 2.3.4), but did not observe a similar trend in murine monocytes (3.3.4). Contrary to our previous hypothesis that osteomyelitis would enhance murine monocyte chemotaxis compared to monocytes from tumor-bearing mice, we found that monocytes from osteomyelitis mice exhibited significantly decreased chemotaxis compared to monocytes from tumor control (Chapter 3, 3.3.4). We therefore asked if MCL-hyperthermia therapy may have a similar or opposite effect on murine monocytes. We did not find any significant difference in murine monocyte

chemotaxis between mice with OS and hyperthermia mice ($p = 1.0$ with MCP, $p = 0.3673$ with SDF).

4.3.6 Histopathologic Evaluation

The morphologic features of masses that appeared at the injection site of all mice were histologically identical, confirming the presence of primary OS. The masses were composed of bundles, streams and sheets of neoplastic mesenchymal cells that expanded the subcutis and infiltrated and replaced dermis and underlying musculature. The neoplastic cells rested on scant collagenous stroma and typically had a moderate amount of pale eosinophilic cytoplasm and poorly defined cell boarders. Nuclear atypia was common with round to oval nuclei that contained coarsely clumped chromatin and multiple prominent nucleoli. Mitotic activity was brisk with 10-13 mitotic figures observed per 10 high power field. In both primary and metastatic lesions, the neoplastic masses often had curvilinear areas of necrosis. Tumor morphology from all presumed metastatic lesions was identical to that observed in the primary injection site. The most frequent sites of metastasis in these mice were liver (17.9%), ovary (7.7%), and lung (7.7%).

To assess the depth and delivery of the MCLs, primary tumors were further assessed for presence of a dark brown-black granular material. In the hyperthermia and vehicle control groups, the MCLs were easily visualized in large lakes that were distributed unevenly throughout the masses (Fig. 2).

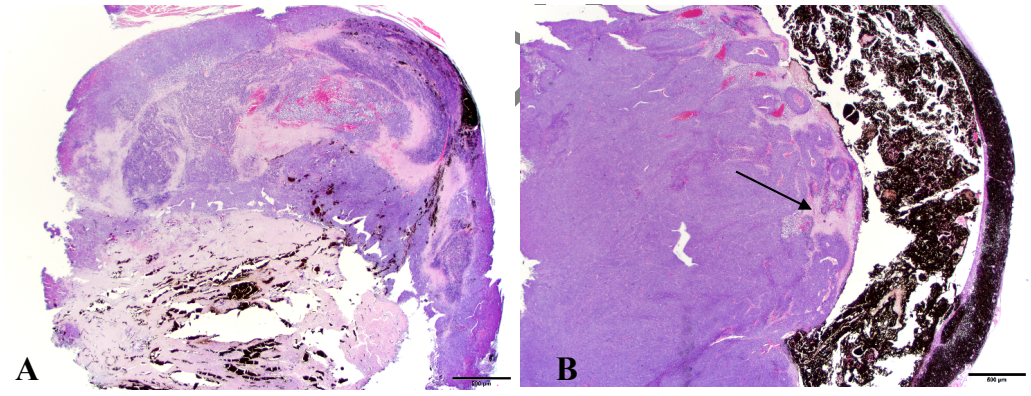

Figure 2: Distribution of nanoparticles in tumors arising at injection sites and tumor histopathology

Photomicrographs of hematoxylin and eosin stained sections from MCL-injected tumors from 2 mice. Note the uneven distribution of black nanoparticle material and areas of necrosis (arrows).

In mice that were treated with hyperthermia therapy, tumor lysis and changes in the epidermis and subcutis consistent with thermal injury were observed. These changes consisted of homogeneously pale eosinophilic staining with retention of tissue architecture (Fig. 3).

Figure 3: Photomicrographs of hematoxylin and eosin stained sections of tumors arising from injection sites

Panel A – neoplastic cells only (tumor control mice). The subcutis contains a large expansile neoplasm that extends into the subjacent musculature. The overlying skin is intact. Panel B – neoplastic cells and MCLs (vehicle control mice). The neoplasm arising from the subcutis has large areas of necrosis (arrows) and intralesional black nanoparticle material was observed. Panel C- neoplastic cells, MCLs and hyperthermia therapy (hyperthermia mice). There is extensive coagulation necrosis consistent with thermal injury that extends from the epidermis into the panniculus and affects approximately 75% of the neoplasm.

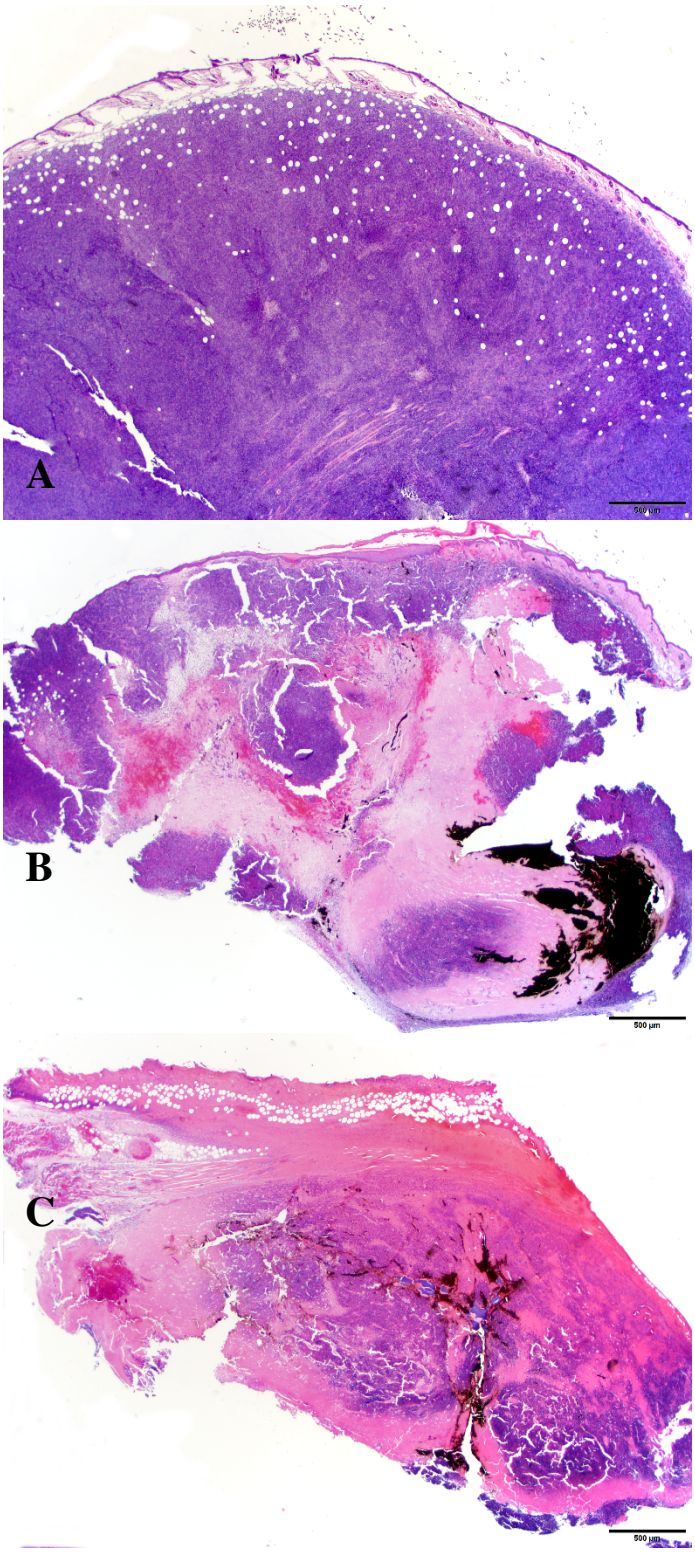
A
B
C

4.3.7 Survival Analysis

In order to evaluate the effects of MCL-hyperthermia treatment on survival in OS, we performed a Kaplan-Meier survival analysis comparing survival between hyperthermia mice, vehicle control mice, and tumor-bearing mice. Median survival for hyperthermia mice was 28 days, for vehicle control mice was 26 days, and for tumor control mice was 25 days. We did not find a statistically significant difference in median survival between experimental groups ($p = 0.53$).

4.4. Discussion

The goal of the study in this chapter was to evaluate the efficacy of MCL-hyperthermia therapy using a syngeneic murine model of OS, and to further characterize the role of monocyte / macrophages in driving an anti-tumor response. We hypothesized that mice with OS treated MCL-hyperthermia therapy will experience longer survival compared to mice with OS alone; that MCL-hyperthermia therapy will reverse the effects of OS on monocyte receptor expression and chemotaxis, and induce an inflammatory tumor mRNA signature. The potential efficacy of MCL-hyperthermia therapy had been demonstrated in a hamster model of OS - hamsters with implanted OS were treated with MCL-hyperthermia therapy at 42°C for 30 minutes every 24 hours for a total of 3 treatments.[16] All tumors in the treatment group reportedly resolved grossly by day 15 post treatment, and no local recurrence of tumor was observed for 3 months.[16] In contrast, we did not demonstrate a survival benefit afforded by MCL-hyperthermia therapy. The MCL-hyperthermia mice exhibited signs of thermal injury at their treatment site, as evidenced by the gross presence of an eschar, and

histologic presence coagulative necrosis. One potential explanation for this observation is the administration of a single large volume (300 μl) of MCLs into each tumor, which prevented the MCLs from distributing in a more diffuse pattern through the tumor (Fig. 4). Such an accumulation of all injected MCLs within one region of the tumor may have resulted in excessive focal heat production during AMF application. We are currently investigating the effects of dividing up the MCL dose into 3 smaller volumes injected into 3 tangential sites within the tumor to achieve a more diffuse distribution of MCLs through the tumor.

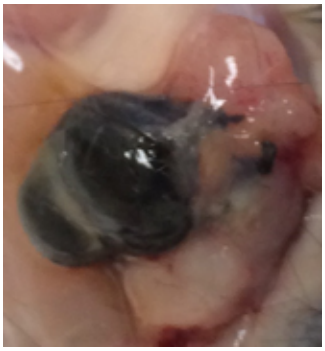

Figure 4: Photograph of MCLs accumulating in only 1 region grossly within the tumor.

Our flow cytometric analysis did not reveal a restoration of monocyte CCR7 receptor expression in hyperthermia mice to that similar to monocytes from normal controls, which suggests the lack of efficacy in our hyperthermia treatment protocol. We had noted a restoration of monocyte chemokine receptors in dogs with OS and a concurrent surgical site infection, which suggested that infection could stimulate an inflammatory response reversing the effects of OS on monocytes. Similar observations were made in mice with OS and osteomyelitis (Chapter 3, Fig. 3). We also observed higher CCR2 and lower CXCR4 expression in the $Ly6C^{hi}$ monocytes of hyperthermia mice compared to their $Ly6C^{lo}$

monocytes, similar to our observations in tumor-bearing mice (Chapter 2, Fig. 5b). As discussed in Chapter 2, the higher CCR2 expression in the Ly6C^{hi} monocytes hyperthermia mice, similar to the OS-bearing mice, may represent tumor-driven upregulation of CCR2 expression to facilitate Ly6C^{hi} monocyte migration towards the tumor. Similarly, the CXCR4 expression on the Ly6C^{hi} monocytes of hyperthermia mice that follows the same pattern as OS-bearing mice could represent another mechanism by which the tumor recruits monocytes. Such similarity in CCR2 and CXCR4 expression in monocytes from MCL-hyperthermia treated mice to tumor control mice suggests the lack of efficacy of our MCL-hyperthermia treatment protocol.

We did not find significant differences in relative mRNA expression of IL-6, TNF-α, arginase, Fizz, and CD206 in the tumor tissue from hyperthermia and vehicle control mice compared to tumor tissue from tumor control mice. CD206, or mannose receptor, is a pattern recognition receptor expressed on macrophages, and has been used to differentiate between macrophage subsets, with M2 macrophages exhibiting higher expression of CD206.[17] There was a trend towards decreased CD206 expression in tumors from hyperthermia mice compared to tumor control mice ($p = 0.0513$), suggesting a shift away from M2 polarization. TAMs are thought to adopt an M2-like phenotype, which helps promote angiogenesis and tumor metastasis, compared to the M1 macrophages that promote inflammatory anti-tumor responses.[18] We hypothesized that MCL-hyperthermia would induce an inflammatory tumor mRNA signature, and the decreasing trend of CD206 expression in tumors from hyperthermia mice compared to tumor control mice suggests that MCL-hyperthermia therapy affects local macrophage inflammatory polarization within the tumor tissue. Further studies

with an optimized MCL-hyperthermia therapy protocol are needed to evaluate the inflammatory M1-polarizing effects of the therapy on TAMs.

This study had limitations. One potential issue was the use of small batch-manufactured MCLs in our laboratory, hence there may have been inconsistencies in the performance of the MCLs. The large volume of MCLs injected into a single site may have contributed to the thermal damage evident at the treatment sites. Current optimization studies using commercial pharmaceutical grade MCLs and injection of smaller volumes of MCLs into multiple sites within each tumor are yielding promising results, with more uniform tumor heating and the absence of gross thermal injury.

Even though the current study did not identify a survival benefit conferred by either MCL-hyperthermia therapy, we have identified features of the MCL-hyperthermia therapy that we can optimize for follow-up studies. We observed higher CCR7 monocyte expression in normal control mice compared to other experimental groups, similar to our previous observations in dogs with OS and normal control dogs. We also identified monocyte surface expression of CCR2 as a potential mechanism by which tumors recruit monocytes, which warrants further investigation as CCR2 blockade is a potential anti-tumor strategy.

REFERENCES

1. Fenger JM, London CA, Kisseberth WC. Canine osteosarcoma: a naturally occurring disease to inform pediatric oncology. *ILAR J* 2014;55:69-85.

2. Friebele JC, Peck J, Pan X, et al. Osteosarcoma: A Meta-Analysis and Review of the Literature. *Am J Orthop (Belle Mead NJ)* 2015;44:547-553.

3. Selmic LE, Burton JH, Thamm DH, et al. Comparison of carboplatin and doxorubicin-based chemotherapy protocols in 470 dogs after amputation for treatment of appendicular osteosarcoma. *J Vet Intern Med* 2014;28:554-563.

4. Alvarez FJ, Kisseberth W, Hosoya K, et al. Postoperative adjuvant combination therapy with doxorubicin and noncytotoxic suramin in dogs with appendicular osteosarcoma. *J Am Anim Hosp Assoc* 2014;50:12-18.

5. Meazza C, Scanagatta P. Metastatic osteosarcoma: a challenging multidisciplinary treatment. *Expert Rev Anticancer Ther* 2016.

6. O'Neal DP, Hirsch LR, Halas NJ, et al. Photo-thermal tumor ablation in mice using near infrared-absorbing nanoparticles. *Cancer Lett* 2004;209:171-176.

7. Hirsch LR, Stafford RJ, Bankson JA, et al. Nanoshell-mediated near-infrared thermal therapy of tumors under magnetic resonance guidance. *Proc Natl Acad Sci U S A* 2003;100:13549-13554.

8. Loo C, Lin A, Hirsch L, et al. Nanoshell-enabled photonics-based imaging and therapy of cancer. *Technol Cancer Res Treat* 2004;3:33-40.

9. Moy AJ, Tunnell JW. Combinatorial immunotherapy and nanoparticle mediated hyperthermia. *Adv Drug Deliv Rev* 2017.

10. Ito A, Tanaka K, Kondo K, et al. Tumor regression by combined immunotherapy and hyperthermia using magnetic nanoparticles in an experimental subcutaneous murine melanoma. *Cancer Sci* 2003;94:308-313.

11. Kawai N, Ito A, Nakahara Y, et al. Complete regression of experimental prostate cancer in nude mice by repeated hyperthermia using magnetite cationic liposomes and a newly developed solenoid containing a ferrite core. *Prostate* 2006;66:718-727.

12. Motoyama J, Yamashita N, Morino T, et al. Hyperthermic treatment of DMBA-induced rat mammary cancer using magnetic nanoparticles. *Biomagn Res Technol* 2008;6:2.

13. Shinkai M, Yanase M, Honda H, et al. Intracellular hyperthermia for cancer using magnetite cationic liposomes: in vitro study. *Jpn J Cancer Res* 1996;87:1179-1183.

14. Ito A, Tanaka K, Honda H, et al. Complete regression of mouse mammary carcinoma with a size greater than 15 mm by frequent repeated hyperthermia using magnetite nanoparticles. *J Biosci Bioeng* 2003;96:364-369.

15. Ito A, Shinkai M, Honda H, et al. Heat shock protein 70 expression induces antitumor immunity during intracellular hyperthermia using magnetite nanoparticles. *Cancer Immunol Immunother* 2003;52:80-88.

16. Matsuoka F, Shinkai M, Honda H, et al. Hyperthermia using magnetite cationic liposomes for hamster osteosarcoma. *Biomagn Res Technol* 2004;2:3.

17. Davis MJ, Tsang TM, Qiu Y, et al. Macrophage M1/M2 polarization dynamically adapts to changes in cytokine microenvironments in Cryptococcus neoformans infection. *MBio* 2013;4:e00264-00213.

18. Mantovani A, Marchesi F, Malesci A, et al. Tumour-associated macrophages as treatment targets in oncology. *Nat Rev Clin Oncol* 2017.

CHAPTER 5

Conclusions, Ongoing Studies, and Future Directions

5.1 Conclusions

These studies enhanced our understanding of the effects of OS on monocytes and macrophages across species, and evaluated the immunostimulatory potential of bacteria and hyperthermia therapy on monocytes and macrophages in the presence of OS. This dissertation represents one of the only reports of cross-species comparative studies in OS using the dog, human and mouse. We demonstrated that OS influences host immune response in dogs by downregulating monocyte chemokine receptor expression and inhibiting monocyte chemotaxis. This dampening effect on monocyte chemokine receptors appears to be attenuated by the presence of a bacterial infection, as dogs with OS and a concurrent surgical site infection have significantly higher monocyte chemokine receptor expression than dogs with untreated OS. The limitations posed by sample acquisition from distant collaborators precluded assessment of monocyte chemotaxis in OS dogs with an infection. We also demonstrated increased PGE_2 secretion from monocytes of untreated OS dogs, which correlates with inhibition of monocyte chemotaxis, causing immunopathology in OS. Parallel flow cytometric analysis of peripheral monocyte receptor expression in human OS patients and murine models of OS did not yield a uniform pattern of monocyte chemokine receptor downregulation across species. However, our cross-species studies have identified receptors that are dysregulated across species, specifically CCR2, CCR7, CXCR2, and CX3CR1, thereby increasing the specificity of follow-up studies focusing on these receptors and their respective ligands (CCL2, CCL19/CCL21, CXCL1-7, CX3CL1 respectively) in

monocytes (Table 1). We did not demonstrate parallel patterns of monocyte chemotaxis between the dog and the mouse (Table 2).

Table 1: Summary of differences (increased or decreased) in monocyte surface markers in dogs, humans and mice as determined by flow cytometry in (a) OS-bearing subjects compared to normal controls; (b) OS-bearing subjects with infections compared to OS-bearing subjects without infections (significant differences are marked with an *)

Table 1a: OS-bearing subjects compared to normal controls

Monocyte markers	Canine OS	Human OS	Murine OS (SQ model)	Murine OS (Orthotopic model)
CCR2	↓*	↑*	↑	↑
CCR7	↓*	↑	↓*	↑*
CXCR2	↓*	↓*	↓	↓
CX3CR1	↓*	↓	↓	↓*
CD62L	↓*	↑	↑	↑*

Table 1b: OS-bearing subjects with infections compared to OS-bearing subjects without infections

Monocyte markers	Infected OS dogs	Infected OS mice
CCR2	↑*	↑
CCR7	↑*	↑*
CXCR2	↑*	↓
CX3CR1	↑*	↑
CD62L	↑	↑

Table 2: Summary of differences in monocyte chemotaxis in dogs and mice

Table 2: Monocyte chemotaxis compared between OS-bearing subjects and normal controls; OS-bearing mice with infections and OS-bearing mice without infections

	OS dogs compared to controls	OS mice compared to controls	Infected OS mice compared to non-infected OS mice
Chemotaxis	↓*	No difference	↓*

Our macrophage studies showed that even though OS can induce a protumorigenic inflammatory response in macrophages, the additional influence of bacteria can upregulate the macrophage inflammatory response to a higher intensity, potentially turning it into an M1-like macrophage anti-tumor response. A summary of the differences (increased and decreased) in macrophage cell surface markers, cytokine levels and mRNA expressions between canine and human macrophages cultured with OS and macrophages cultured alone, and between macrophages cultured with OS + *S. aureus* and macrophages cultured with OS is listed in Table 3.

Table 3: Summary of differences (increased or decreased) in macrophage surface receptors in canine and human macrophages. Comparisons are made between macrophages cultured with OS versus macrophages cultured alone; macrophages cultured with OS + *S. aureus* versus macrophages cultured with OS (significant differences are marked with an *; N/A = not assessed)

Table 3: Macrophages + OS compared to normal controls; macrophages + OS + *S. aureus* compared to macrophages + OS

	Canine Mφ + OS vs. controls	Canine Mφ + OS + *S. aureus* vs. Mφ + OS	Human Mφ + OS vs. controls	Human Mφ + OS + *S. aureus* vs. Mφ + OS
CD80 (surface receptor)	↑*	↑	N/A	N/A
CCR2 (surface receptor)	N/A	N/A	↓*	↓
CD86 (surface receptor)	N/A	N/A	↑*	↑*
TNF-α (cytokine)	↑	↑*	↑	↑*
TGF-β (cytokine)	↑	↓*	↑	↓*
IFN-γ (cytokine)	↑	↑	↑	↑*
MCP-1 (cytokine)	↑*	↓*	↑	↑*
TNF-α (mRNA)	↑*	↓	↑	↑*
IL-10 (mRNA)	↑*	↓	↑	↑*

In summary, the most pertinent finding from our monocyte studies is that bacterial infection attenuates the suppression of canine monocyte chemokine receptors observed in OS dogs. The most pertinent finding from our macrophage studies is that bacteria intensify the canine and human macrophage inflammatory response in the presence of OS. Even though these studies did not demonstrate perfectly parallel findings between dogs, humans and mice, they provide us with valuable information about the utility of the different models. The differences in findings between the subcutaneous syngeneic and orthotopic OS murine models suggest that there may be variation in quality of the models. Given that OS is a tumor originating from bone, the subcutaneous OS mouse may not be as relevant a model compared to the orthotopic mouse, hence accounting for the differences in experimental observations between the 2 models. Further work needs to be done to validate the orthotopic model and determine whether it is truly a more relevant and therefore superior model for OS compared to the subcutaneous syngeneic model. The differences observed in monocyte receptor expression between canine and human experiments do not necessarily negate the canine as a relevant model for human OS. The human patients recruited in this study were of a more heterogeneous population compared to the canine patients – human patients had a larger variation in treatments (e.g. chemotherapy) administered prior to sample collection, versus the canine patients that were a relatively homogeneous population, all of them being dogs that were diagnosed with osteosarcoma that had not received any treatment. Potentially, a larger sample of human OS patients may be needed due to the heterogeneity of that population. The results of our macrophage studies have more consistent similarities between human and canine samples, which may be explained by the *ex vivo* / *in vitro* nature of these

studies. These similarities emphasize the strength of the canine as a highly relevant model for human OS. Our priority is to identify a clinically safe and effective stimulus that can trigger the desired anti-OS inflammatory response in canine and human monocytes and macrophages.

5.2 Ongoing Studies

Manipulation of macrophage polarization is a promising therapeutic strategy in tumor immunotherapy. Macrophages display a high degree of polarization plasticity, which is a feature we can exploit to the host's advantage to induce an anti-tumor immune response. Tumor-associated macrophages (TAMs) primarily exhibit an immunosuppressive M2-like phenotype, shown to be pro-tumorigenic in many cancers.[1] Curiously, increased infiltration of M1/M2 TAMs was associated with improved survival in high-grade human OS, but the heterogeneous TAM population precluded conclusions about the anti-tumor mechanism.[2] Recent OS studies show M2 TAMs to be tumorigenic – a murine OS study found M1 TAMs polarizing to M2 TAMs within the first 3 weeks, with M2 TAMs promoting tumor growth, and another study demonstrated suppression of anti-tumor T-cells by M2 TAMs.[3,4] Interestingly, a murine study demonstrated induction of anti-OS activity in tumor-bearing mice with concurrent bacterial osteomyelitis.[5] This anti-tumor response corresponded with an increase in circulating inflammatory monocytes that potentially could be a source of the increased number of TAMs observed in the OS mice with osteomyelitis.[5] These TAMs were not further identified as M1 versus M2 TAMs, thus this study raises the intriguing question whether the observed anti-tumor response was elicited by increased numbers of bacteria-

induced M1 TAMs. Our studies have demonstrated the induction of an M1-like inflammatory response in macrophages co-cultured with OS and exposed to *S. aureus*. Consistent with our findings, a previous study demonstrated that macrophages activated by liposomal encapsulated muramyl tripeptide phosphatidyl ethanolamine (L-MTP-PE) mount an anti-OS response.[6,7] L-MTP-PE is a synthetic derivative of muramyl dipeptide (MDP), a bacterial cell wall component. Even though results from human clinical trials did not demonstrate an unequivocal survival benefit with the addition of L-MTP-PE, there were sufficiently positive results to support the efficacy of macrophage stimulation in OS treatment.[8,9] Therefore, finding novel effective ways of activating macrophages towards the inflammatory M1 phenotype is a promising anti-tumor strategy against metastatic OS.

One potential strategy for influencing macrophage polarization towards an M1-like anti-tumor phenotype is by manipulation of microRNAs (miRNAs), which are small, non-coding single-stranded RNAs that regulate many cellular processes such as proliferation, apoptosis, and differentiation, including macrophage polarization. miRNAs generally bind to the 3'/5' untranslated region of the target mRNA transcript, resulting in mRNA degradation or inhibition of translation of the transcript.[10] Manipulation of miRNA regulation of cellular functions thus has therapeutic potential. Using miRNAs to activate M1 anti-tumor macrophage polarization against OS has potential as a novel treatment strategy. miRNA profiles differ between M1 versus M2 macrophages – for example miR-155 is up-regulated in M1 macrophages whereas miR-125b is up-regulated in M2 macrophages.[11,12] miRNAs have been shown to induce anti-tumor M1 macrophages, or be secreted by tumors to generate M2 macrophages.[13,14] Manipulating macrophage miRNA can rescue an anti-tumor M1

phenotype in M2 TAMs,[15] thus, developing a technique for macrophage miRNA manipulation in OS has anti-metastatic therapeutic potential.

In order to develop miRNA manipulation as a therapeutic technique, we first need to elucidate the miRNA profiles of macrophages co-cultured with OS, with and without the influence of bacteria. Comparing the differences in miRNA profiles under these conditions would allow us to identify the miRNAs associated with inducing the heightened inflammatory response of macrophages co-cultured with OS and exposed to bacteria. By performing the experiments in human and canine macrophages, we aimed to identify miRNAs common, and thus most relevant, to both species that are associated with bacteria-induced macrophage inflammation. As a preliminary experiment to verify the feasibility of miRNA identification in canine cells, we utilized the canine miFinder® miRNA array from Qiagen to compare monocyte miRNA expression in dogs with untreated OS (n = 2) to healthy controls (n = 2). After gaining positive results with our preliminary experiment, we then proceeded to evaluate miRNA profiles from canine and human macrophages in the following experimental groups: macrophages cultured alone, macrophages cultured with OS, macrophages cultured with OS and *S. aureus*. The description of the materials and methods, and results of these experiments are provided below.

Materials and methods

Sample acquisition / preparation

Canine monocyte samples were obtained by high-speed cell sorting as described in Chapter 2. Samples were collected from 2 dogs with untreated OS and 2 healthy controls. Canine and human primary macrophage cultures were prepared as described in Chapter 3,

and at least 5 samples were prepared for each of the following experimental groups: macrophages cultured alone, macrophages cultured with OS, macrophages cultured with OS and *S. aureus*.

RNA extraction, reverse transcription, and miRNA PCR array

RNA was extracted from sorted canine monocytes using the miRNeasy® mini kit according to the manufacturer's protocol. Macrophages were collected from culture wells by addition of Tri-Reagent (Zymo Research) directly into the wells to lyse the cells, and stored at -80°C for subsequent PCR analysis. The Direct Zol RNA Microprep™ kit (Zymo Research) was used to extract total RNA from macrophages according to the manufacturer's protocol. The concentration and quality of the extracted RNA was determined using a NanoDrop 2000c spectrophotometer as well as the Agilent Bioanalyzer, and the RNA samples were stored at -80°C until processing. cDNA was synthesized from 125 ng RNA per sample using the miScript® II RT kit according to manufacturer's directions, and the RT reactions were carried out in a GeneAmp®PCR System 9700 thermal cycler. miRNA gene expression was determined with SYBR Green qPCR using the miScript® SYBR Green PCR kit per manufacturer's directions, and reactions cycled in a Roche Lightcycler 480. The ΔΔCT method of relative quantification was used to analyze data from the miScript® miRNA PCR array.

Results

Canine monocytes: Pairwise comparisons focused the miRNAs consistently different between groups. miR-126, miR- 130a, miR-204, miR-335, miR-29b, miR-451, miR-96 were over- expressed, and miR-122, miR-200a, miR-218, miR-223, miR-9 were under-expressed in 2 untreated OS dogs vs. 2 healthy controls.

Canine macrophages: In canine macrophages, a similar panel of miRNAs were differentially expressed between macrophages cultured with OS, and macrophages cultured with OS + *S. aureus* and macrophages cultured alone (controls) (Figure 1). This observation potentially supports our previous finding that macrophages cultured with OS assume an inflammatory phenotype, similar to macrophages cultured with OS and *S. aureus,* but to a lesser degree. Some of these miRNAs such as miR-125a, miR-146a are associated with macrophage polarization and the inflammatory response, and could be trending in similar patterns in macrophages + OS, and macrophages + OS + *S. aureus* due to the inflammatory response induced in both groups.

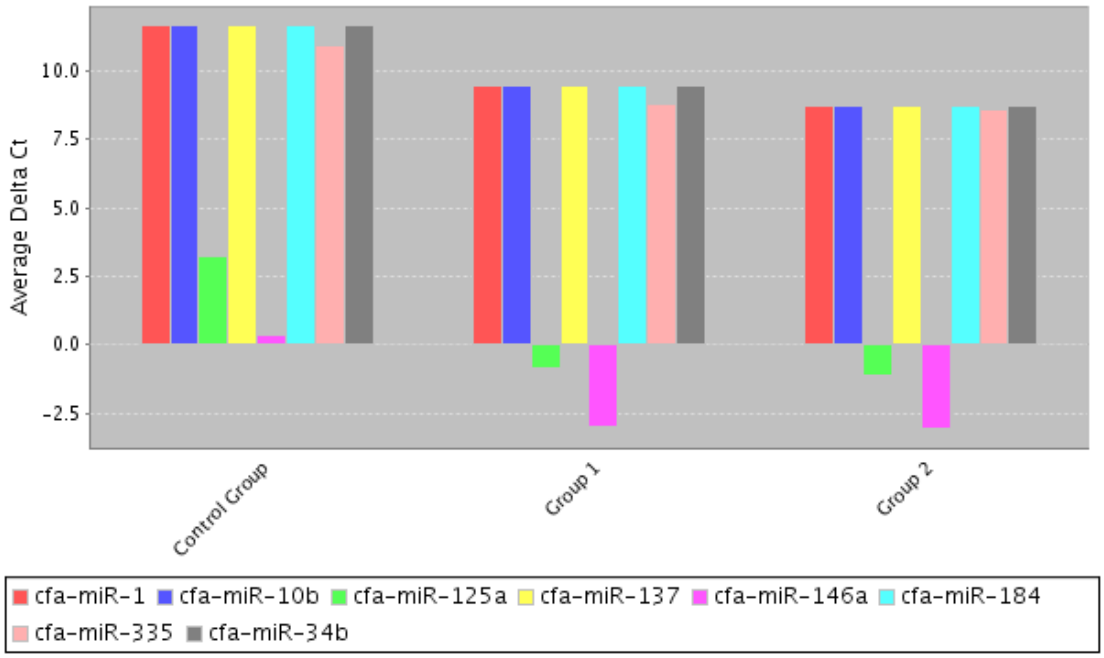

Figure 1: miRNAs differentially expressed in macrophages cultured with OS and macrophages cultured with OS + *S. aureus* compared to controls

Bar graphs showing individual miRNAs (color-coded by miRNA) expressed by macrophages from the 3 experimental groups (control = macrophages cultured alone, n=5; Group 1 = macrophages cultured with OS, n=7; Group 2 = macrophages cultured with OS + *S. aureus*, n=7). The y-axis represents the average delta Ct of each miRNA. Differential expression of miRNAs by Group 1 and Group 2 macrophages compared to control macrophages occurs in a similar pattern in Group 1 and 2 macrophages.

miR-451 was differentially expressed in macrophages cultured with OS compared to macrophages cultured with OS + *S. aureus* (Figure 2). miR-451 is involved with cellular differentiation and growth, and one of the primary targets of miR-451 is macrophage migration inhibitory factor (MIF).[16] MIF is a cytokine associated with tumor progression, for example, in colorectal cancer, and its expression is inversely related to miR-451 expression.[16] In OS, MIF has also been shown to induce VEGF and promote cellular invasion.[17] miR-451

was demonstrated to be overexpressed in canine OS compared to normal controls, however, miR-451 has been shown to be upregulated in murine M1-macrophages.[12,18] Therefore, decreased expression of miR-451 in macrophages cultured with OS + *S. aureus* (Group 2) is unexpected and warrants further investigation.

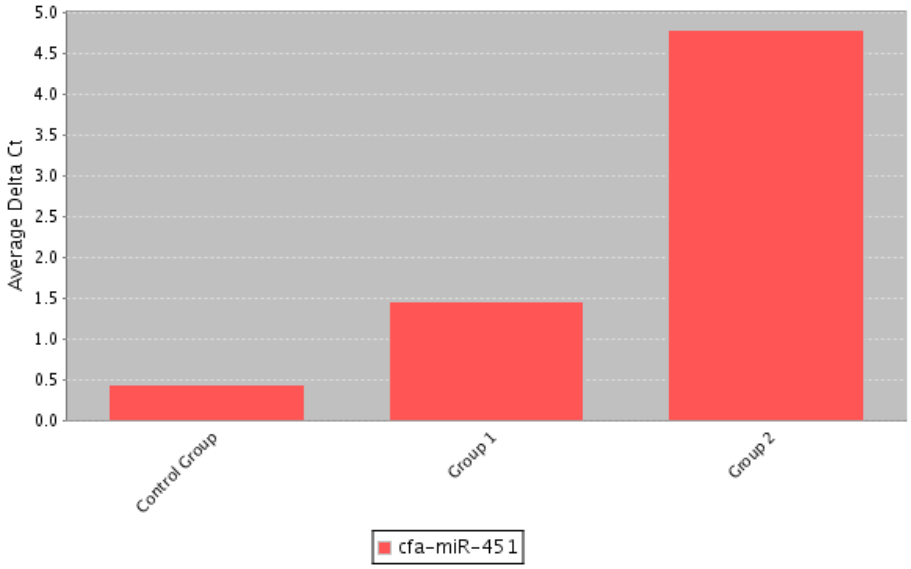

Figure 2: miR-451 is differentially expressed in macrophages cultured with OS + *S. aureus* compared to macrophages cultured with OS and controls

Bar graphs showing individual miR-451 expression by macrophages from the 3 experimental groups (control = macrophages cultured alone, n=5; Group 1 = macrophages cultured with OS, n=7; Group 2 = macrophages cultured with OS, n=7. The y-axis represents the average delta Ct of each miRNA. miR-451 expression is decreased in macrophages cultured with OS + *S. aureus* compared to macrophages cultured with OS and control macrophages.

Human macrophages: In human macrophage cultures, we observed 3 miRNAs that were differentially expressed between groups – miR-155, miR-30e, miR-144 (Fig. 3). miR-155 is a proinflammatory microRNA of macrophages, upregulated in M1-macrophages,[12,19] thus its increased expression in macrophages cultured with OS and macrophages cultured

with OS + *S. aureus* correlates with our previous observations that OS induces an inflammatory response in macrophages that is heightened by exposure to *S. aureus*. The expression of miR-30e and miR-144 in macrophages cultured with OS + *S. aureus* appear to be restored to their baseline levels expressed in macrophages cultured alone. The function of miR-30e and miR-144 are not well defined in macrophage polarization. In OS, miR-144 is downregulated in human OS cells and low expression correlated with poorer prognosis.[20] In canine OS, miR-30e was shown to be overexpressed in OS cells compared to normal controls.[18] Further work needs to be performed to understand the effects of miR-30e and miR-144 on macrophage polarization.

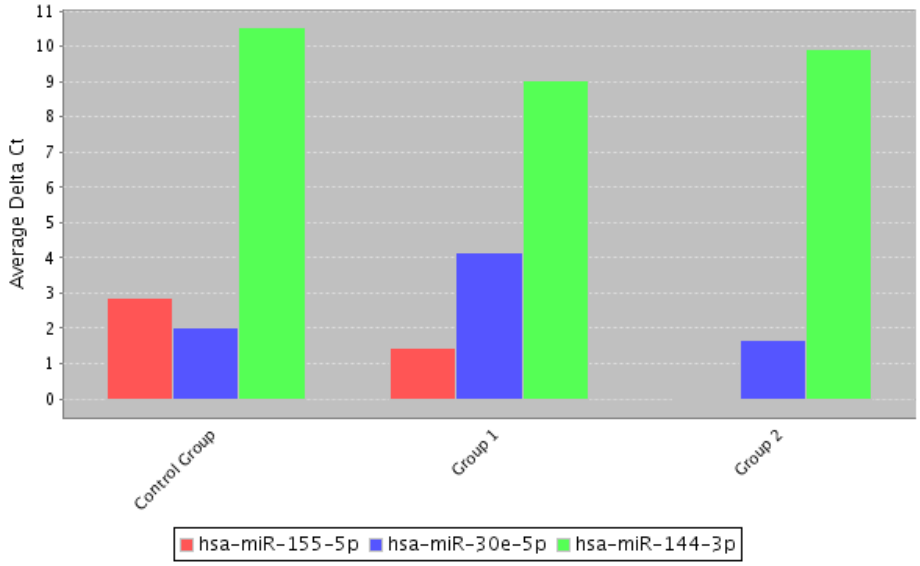

Figure 3: miR-155, miR-30e, miR-144 are differentially expressed in macrophages cultured with OS + *S. aureus* compared to macrophages cultured with OS

Bar graphs showing individual miR-451 expression by macrophages from the 3 experimental groups (control = macrophages cultured alone, n=5; Group 1 = macrophages cultured with OS, n=7; Group 2 = macrophages cultured with OS, n=7. The y-axis represents the average delta Ct of each miRNA. miR-451 expression is decreased in macrophages cultured with OS + *S. aureus* compared to macrophages cultured with OS and control macrophages.

5.3 Future Directions

Further work is needed to elucidate the effects of miR-451, miR-30e, miR-155 and miR-144 on macrophage polarization in the presence of OS, and to identify miRNAs in human and canine macrophages that express similar patterns under the described experimental conditions. One of the limitations of the miFinder® miRNA array is the dissimilarity in some miRNAs included in the arrays between species. We are currently planning first to determine whether we observe a similar trend in the expression of miR-30e in canine macrophages as our observations in human macrophages. Finding miRNAs with a similar pattern of expression in canine and human macrophages under the 3 experimental culture conditions described will enhance the specificity and relevance of the miRNA for future studies. We will then seek to determine whether manipulation of the miRNAs with common expression in the dog and human via transfection of mimics or inhibitors can induce an M1-like macrophage polarization capable of killing tumor cells. Identification of a miRNA that can be used to induce an inflammatory anti-tumor macrophage phenotype in both canine and human macrophages will forward our efforts in developing a therapeutic strategy aimed at immunostimulation against metastatic OS. Our ultimate goal is to improve OS survival in both humans and dogs using a novel immunotherapeutic approach. Using the dog as a model for comparative OS research takes advantage of the biologic similarities between canine and human OS to produce maximally translatable results to progress human OS research.

REFERENCES

1. Komohara Y, Jinushi M, Takeya M. Clinical significance of macrophage heterogeneity in human malignant tumors. *Cancer Sci* 2014;105:1-8.

2. Buddingh EP, Kuijjer ML, Duim RA, et al. Tumor-infiltrating macrophages are associated with metastasis suppression in high-grade osteosarcoma: a rationale for treatment with macrophage activating agents. *Clin Cancer Res* 2011;17:2110-2119.

3. Xiao Q, Zhang X, Wu Y, et al. Inhibition of macrophage polarization prohibits growth of human osteosarcoma. *Tumour Biol* 2014;35:7611-7616.

4. Han Q, Shi H, Liu F. CD163(+) M2-type tumor-associated macrophage support the suppression of tumor-infiltrating T cells in osteosarcoma. *Int Immunopharmacol* 2016;34:101-106.

5. Sottnik JL, U'Ren LW, Thamm DH, et al. Chronic bacterial osteomyelitis suppression of tumor growth requires innate immune responses. *Cancer Immunol Immunother* 2010;59:367-378.

6. Pahl JH, Kwappenberg KM, Varypataki EM, et al. Macrophages inhibit human osteosarcoma cell growth after activation with the bacterial cell wall derivative liposomal muramyl tripeptide in combination with interferon-gamma. *J Exp Clin Cancer Res* 2014;33:27.

7. Kurzman ID, Shi F, Vail DM, et al. In vitro and in vivo enhancement of canine pulmonary alveolar macrophage cytotoxic activity against canine osteosarcoma cells. *Cancer Biother Radiopharm* 1999;14:121-128.

8. Meyers PA, Schwartz CL, Krailo MD, et al. Osteosarcoma: the addition of muramyl tripeptide to chemotherapy improves overall survival--a report from the Children's Oncology Group. *J Clin Oncol* 2008;26:633-638.

9. Meyers PA. Muramyl tripeptide (mifamurtide) for the treatment of osteosarcoma. *Expert Rev Anticancer Ther* 2009;9:1035-1049.

10. Brown BD, Naldini L. Exploiting and antagonizing microRNA regulation for therapeutic and experimental applications. *Nat Rev Genet* 2009;10:578-585.

11. Cobos Jimenez V, Bradley EJ, Willemsen AM, et al. Next-generation sequencing of microRNAs uncovers expression signatures in polarized macrophages. *Physiol Genomics* 2014;46:91-103.

12. Zhang Y, Zhang M, Zhong M, et al. Expression profiles of miRNAs in polarized macrophages. *Int J Mol Med* 2013;31:797-802.

13. Squadrito ML, Etzrodt M, De Palma M, et al. MicroRNA-mediated control of macrophages and its implications for cancer. *Trends Immunol* 2013;34:350-359.

14. Jinushi M, Komohara Y. Tumor-associated macrophages as an emerging target against tumors: Creating a new path from bench to bedside. *Biochim Biophys Acta* 2015;1855:123-130.

15. Cai X, Yin Y, Li N, et al. Re-polarization of tumor-associated macrophages to pro-inflammatory M1 macrophages by microRNA-155. *J Mol Cell Biol* 2012;4:341-343.

16. Mamoori A, Gopalan V, Lu CT, et al. Expression pattern of miR-451 and its target MIF (macrophage migration inhibitory factor) in colorectal cancer. *J Clin Pathol* 2017;70:308-312.

17. Han I, Lee MR, Nam KW, et al. Expression of macrophage migration inhibitory factor relates to survival in high-grade osteosarcoma. *Clin Orthop Relat Res* 2008;466:2107-2113.

18. Fenger JM, Roberts RD, Iwenofu OH, et al. MiR-9 is overexpressed in spontaneous canine osteosarcoma and promotes a metastatic phenotype including invasion and migration in osteoblasts and osteosarcoma cell lines. *BMC Cancer* 2016;16:784.

19. Essandoh K, Li Y, Huo J, et al. MiRNA-Mediated Macrophage Polarization and its Potential Role in the Regulation of Inflammatory Response. *Shock* 2016;46:122-131.

20. Wang W, Zhou X, Wei M. MicroRNA-144 suppresses osteosarcoma growth and metastasis by targeting ROCK1 and ROCK2. *Oncotarget* 2015;6:10297-10308.